



## **Dissertation**

zur Erlangung des Doktorgrades der Fakultät für Biologie

der Ludwig-Maximilians-Universität München

---

---

### **Molecular characterization of two chloroplast biogenesis regulators in *Arabidopsis thaliana***

---

---

*Vorgelegt von:* Nicola ZAGARI

Diese Dissertation wurde angefertigt  
unter der Leitung von Prof. Dr. Dario Leister  
im Bereich von Fakultät für Biologie  
an der Ludwig-Maximilians-Universität München

Gutachter: 1. Prof. Dr. Dario Leister

2. Prof. Dr. Wolfgang Frank

Tag der Abgabe:: 22.11.2018

Tag der mündlichen Prüfung: 29.05.2019

## Index

<b>Summary .....</b>	<b>8</b>
<b>Abbreviations.....</b>	<b>10</b>
<b>1. Introduction.....</b>	<b>12</b>
1.1 The identification of a putative chloroplast ribosome subunit .....	12
1.2 A hypothetical link between leaf variegation and a DNA-J like protein.	17
<b>2. Materials and Methods.....</b>	<b>20</b>
2.1 Plant material, propagation and growth conditions .....	20
2.2 Nucleic acid analysis .....	21
2.3 Fluorescence measurements .....	22
2.4 Pigments .....	23
2.5 Metabolite analysis .....	24
2.6 Phylogenetic analysis.....	24
2.7 Protein isolation and immunoblot analysis.....	25
2.8 Thylakoid Isolation and SDS–PAGE .....	25
2.9 Low-Temperature (77-K) Fluorescence Measurements .....	26
2.10 Immunoprecipitation analysis .....	26
2.11 Size exclusion chromatography (SEC) and sucrose gradient .....	26
2.12 In vivo protein labeling.....	27
2.13 Polysome analyses .....	27
2.14 Mass spectrometry .....	27
2.15 RNA gel blot analysis and polysome loading.....	28
2.16 RNA sequencing, mapping and slot-blot analysis .....	28
2.17 Yeast two-hybrid analysis.....	29
2.18 In vivo translation assay.....	29
2.19 Confocal microscopy .....	29
2.20 Accession numbers .....	30
<b>3. Results CRASS.....</b>	<b>31</b>
3.1 CRASS is coregulated with plastidial ribosomal proteins.....	31
3.2 CRASS is present in green plants but not in Chlorophyta.....	32
3.3 CRASS is a non-essential protein localized in the chloroplast stroma....	33
3.4 CRASS does not alter rRNA accumulation under control conditions.....	35
3.5 The absence of CRASS triggers a reduced translational activity .....	36
3.6 CRASS is necessary for cold stress tolerance .....	36
3.7 Chloroplast 16S rRNA coimmunoprecipitates with CRASS .....	38
3.8 CRASS interacts with PRPS1 in a RNA-independent manner .....	41
3.9 Synergistic effect between CRASS and PRPS17 .....	43

---

<b>4. Results SCO2</b> .....	<b>45</b>
4.1 Absence of SCO2 results in leaf variegation in <i>L. japonicus</i> .....	45
4.2 LjSCO2 is essential for photosynthetic activity in <i>L. japonicus</i> .....	49
4.3 Variegated leaves display altered protein profiles in <i>L. japonicus</i> .....	52
4.4 SCO2 is involved in the assembly or repair of PSII complexes.....	53
4.5 SCO2 has also a role in variegation in <i>A. thaliana</i> .....	57
<b>5. Discussion</b> .....	<b>58</b>
5.1 CRASS is located in the stroma of <i>Arabidopsis thaliana</i> chloroplasts ...	58
5.2 The HMA domain of CRASS lost its function during evolution .....	59
5.3 CRASS assists ribosome assembly when stress is applied.....	59
5.4 CRASS interacts with chloroplastic small ribosomal proteins.....	60
5.5 CRASS is directly involved in ribosome functionality .....	61
5.6 SCO2 is a DNAJ-related protein involved in chloroplast biogenesis.....	62
5.7 SCO2 is required for the assembly or repair of LHC .....	62
5.8 SCO2 constitutes a novel factor involved in leaf variegation .....	64
5.9 Stressful environmental conditions facilitate protein characterization....	65
<b>6. Appendix</b> .....	<b>67</b>
<b>7. References</b> .....	<b>86</b>
<b>8. Eidesstattliche Erklärung</b> .....	<b>96</b>
<b>9. Curriculum vitae</b> .....	<b>97</b>
<b>10. Acknowledgements</b> .....	<b>99</b>

---

## Figures and tables index

Figure 1.1 Chloroplast ribosome subunits.....	13
Figure 3.1 Coexpression and phylogeny of CRASS .....	32
Figure 3.2 Characterization of CRASS mutants and analysis of subcellular localization. ....	34
Figure 3.3. Analysis of the effect of CRASS on the accumulation of plastid rRNA and protein levels.....	35
Figure 3.4. Effects of the inhibition of chloroplast translation by lincomycin on CRASS mutants. ....	36
Figure 3.5. CRASS is required for cold stress tolerance. ....	38
Figure 3.6. RNA co-immunoprecipitation with CRASS. ....	39
Figure 3.7. Crass co-immunoprecipitation analysis .....	40
Figure 3.8. Analysis of RNA-dependency of CRASS interaction with ribosomal proteins.....	42
Figure 3.9. Genetic interactions between CRASS and ribosomal proteins. ....	43
Figure 4.1 Mutation of LjSCO2 impairs chloroplast development in cotyledons and true leaves in <i>Lotus japonicus</i> .....	47
Figure 4.2 Greening and photosynthetic measurements confirm conserved roles of SCO2 between <i>A. thaliana</i> and <i>L. japonicus</i> . ....	48
Figure 4.3 Analysis of the leaf phenotype of the <i>ljSCO2-1</i> mutant under different growth conditions. ....	49
Figure 4.4 <i>L. japonicus ljSCO2-1</i> mutant displays impaired photosynthesis.....	51
Figure 4.5 Western-blot analyses of cotyledons and true leaves in <i>L. japonicus</i> . ....	53
Figure 4.6 SCO2 is required for PSII supercomplex and megacomplex accumulation.....	55

---

Figure 4.7 Inhibition of translation in the chloroplast does not suppress variegation in <i>ljSCO2</i> mutants .....	56
Figure 4.8 <i>Arabidopsis thaliana</i> double mutant <i>atsCO2 atclpr1</i> displays a variegated phenotype. ....	57
Supplemental Figure 6.1 The coexpression regulon of plastid ribosomal proteins.....	67
Supplemental Figure 6.2 Sequence alignment of CRASS and bacterial heavy metal associated (HMA) proteins. ....	68
Supplemental Figure 6.3 Altered CRASS levels do not affect photosynthetic efficiency.....	69
Supplemental Figure 6.4 Analysis of the effect of CRASS on polysome loading of <i>psaA</i> and <i>rbcL</i> .....	69
Supplemental Figure 6.6 Analysis of the inhibition of chloroplast translation in overexpressor lines.....	70
Supplemental Figure 6.5 Yeast two-hybrid analysis of CRASS and ribosomal proteins. ....	70
Supplemental Figure 6.7 Analysis of plant development in short day conditions in the absence of plastidial ribosomal proteins. ....	71
Supplemental Figure 6.8 Characterization of three independent mutant lines for SCO2 in <i>Lotus japonicus</i> .....	72
Supplemental Figure 6.9 Sequence and phylogenetic analysis of SCO2.....	74
Supplemental Figure 6.10 77K fluorescence emission spectra of thylakoid samples.....	74
Supplemental Figure 6.11 Analysis of the cotyledon phenotype of the <i>atsCO2</i> mutant under different light regimes. ....	75
Supplemental Figure 6.12 Metabolic analyses of <i>L. japonicus</i> plants. ....	76
Supplemental Figure 6.13 PsbD and LHCB1 accumulation in <i>L. japonicus</i> true leaves.....	77

---

Supplemental Figure 6.14 SCO2 is required for PSII megacomplex accumulation. ....	78
Supplemental Figure 6.15 LjSCO2 is not required for state transitions.....	79
Supplemental Figure 6.16 Chloroplast translation inhibitors do not suppress variegation in <i>ljSCO2</i> mutants.....	80
Supplemental Figure 6.17 The <i>Arabidopsis thaliana</i> double mutant <i>atsCO2 atclpr1</i> contains the same point mutation as the <i>sco2</i> single mutant. ....	81
Supplemental Figure 6.18 Model of SCO2 function in the assembly or repair of photosynthetic complexes. ....	82
Table 3-1 CRASS coimmunoprecipitates with plastid ribosomal proteins. ....	44
Supplemental Table 6-1 Data set of protein coimmunoprecipitation experiments.....	82
Supplemental Table 6-2 Data set of RNA coimmunoprecipitation with CRASS. ....	83
Supplemental Table 6-3 List of primers used in this work.....	84
Supplemental Table 6-4 List of primers used in this work.....	85

## Summary

Plastid ribosomes are derived from ancestral endosymbiotic cyanobacteria and are composed of a large (50S) and a small (30S) subunit. Each subunit contains ribosomal proteins and ribosomal RNAs. The majority of these ribosomal proteins are also involved with ribosome biogenesis and functioning and are encoded in the nucleus. However only a small percentage of ribosomal proteins are chloroplast encoded. The first part of this doctoral thesis reports the identification and characterization of the *Arabidopsis thaliana* nuclear encoded CHLOROPLAST RIBOSOME ASSOCIATED (CRASS) protein. This protein has emerged during embryophyta evolution and resides in the chloroplast stroma of land plants but not in green algae or cyanobacteria. Under optimal growth conditions CRASS is not required for plant survival and *crass* mutants show minor defects in photosynthesis and plant fitness. On the other hand, translation inhibitors (lincomycin and chloramphenicol) and cold stress exacerbate the mutant plant phenotype. In co-immuno-precipitation experiments, CRASS is pulled down with 16S RNA and with the small ribosomal subunits PRPS1 and PRPS5. CRASS interacts with ribosomal proteins independently of ribosomal RNAs, suggesting a protein-protein interaction with other subunits or structural components of the ribosome. Double mutants have a synergistic mutant phenotype confirming that CRASS plays a role in the stability of the chloroplast and becomes crucial when stress conditions interfere with ribosome biogenesis and activity.

An additional crucial role in the development of the chloroplasts is played by the assembly factors which allow correct formation of thylakoid membrane complexes needed to sustain phototrophic growth. The second part of this dissertation focuses on a DNAJ related protein, SNOWY COTYLEDON2 (SCO2), required for thylakoid complex assembly and protein interaction with the light-harvesting chlorophyll-binding protein LHCB1. Its role in chloroplast biogenesis in true leaves of *Arabidopsis thaliana* and *Lotus japonicus*, previously thought to be a protein acting exclusively in cotyledon greening, is here analysed. The lack of SCO2 in *Arabidopsis* results in a drastic decrease in plant growth and photosynthesis efficiency under short-day conditions, while SCO2 disruption in *Lotus* induces white and green variegated leaves and stunted growth. In this case, inhibition of translation rates does not decrease the variegation phenotype as in other variegated mutants. Furthermore, in *Arabidopsis*, the combined absence of SCO2 and ClpR1 causes a severe variegated phenotype. These effects suggest that SCO2 can be considered a new component able to suppress leaf variegation.

Taken together, the results of this thesis highlight the possibility to discover new gene functions, such as CRASS and SCO2. These genes have been functionally characterized by inducing stresses that enhanced otherwise undetected phenotypes.

## Zusammenfassung

Plastide Ribosomen stammen von endosymbiontischen Cyanobakterien ab und bestehen aus einer großen (50S) und einer kleinen (30S) Untereinheit. Jede Untereinheit enthält ribosomale Proteine und ribosomale RNAs. Die Mehrzahl dieser ribosomalen Proteine, die auch an der Ribosomenbiogenese und -funktion beteiligt sein könnten, wird im Kern kodiert, während nur ein geringer Prozentsatz im Chloroplasten kodiert wird. Im ersten Teil dieser Doktorarbeit wird über die Identifizierung und Charakterisierung des durch *Arabidopsis thaliana* kerncodierten Proteins CHLOROPLAST RIBOSOME ASSOCIATED (CRASS) berichtet. Dieses Protein wurde während der Embryophyten-Evolution erworben und befindet sich im Chloroplastenstroma von Landpflanzen, jedoch nicht in Grünalgen oder Cyanobakterien. Unter optimalen Wachstumsbedingungen ist CRASS für das Überleben der Pflanze nicht erforderlich. *Arabidopsis thaliana* Mutanten weisen nur geringfügige Defekte in der Photosyntheseeffizienz und der Fitness der Pflanze auf. Allerdings verstärken Translationsinhibitoren (Lincomycin und Chloramphenicol) und Kältestress den Phänotyp der mutierten Pflanzen. In Co-immunpräzipitationsexperimenten wandert CRASS mit 16S-RNA und dementsprechend mit den Proteinen der kleinen ribosomalen Untereinheit, insbesondere PRPS1 und PRPS5. Trotzdem interagiert CRASS mit ribosomalen Proteinen unabhängig von ribosomalen RNAs, was auf eine Protein-Protein-Interaktion mit anderen Untereinheiten oder Strukturkomponenten des Ribosoms schließen lässt. Doppel Mutanten haben einen synergistisch Mutanten Phänotyp. Dieser bestätigt dass CRASS eine Rolle für die Stabilität des Chloroplasten spielt und entscheidend wird, wenn Stressbedingungen die Ribosomenbiogenese und -aktivität beeinträchtigen.

Eine weitere entscheidende Rolle bei der Entwicklung der Chloroplasten spielen die Assemblierungsfaktoren, die die korrekte Bildung von Thylakoid-Membrankomplexen ermöglichen, die zur Aufrechterhaltung des phototrophen Wachstums erforderlich sind. In diesem Zusammenhang konzentriert sich der zweite Teil dieser Dissertation auf ein DNA-J- verwandtes Protein, SNOWY COTYLEDON2 (SCO2), das für die Thylakoid-Assemblierung und die Interaktion mit dem Lichtsammel-Chlorophyll-Bindungsprotein LHCB1 benötigt wird. Bisher wurde davon ausgegangen, dass es ein Protein ist, das ausschließlich in der Cotyledon-Begrünung wirkt. Hier wird seine Rolle bei der Chloroplastenbiogenese in echten Blättern von *Arabidopsis thaliana* und *Lotus japonicus* analysiert. Das Fehlen von SCO2 bei *Arabidopsis* führt zu einer drastischen Abnahme des Pflanzenwachstums und der Photosyntheseeffizienz unter kurzen Tagesbedingungen, während in *Lotus* weiße und grüne Blätter und Wachstumsstörungen induziert werden. In diesem Fall verringert die Inhibierung der Translationsraten den Variationsphänotyp nicht wie bei anderen enlichen Mutanten. Darüber hinaus induziert in *Arabidopsis* die Kombination der Abwesenheit von SCO2 und ClpR1 einen stärker mutierten Phänotyp. Diese Effekte legen nahe, dass SCO2 als neue Komponente betrachtet werden kann, die die Färbung des blattes unterdrückt. Die Ergebnisse dieser Arbeit haben gezeigt, dass neue Genfunktionen entdeckt werden können, wie im Fall von CRASS und SCO2. Diese wurden dadurch charakterisiert, dass Stress ausgeübt wurde und das unentdeckte Phänotypen verstärkt wurden.

## Abbreviations

°C	Celsius degrees
μ	Micro
ATP	Adenosine triphosphate
Bp	Base pairs
cDNA	Complementary deoxyribonucleic acid
CDS	Coding sequence
Col	<i>Arabidopsis thaliana</i> . var. Columbia
CRASS	CHLOROPLAST RIBOSOME ASSOCIATED protein
CTP	Chloroplast transit peptide
Da	Dalton
ddH <sub>2</sub> O	distilled water
DEPC	Di-ethylpyrocarbonate
DNA	Deoxiribonucleic acid
dNTPs	Deoxyribonucleotides
DTT	Dithiothreitol
<i>E. coli</i>	<i>Escherichia coli</i>
ECL	Enhanced chemiluminescence
EDTA	Ethylendiamintetraacetate
ETR	Electron transport rate
g	Gram
<i>g</i>	Gravity force
GFP	Green Fluorescent Protein

h	Hour
l	Liter
LIN	Lincomycin
M	Mol per liter
mol	Mol
MS	Mass spectrometry
PAGE	Polyacrylamide Gel electrophoresis
PCR	Polymerase chain reaction
PVDF	Polyvinylidene difluoride
rRNA	Ribosomal RNA
RT	Room temperature
SDS	Sodium dodecylsulfate
T-DNA	Transfer DNA
TRIS	Tris (hydroxymethyl) aminomethane
tRNA	Transfer RNA
WT	Wild type
YFP	Yellow Fluorescent Protein

# 1. Introduction

## 1.1 The identification of a putative chloroplast ribosome subunit

Plastids of plants and algae evolved from a single endosymbiotic event involving the incorporation of an ancient photosynthetic cyanobacterium into a eukaryotic host. The name “plastids” has been given to these organelles because of their plasticity, since there are many plastid types with very different functions such as amyloplasts, leucoplasts, chromoplasts and chloroplasts, which differentiate from proplastids (Lopez-Juez & Pyke 2005; Sakamoto et al. 2008). For instance, the transition from a small undifferentiated proplastid to a mature chloroplast is characterized by a large increase in size, an accumulation of plastid-specific pigments (carotenoids and chlorophylls), a rapid production of photosynthetic proteins and formation of the thylakoid membranes. The last step is the assembly of the light harvesting antenna complexes (LHCs) to allow photosynthesis in the mature chloroplast (Jarvis & López-Juez 2013).

Many features of the original bacterial ancestor are still present in the modern chloroplast (Moreira et al. 2000). These include a circular genome with about 120 genes encoding ribosomal RNA (rRNA), transfer RNA (tRNA), subunits of the translational apparatus (polymerases, ribosomal proteins and assembly factors), components of the two photosystems such as ATP synthase, NADH dehydrogenase, cytochrome  $b_6f$ , subunits of the ATP synthase and the Rubisco large subunit which is likely the most abundant protein on Earth. The abundance of Rubisco and other crucial components of the photosynthetic machinery might be the reason why their protein synthesis takes place in the chloroplast by plastidial ribosomes, even if 95 % of the plastid proteins are nuclear encoded (Barbrook et al. 2006).

The ancestral cyanobacterial genome was composed of 1500-3000 genes of which only a minor fraction (usually less than 150) is still present in the current chloroplasts genomes of higher plants. The strong reduction of gene number is the consequence of symbiosis that made many genes become dispensable and of a massive gene transfer to the host’s nuclear genome (Bock & Timmis 2008; Kleine et al. 2009). As a consequence, nucleus-encoded proteins have to be transported into the chloroplast. Thus chloroplast biogenesis depends on anterograde signaling from nucleus to chloroplast, and vice versa, retrograde signaling to properly coordinate the assembly of the photosynthetic apparatus starting from proteins encoded in different compartments (Ruckle & Larkin 2009). Two RNA polymerases are present in the

plastids: a nuclear-encoded bacteriophage-type and a plastid-encoded, bacterial-type which transcribes most of the plastid genes (Fristedt et al. 2014).

Ribosomes were first found in 1953 by George Emil Palade using an electron microscope on rat liver homogenates, while their name has been given few years later to abbreviate ‘microsomal ribonucleoproteins’ (Oota & Takata 1959; Palade & Siekevitz 1956). Ribosomes are a macromolecular complex inside eukaryotic and prokaryotic cells responsible for protein synthesis.

Eukaryotic ribosomes are larger than their prokaryotic counterparts, which differ from mitochondrial (called mitoribosomes) and chloroplastic ribosomes. Plastid ribosomes are of cyanobacterial origin and are composed of a small subunit with a 30S sedimentation factor and a large 50S subunit which together form the 70S ribosome that decodes and translates mRNAs into the corresponding polypeptide chains (Harris et al. 1994). Both subunits are composed of RNA and proteins forming a macromolecular complex. To date more than 50 plastid ribosomal proteins (PRP) and four ribosomal RNAs (rRNAs) are known while only few ribosome-associated proteins and assembly factors have identified.

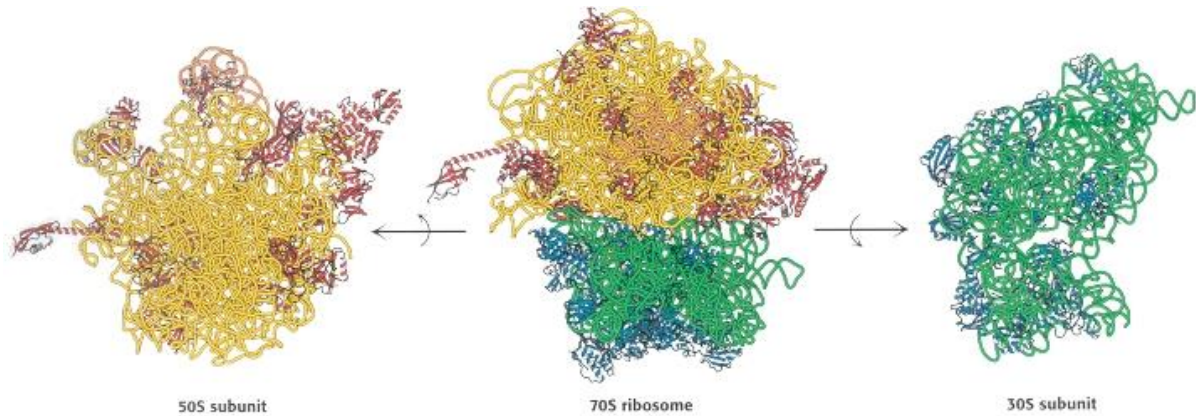


**Figure 1.1 Chloroplast ribosome subunits**

Graphic representation of the 50S large subunit and the 30S small subunit of plastidial ribosomes. Adapted from: [bifi.es/~jsancho/estructuramacromoleculas/](http://bifi.es/~jsancho/estructuramacromoleculas/)

Even if very distant in evolutionary terms, most plastid encoded genes are organized in operons and are transcribed as polycistronic transcriptional units. Moreover, the chloroplast rRNA is composed of 16S, 23S, 4.5S, and 5S rRNAs, and three tRNAs, thus maintaining the

same order as found in the bacterial operons (Strittmatter & Kossel 1984). The three tRNAs are located between the 30S and 50s subunits and their binding sites are called A (aminoacyl), P (peptidyl), and E (exit). The mRNA is associated to the 30S subunit and is bound to the A and P site to two tRNAs. The third tRNA is bound to the E site which is the last position of the tRNA before it exits the ribosome (Rogalski et al. 2008).

Although ribosome biogenesis involves a tight coordination with cell growth and proliferation and is regulated by a plethora of evolutionarily conserved assembly factors, including small nucleolar ribonucleoproteins (SnoRNPs), nucleases, RNA helicases, RNA chaperones, kinases, ATPases, and GTPases, only a few have been functionally characterized (Pendle et al. 2005; Weis et al. 2014). For many years, rRNAs have been considered to function mainly as a scaffold for ribosomal proteins to be properly positioned for protein synthesis. However, this view has changed considerably since the discovery of catalytically active rRNA granules. This observation led to the assumption that rRNAs play a major posttranscriptional role while associated proteins act in modulating ribosome activity (Anderson & Kedersha 2006). Currently, ribosome assembly and mRNA processing are thought to occur in association with nucleoids (Chotewutmontri & Barkan 2016). Plastid nucleoids are DNA-rich structures in proximity of thylakoids or envelope membranes. Proteomic studies of nucleoids revealed a diverse and heterogeneous amount of proteins. Therefore, the lack of a membrane surrounding the nucleoid might allow a very dynamic organization with transitory interactions. However in the nucleoid proteome, ribosomal subunits, RNA processing proteins and ribosome assembly factors are always abundant, suggesting that ribosome biogenesis takes place in close association with the nucleoids (Powikrowska et al. 2014; Melonek et al. 2016).

Interestingly, many of the chloroplast ribosomal proteins are larger than their bacterial orthologues, mainly due to short insertions or extensions at their N- or C-termini (Marín-Navarro et al. 2007) while only minor differences occur in the large and small subunit rRNAs. Regulation of translation, together with its initiation and elongation modulates gene expression in such a way that minor defects in ribosome assembly generally lead to a plethora of pleiotropic mutant phenotypes (Pesaresi 2006).

Furthermore, it is well known that defects in ribosomal subunits in chloroplasts lead to a different and often stronger phenotype than their prokaryotic counterpart in bacteria. For instance, several mutants for ribosomal proteins in bacteria lead to a mild phenotype, such as

a slower growth rate, whilst their plastidial orthologs lead to embryo lethality also with a complete loss of the ability to perform protein translation (Fleischmann et al. 2011). Reasons for such diversity probably reside in the higher specialization and complexity of eukaryotic organisms which need the transfer of proteins across compartments within the cell (Dinman 2009).

PRPL11, for example, is a subunit localized in the ribosome near to the GTPase binding site and the 23S rRNA (Ban et al. 1999). Plants with a reduced expression of PRPL11 show pale green true leaves and cotyledons together with a delay in plant growth and senescence (Pesaresi et al. 2001). This mutant lacks completely the subunit and its phenotype confirms a key role in ribosome stability. Similarly to their plant counterparts, bacterial mutants lacking PRPL11, show an increased generation time and decreased rates of in vitro protein synthesis (Stark & Cundliffe 1979).

A knockdown insertion in the PRPS17 gene results in a delayed leaf senescence (Woo et al. 2002), supposedly caused by a decreased translation rate similar to what happens after cold stress. This has been shown also in *C. elegans* where a reduced messenger RNA translation rate leads to an extension of life span (Arquier et al. 2005; Hansen et al. 2007; Syntichaki et al. 2007). Cold stress sensitivity found in PRPS17 mutants might be associated to a delay in ribosome assembly or defective retrograde signalling pathway involving cold responsive genes (Yu et al. 2012).

Cold sensitivity is a common ribosome-associated phenotype because the translation rate is reduced at low temperatures and hence it is further affected in plants which lack parts of the ribosomal machinery (Rogalski et al. 2008). Plants lacking another 30S subunit, PRPS5, show pale inner leaves and a retarded growth, typical phenotypes induced by plastidial ribosome defects especially under cold stress. On the other hand, lack of PRPS5 induces defects in the whole chloroplast biogenesis, this might modify expression levels of target nuclear genes through a retrograde plastid-to-nucleus signaling affecting nuclear gene expression (Zhang et al. 2016).

The largest ribosomal protein in *E. coli*, PRPS1, consists of a series of repetitions of the same domain called S1 domain which can be found across kingdoms and is involved in RNA metabolism (Salah et al. 2009). In *E. coli*, it allows the binding of the transcripts with the 30S small subunit (Sørensen et al. 1998). In Arabidopsis, knocking down PRPS1 resulted in pale and heat sensitive mutants likely due to a down regulation of the expression of heat

responsive genes suggesting the existence of a retrograde signaling pathway (Yu et al. 2012). Further studies demonstrated that PRPS1 interacts with GUN1 (GENOMES UNCOUPLED 1), one of the best known master regulators of retrograde signaling (Tadini et al. 2016). Interestingly, PRPS1 is the only ribosomal subunit which is found both in ribosome-bound and ribosome-free forms (Merendino et al. 2003; Delvillani et al. 2011). However, double mutants *gun1 prps1* showed no sensitivity to heat shock treatments, suggesting that GUN1 delivers the signal of delayed ribosome biogenesis to the nucleus thus regulating PRPS1 expression levels post-transcriptionally (Colombo et al. 2016; Tadini et al. 2016).

RBD1 is an RNA-binding protein found in chloroplast nucleoids involved in ribosome assembly through 23S rRNA processing. Cold stress experiments leads to a deficient greening in young leaves in mutant plants which is restored under normal growth temperature conditions (Wang et al. 2016c). Although it is not clear how low temperatures are affecting translation, it is hypothesized that the presence of an RNA-binding protein might prevent the formation of unstable RNA secondary structures which are frequent under low temperatures (Lorsch 2002; Jones & Inouye 1996).

RBF1 Ribosome Binding Factor 1 has a role in the biogenesis and coordination of the 30S subunit of the plastidial ribosome (Fristedt et al. 2014). Knocking down RBF1 impairs chloroplast development as a consequence of a reduced translation rate (Fristedt et al. 2014). Minor defects in the translation apparatus can yield a delay in greening in new leaves. Older leaves require low translational activity that allows them to reach wild type quantities of chlorophyll and photosynthesis efficiency (Fleischmann et al. 2011).

Transcriptomics studies led to the comparison of patterns and intensities of expression of all the mRNAs in different cells or tissues. Using a ‘guilt-by-association’ approach, it is possible to have an indication of protein function by comparing gene expression across tissues and developmental stages. Co-regulation of gene expression can be seen as a mechanism to provide the correct amount of proteins belonging to the same metabolic pathway at the right time in processes such as photosynthesis. 101 conditions have been clustered and then subdivided in 23 regulons based on their mRNA expression profiles (Richly et al. 2003; Biehl et al. 2005). On average, regulon 1 and 2 are very distant in localization compared to the rest of the dataset because they are mainly chloroplast targeted. While regulon 1 could be assigned to photosynthesis, most of the genes in regulon 2 encode subunits of the chloroplast ribosome or proteins presumably involved in the transcription or translation of plastid genes.

During this doctoral thesis it has been characterized CHLOROPLAST RIBOSOME ASSOCIATED (CRASS), a nuclear encoded gene belonging to regulon 2 encoding for a 16 kD protein characterized by the presence of a putative heavy-metal-associated domain (HMA) and a chloroplast transit peptide at the C-terminus. The HMA is a well conserved sequence of 20-40 amino acids found in a plethora of ATP dependent proteins, from Archea to mammals, trafficking or detoxifying heavy metals. The binding site for metals resides within the HMA domain and consists of two cysteins. These two cysteins, are absent in CRASS. Thus the protein might have lost the metal coordination function during evolution or evolved a different role specific for plants. In fact, CRASS is only present in Embryophytae and no orthologues can be found in bacteria or animals.

## 1.2 A hypothetical link between leaf variegation and a DNA-J like protein.

Correct chloroplast biogenesis is essential for plant fitness. Mutants affected in chloroplast biogenesis often display severe pale or albino phenotypes that can lead to plant death. However, in some cases these mutants display a phenotype called “variegated phenotype”, i.e. leaves are characterized by white and green sectors distributed without a predictable pattern. In some plant species these sectors can also overlap yielding to different shades of green. The common characteristic is that chloroplasts develop normally and are fully functional in the green areas, while chlorophyll synthesis is aborted in the white areas (Aluru et al. 2006; Putarjunan et al. 2013)

Several hypothesis exist to explain this phenomenon at the molecular level, but most lack a precise molecular explanation.

The best studied type of leaf variegation occurs in *var1* and *var2* mutants which are lacking FTSH5 and FTSH2 respectively, two proteins belonging to the FTSH (filamentation temperature sensitive H) protease family. FTSH heterocomplexes have several functions ranging from chaperone activity to ATPases and are crucial for photodamaged D1 degradation (Lu 2016). At least two minor isoforms are present in these complexes, FTSH1 and FTSH8, whose mutants do not show obvious phenotypes (Sakamoto 2003; Zaltsman et al. 2005). Their expression levels instead determine the functionality of the complex when one of the main isoforms is lacking, indicating a high (but not complete) level of redundancy among the 12 FTSH gene family members. In fact, the hypothesis from Yu et al. (2004) for the *var1* and *var2* variegated phenotype is based on a “molecular threshold”, implying that there is a

minimum amount of FTSH complexes needed in the thylakoid membrane to efficiently carry out the repair of degraded photosystem II reaction center protein D1. Below a certain level, the repair rate of damaged D1 is too low, inducing photooxidation and non photosynthetic white chloroplasts. Interestingly, both types of chloroplasts are viable and capable of division giving rise to white or green groups of cells in distinct sectors of the leaf. This model assumes that the expression of certain FTSHs is rather “patchy”, otherwise the sectors would present a clearly defined pattern based on the initial concentration of specific FtsHs in the meristem. The hypothesis has been further strengthened by the consideration that several suppressors of variegated phenotype act by slowing down protein biosynthesis in the plastid which affects D1 turnover and the amounts of reactive oxygen species (ROS) (Miura et al. 2007; Kato et al. 2009).

Cotyledons are usually not affected by this phenotype, because if seed quality is normal, there is sufficient energy stored for a regular chloroplast biogenesis (Stoynova-Bakalova et al. 2004). An exception is a class of mutants called SNOWY COTYLEDONS (SCO) which are exclusively affected at their cotyledon stage but display unaffected green true leaves that carry out WT levels of photosynthesis (Albrecht et al. 2006).

The gene SNOWY COTYLEDON 2 (SCO2)/CYO1 encodes a DNAJ-related protein with a conserved zinc-finger domain, and is required for normal accumulation of the photosynthetic machinery in cotyledons (Shimada et al. 2007; Albrecht et al. 2008). Other chloroplastic members of the DNAJE clade (Pulido & Leister 2018) have been shown to exhibit chaperone/assembly activity even when lacking the J-domain required for HSP70 binding. For instance, PSA2 is required for proper photosystem I (PSI) assembly (Fristedt et al. 2014), LQY1 for photosystem II (PSII) repair after stress (Lu et al. 2011), and OR for accumulation of its substrate phytoene synthase in carotenoid biosynthesis (Zhou et al. 2015). Similarly, SCO2/CYO1 is required for the accumulation of the light harvesting chlorophyll-binding protein LHCB1 (Tanz et al. 2012). However, SCO2/CYO1 has been proposed to facilitate targeting of LHCB1 to the thylakoid membrane rather than having a function in the assembly of the photosynthetic complexes (Tanz et al. 2012). In addition, SCO2/CYO1 was found to interact with several PSI and PSII subunits in yeast two-hybrid experiments (Muranaka et al. 2012).

PSII assembly has yet to be fully unravelled. Its main components and steps involved are known but we are far from fully deciphering the construction of such a complicated

machinery. Several approaches have been tried to get closer to a full picture of all the components involved in the photosystems and in their assembly. Classical genetics yielded and continue to provide the characterization of new components by knocking out genes and assessing the resulting mutant phenotypes. Functionality of assembly factors is different across species and the importance of a specific component is sometimes overrated when its presence is demonstrated in a single species. Since more and more plants or algae are fully sequenced and used as model organism, the accuracy of the information is higher and the pleiotropic effects caused by the improper assembly of a crucial machinery are diminished by using different plant backgrounds with different physiology and assembly quality control systems. Another approach is a bottom up way, in which a synthetic scaffold is used to generate an artificial photosynthetic organism with functional photosystems. Missing or undiscovered genes can be provided through a cDNA library. Technical difficulties arise with the increase of the complexity of the host organism which has to be engineered, such as cyanobacteria or plants. *E. coli* instead can carry out homologous recombination of large synthetically designed DNA fragments potentially providing a scaffold more efficient than photosynthetic organisms. (Rühle & Leister 2016)

Since its mechanism of action is well known, the use of lincomycin (LIN) at sub-lethal levels is often used to study the effects of a reduced protein translation. LIN is a lincosamide antibiotic which inhibits the peptidyl transferase reaction by competing for several binding sites in common with those of the peptidyl transferase substrates (Tenson et al. 2003). This crucial reaction carried out by ribosomal RNA in the major subunit of the ribosome binds adjacent amino acids thus constituting the core of protein biosynthesis. When there is a minor defect in ribosome assembly or in chloroplast biogenesis the LIN-induced reduction of proteins leads to an evident pale or variegated phenotype (Llamas et al. 2017).

In this work, we report that the mutations in *SCO2* in *Lotus japonicus*, besides paler cotyledons, result in variegated true leaves. Similarly, the absence of *SCO2* in *A. thaliana* affects true leaf development, specially under short-day conditions. In both plant species, we demonstrate a role for *SCO2* in the assembly or repair of photosystem complexes. Furthermore, an *A. thaliana* double mutant in which *atsco2* is combined with a mutation in *SUPPRESSOR OF VARIATION2 (svr2/atclpr1)* shows an unexpected additive variegated phenotype. Therefore, we propose a mechanistic model for *SCO2*-dependent variegation, which is insensitive to previously described suppressors of variegation.

## 2. Materials and Methods

### 2.1 Plant material, propagation and growth conditions

The *Arabidopsis thaliana crass-1* (line 84-776) and *crass-2* (line: 72-131) mutants in Col-0 background have been obtained from the Koncz (Max Planck Institut, Köln) collection (Ríos et al. 2002). To generate the *oeCRASS-YFP* overexpressing lines, the coding sequence of CRASS (At5G14910) was PCR-amplified using a gene specific primer pair (Supplemental Table 6.3) and the gel-purified PCR product was used for BP and LR Clonase reactions (Invitrogen). The resulting product was cloned in-frame into the Gateway binary vector pGWB641 containing a 35S promoter and YFP (Invitrogen). *Agrobacterium tumefaciens* mediated transformation has been performed by floral dipping densely sown plants in a solution of transformed *Agrobacterium tumefaciens* (strain GV3101). Transgenic plants were selected on the basis of their resistance to BASTA, propagated and genotyped. Mutants *prpl11-1* and *prps17-1* have been described before (Pesaresi et al. 2001; Tadini et al. 2016). After stratification for 3 days in darkness at 4 °C, wild-type and mutant plants were grown on soil or MS agar plates with 1% sucrose. Plants were grown under controlled conditions in growth chambers at 22°C in long day (LD, 16 h light/8 h dark, 100  $\mu\text{mol photons m}^2 \text{s}^{-1}$ ) or short day (SD, 8 h light/16 h dark, 100  $\mu\text{mol photons m}^2 \text{s}^{-1}$ ). 21 days after germination, plants were harvested for weight measurement or in liquid nitrogen for protein extraction. For co-immunoprecipitation experiments, wild-type (WT) and *oeCRASS* lines were grown on soil in a 12 h light/12 h dark cycle (100  $\mu\text{mol photons m}^2 \text{s}^{-1}$ ) for two weeks. For cold stress experiments in soil, adult plants were grown on soil in long day (16 h light / 8 h dark) for two weeks at 22°C and moved to a 4 °C chamber (Percival Scientific LED 41HL2) equipped with white and red LEDs set at 18% intensity (equivalent to 100  $\mu\text{mol photons m}^2 \text{s}^{-1}$ ) for 5 weeks. Alternatively, plants were germinated and grown on plates for six weeks in the same chamber and conditions. Seedlings were otherwise grown for 10 days in plates supplemented with the indicated concentrations of lincomycin (LIN).

*Lotus japonicus sco2* mutants in the Gifu genetic background originate from the LORE1 endogenous retrotransposon mutant population ([www.lotus.au.dk](http://www.lotus.au.dk)) (Małolepszy et al. 2016). Three independent lines with a similar variegated phenotype identified as *ljSCO2-1* (30096086), *ljSCO2-2* (30099994), and *ljSCO2-3* (30006602) were found to disrupt the coding region of the LjSCO2 gene (Lj3g3v0537380.1). The ecotype Gifu B-129 served as the WT

control. Lotus seeds were surface sterilized (Handberg & Stougaard 1992) and grown on soil or solid Murashige and Skoog (MS) medium. For greening experiments, plants were exposed to light ( $100 \mu\text{mol photons m}^{-2} \text{s}^{-1}$ ) for 4 h, then incubated in the dark at 22 °C for 8 days. Pigments were extracted from whole seedlings immediately, and after 1 and 8 days of growth under long-day conditions ( $100 \mu\text{mol photons m}^{-2} \text{s}^{-1}$ ). The *A. thaliana sco2* mutant (NASC: N68145) in the Landsberg erecta background was initially isolated in an ethyl methanesulfonate screen for plants with pale cotyledons and green true leaves (Albrecht et al. 2008). The *atclpr1* mutant (SALK\_088407) in the Columbia-0 background has been described previously (Koussevitzky et al. 2007; Pulido et al. 2016). After stratification for 3 days at 4 °C, WT and mutant plants were grown on soil or MS agar plates with 1% sucrose. Both Arabidopsis and Lotus plants were grown under controlled conditions in growth chambers at 22 °C in long-day (16 h light/8 h dark,  $100 \mu\text{mol photons m}^{-2} \text{s}^{-1}$ ), short-day (8 h Light/16 h dark,  $100 \mu\text{mol photons m}^{-2} \text{s}^{-1}$ ), continuous light ( $100 \mu\text{mol photons m}^{-2} \text{s}^{-1}$ ), or high light (16 h light/8 h dark,  $400 \mu\text{mol photons m}^{-2} \text{s}^{-1}$ ). When specified, Arabidopsis and Lotus were grown on plates supplemented with the indicated concentrations of chloramphenicol or lincomycin.

## 2.2 Nucleic acid analysis

Arabidopsis genomic DNA was isolated by a phenol and chloroform free method (Edwards et al. 1991). The *crass-1* and *crass-2* T-DNA insertion-junction sites were recovered by PCR using combinations of insertion- and gene-specific primers, and then sequenced. Total RNA was isolated using TRIzol reagent (Invitrogen). Briefly, 1 mL of TRIzol was added to pulverized tissue in liquid nitrogen (50-100 mg). The resuspended sample was centrifuged at 12,000g for 10 min at 4°C. Supernatant was extracted with 200  $\mu\text{L}$  of chloroform mixing vigorously. After 2 min at room temperature, the sample was centrifuged at 12,000 g for 15 min at 4°C. 500  $\mu\text{L}$  of isopropanol was added to the upper aqueous phase and incubated at room temperature for 10 min. Subsequent centrifugation at 12,000 g for 10 min at 4°C precipitate the RNA pellet, that was washed with 1 mL of 75% ethanol. After centrifugation at 7,500 g for 5 min at 4°C, the pellet was dried under hood for 5 min and resuspended in 20  $\mu\text{L}$  of DEPC water. Total RNA was treated with 2 units of DNase I (New England Biolabs) in a final volume of 100  $\mu\text{L}$  at 37°C for 10 min. RNA sample was supplemented with 1  $\mu\text{L}$  of 0.5 M EDTA, heat inactivated at 75°C for 10 min, and precipitated with 10  $\mu\text{L}$  of sodium acetate (pH 5.0) and 200  $\mu\text{L}$  of 100% ethanol over night. Then, RNA was again precipitated (12,000 g

for 10 min at 4°C), washed with 75% ethanol (7,500 g for 5 min at 4°C), dried and resuspended in 20 µL of DEPC water. One microgram of RNA was reverse-transcribed using iScript cDNA Synthesis Kit (Bio-Rad). Quantitative PCR experiments were performed using 7.5 µL of iQ SYBR Green Supermix solution (Bio-Rad), cDNA derived from 15 ng of input RNA, and 0.5 µM of sense and antisense primers in a final volume of 15 µL. A standard thermal profile (95°C for 5 min, 40 cycles of 95°C for 10 s, 55°C for 30 s, and 72°C for 20 s) was used in an IQ5 real-time PCR detection system (Bio-Rad).

The *atclpr1* T-DNA insertion-junction sites were recovered by PCR using combinations of insertion- and gene specific primers (Supplemental Table 6.3) and then sequenced. The whole *AtSCO2* gene was amplified and the band sequenced to detect the point mutation (Supplemental Figure 6.17). *L. japonicus* DNA extraction and library preparation was performed as described earlier, and the sequencing output was analyzed using FSTpoolit v.0.33 software (Urbański et al. 2012). Total RNA was isolated from seedlings and leaf samples frozen in liquid nitrogen using TRIzol reagent (Invitrogen) according to the manufacturer's protocol. For each RNA sample, a pool of at least three individuals was used. One microgram of RNA was primed with oligo(dT) and reverse transcribed into complementary DNA using Superscript III reverse transcriptase (Invitrogen). Relative levels of *LjSCO2* transcripts in WT cotyledons and true leaves (from 25-day-old WT and mutant Lotus plants) were determined by quantitative real-time PCR (for primer sequences see Supplemental Table 6.3), which was performed with iQ SYBR Green Supermix using an IQ5 multicolor real-time PCR detection system (Bio-Rad) following a standard thermal profile (95 °C for 5 min, 40 cycles of 95 °C for 10 s, 55 °C for 30 s, and 72 °C for 20 s). The relative level of each transcript was referred to the level of the corresponding UBIQUITIN transcript. Analysis of the threshold cycles (Ct) with the iQ5 software (Bio-Rad) was performed for determining relative expression.

### 2.3 Fluorescence measurements

In vivo room temperature chlorophyll a fluorescence of leaves of 3-week-old plants and 6-weeks-old plants grown in long day and short day, respectively, were analyzed using an Imaging PAM chlorophyll fluorometer equipped with the computer-operated PAM control unit IMAG-MAXI (Walz) as described previously (Zagari et al. 2017). After a minimum of 30 min of dark adaptation, the minimal fluorescence ( $F_0$ ) was measured. For cold tolerance experiments, dark adaptation has been carried out at 4°C. To determine the maximum

fluorescence ( $F_m$ ), a pulse (0.8 sec) of saturating white light ( $5000 \mu\text{mol photons m}^2 \text{s}^{-1}$ ) was applied. The ratio  $(F_m - F_0)/F_m$  was calculated as  $F_v/F_m$ , the maximum quantum yield of PSII. False-color images representing  $F_v/F_m$  levels in wild-type (WT) and mutant leaves were produced by the Imaging PAM and representative pictures were selected.

*In vivo* room temperature chlorophyll a fluorescence of leaves of 8-week-old Lotus plants was measured using a Dual-PAM 100 (Walz) as described previously (Pesaresi et al. 2009). After a minimum of 30 min of dark adaptation, the minimal fluorescence ( $F_0$ ) was measured. To determine the maximum fluorescence ( $F_m$ ), a pulse (0.8 s) of saturating white light ( $5000 \mu\text{mol photons m}^2 \text{s}^{-1}$ ) was applied. The ratio  $(F_m - F_0)/F_m$  was calculated as  $F_v/F_m$ , the maximum quantum yield of PSII. The electron transport rate through PSII (ETR II) was monitored at increasing light intensities and plotted as a light response curve.

For NPQ induction, plants were dark-adapted overnight and slow kinetics were determined with Dual PAM by applying red actinic light ( $830 \mu\text{mol photons m}^2 \text{s}^{-1}$ ) for 30 min, followed by a succession of white light pulses ( $8000 \mu\text{mol photons m}^2 \text{s}^{-1}$ , duration 600 ms) administered at 60 seconds intervals. NPQ was calculated as  $(F_m F_{m0})/F_{m0}$  and FII as  $(F_m F_s)/F_m$ . False-color images representing  $F_v/F_m$  levels in WT and mutant leaves were produced using an Imaging PAM chlorophyll fluorometer equipped with the computer-operated PAM control unit IMAG-MAXI (Walz). State transitions were measured by pulse-amplitude modulation fluorometry (PAM) as described previously (Pribil et al. 2010). Five plants of each genotype growing under long-day conditions were dark-adapted and analyzed using the Dual-PAM (Walz). Pulses of red light ( $5000 \mu\text{mol photons m}^2 \text{s}^{-1}$ , 0.5 s) were used to determine the maximum fluorescence. After illumination with red light ( $35 \mu\text{mol photons m}^2 \text{s}^{-1}$ , 15 min), state 1 was induced by adding far-red light (maximal light intensity corresponding to level 20 in the Dual-PAM setting, 15 min) and  $F_{M1}$  was determined. Next, state 2 was induced by switching off the far-red light (only red light, 15 min) and  $F_{M2}$  was measured. qT was calculated as  $(F_{M1} F_{M2})/F_{M1}$  (Ruban & Johnson 2009).

## 2.4 Pigments

Chlorophyll quantification was performed as described previously (Lichtenthaler & Wellburn 1983). Briefly, pigments were extracted by shaking 50 mg (fresh weight) of pulverized samples with 1 ml of 80% (v/v) ice-cold acetone in the dark at 4 °C for 30 min. After centrifugation (10,000 g, 10 min, 4 °C),  $A_{663}$ ,  $A_{647}$  and  $A_{470}$  were recorded with a

spectrophotometer (Ultrospec3100, Amersham Biosciences) and pigment levels were calculated according to the following equation: chlorophyll a =  $12.25 A_{663} - 2.79 A_{647}$ ; chlorophyll b =  $21.50 A_{647} - 5.10 A_{663}$ ; chlorophyll tot =  $7.15 A_{663} + 18.71 A_{647}$ ; carotenoids =  $(1000 A_{470} - 1.82 Cl_a - 85.02 Cl_b)/198$ .

## 2.5 Metabolite analysis

Standard chlorophyll determinations were performed as described previously (Lichtenthaler & Wellburn 1983). Alternatively, HPLC analysis of chlorophylls, carotenoids, and tocopherols was performed as described by Rodriguez-Concepcion (2004) using 4 mg of lyophilized 45-day-old Lotus samples and an Agilent 1200 series HPLC system (Agilent Technologies, <http://www.agilent.com>). Canthaxanthin was used as an internal standard for normalization, and appropriate carotenoid and tocopherol standards were used for quantification.

## 2.6 Phylogenetic analysis

CRASS orthologous proteins were identified using BLAST (<http://blast.ncbi.nlm.nih.gov>). Sequences were aligned with MUSCLE ([www.ebi.ac.uk/Tools/msa/muscle](http://www.ebi.ac.uk/Tools/msa/muscle)) and BioEdit Sequence Alignment Editor version 7.0.5. Phylogenetic trees rooted at midpoint were constructed using the neighbour-joining method in MEGA6 ([megasoftware.net](http://megasoftware.net)). The evolutionary distances were computed using the Poisson correction method, and the bootstrap test was performed with 2000 replications.

For sequence comparisons, orthologs of AtSCO2 (AT3G19220) were identified by BLAST. Sequences were aligned with MUSCLE ([www.ebi.ac.uk/tools/msa/muscle](http://www.ebi.ac.uk/tools/msa/muscle)), and a phylogenetic tree rooted at midpoint was constructed using the neighbour-joining method in MEGA6 ([megasoftware.net](http://megasoftware.net)). The RNA evolutionary distances were computed using the Poisson correction method, and the bootstrap test was performed with 2000 replications. Data used to create Supplemental Figure 6.9 can be retrieved under the following accession numbers: *A. thaliana* (AtSCO2, At3g19220; LQY1, AT1G75690; TSIP1, AT2G24860; BSD2, AT3G47650), *Brassica napus* (CDX92309), *Vitis vinifera* (XP\_003631671), *Nicotiana sylvestris* (XP\_009772536; XP\_009761846), *Theobroma cacao* (XP\_007042421) *Solanum tuberosum* (XP\_006346429), *Populus trichocarpa* (XP\_002313849), *L. japonicus* (Lj3g3v0537380), *Cucumis melo* (XP\_008456126), *Cucumis sativus* (XP\_004140700), *Solanum lycopersicum* (XP\_010315236), *Malus domestica* (XP\_017189504), *Glycine max*

(NP\_001242534; XP\_003518841), *Zea mays* (NP\_001144163), *Oryza sativa* (NP\_001063376), *Hordeum vulgare* (BAJ85952), and *Phaseolus vulgaris* (XP\_007156517).

## 2.7 Protein isolation and immunoblot analysis

Protein analyses were performed as described (Pulido et al. 2013). Briefly, total plant protein extracts were obtained from 50 mg of 21-day-old fresh tissue by grinding samples in liquid nitrogen. The powder was resuspended in 100  $\mu$ L of ice-cold TKMES homogenization buffer (100 mM Tricine-KOH, pH 7.5, 10 mM KCl, 1 mM MgCl<sub>2</sub>, 1 mM EDTA, and 10% [w/v] sucrose) supplemented with 0.2% (v/v) Triton X-100, 1 mM DTT, and 20  $\mu$ L/mL protease inhibitor cocktail (Sigma-Aldrich). The resuspended sample was centrifuged at 2,300 g for 10 min at 4 °C, and the supernatant recovered for a second step of centrifugation. Supernatant protein concentration was determined using the Bio-Rad protein assay. After SDS-PAGE, the proteins were electrotransferred to Hybond-P polyvinylidene difluoride membranes (Amersham). After protein transfer was complete, membranes were incubated overnight at 4 °C with the respective specific primary antibody (Agrisera) diluted 1:1000 for ClpC, LHCB1, PsaB, PsaL, PsbO, Cpn60, PsbQ, SVR4, SVR4L, and FNR; diluted 1:5000 for YFP, PRPS1, PRPS5, PRPL2, PRPL11, ClpC, ClpB3, CPN60-1, PSBC, PSBD, PSBR, PSAL, Cytf, Cytb6, actin, LHCB2, LHCB4 and 1:10,000 for HSP70, LHCA1, LHCB2, RBCL, and ATPB. Incubation with the horseradish peroxidase-conjugated secondary antibody (diluted 1:10,000) was performed for 1 h at room temperature. Detection of immunoreactive bands was performed using the ECL Plus reagent (Amersham). Chemiluminescent signals were visualized using a ChemiDoc MP analyzer (Bio-Rad).

## 2.8 Thylakoid Isolation and SDS-PAGE

Four-week-old *A. thaliana* plants (grown under short-day conditions, 100–120  $\mu$ mol photons m<sup>2</sup> s<sup>-1</sup>, 22 °C), or *L. japonicus* plants (grown under long-day conditions, 100–120  $\mu$ mol photons m<sup>2</sup> s<sup>-1</sup>, 22 °C) were used. Thylakoids were isolated in the dark, following a previously described protocol (Järvi et al., 2011). The grinding buffer contained 50 mM HEPES-KOH (pH 7.5), 330 mM sorbitol, 2 mM EDTA, 1 mM MgCl<sub>2</sub>, 5 mM ascorbate, 0.05% BSA, and 10 mM sodium fluoride; shock buffer contained 50 mM HEPES-KOH (pH 7.5), 5 mM sorbitol, and 5 mM MgCl<sub>2</sub>; and storage buffer contained 50 mM HEPES-KOH (pH 7.5), 100 mM sorbitol, and 10 mM MgCl<sub>2</sub>. Total chlorophyll in the thylakoid fractions was determined after

extraction with 80% acetone as described above. For SDS–PAGE, samples containing 0.5, 1, 2, and 3 mg of chlorophyll were resuspended in SDS–PAGE loading buffer supplemented with 200 mM DTT, and boiled at 95 °C for 5 min. The samples were then centrifuged at 21000 *g* for 2 min and loaded in SDS–PAGE gels. For Large-Pore Blue-Native PAGE (lpBN-PAGE), 12 mg of chlorophyll from the thylakoid membranes were incubated with 1% digitonin or 1%  $\beta$ -DM according to Järvi et al. (2011) and the solubilized fraction was loaded on a native gradient gel (3.5%–12.5% [w/v], acrylamide/bisacrylamide ratio 32:1) topped with a 3% (w/v) stacking gel (ratio 1:4). After electrophoresis, the native gel was treated with Laemmli buffer (138 mM Tris–HCl [pH 6.8], 6 M urea, 22.2% [v/v] glycerol, 4.3% [w/v] SDS, and 200 mM DTT), and the separated protein complexes were transferred to a polyvinylidene fluoride membrane using the Turbo Transfer system (Bio-Rad).

## 2.9 Low-Temperature (77-K) Fluorescence Measurements

The accumulation of PSI and PSII was evaluated by using the low-temperature (77-K) fluorescence emission spectra of intact leaves frozen in liquid nitrogen. The fluorescence emission spectra were recorded *in vivo* from 600 to 800 nm using a spectrofluorometer (Photon Technology International, Lawrenceville, NJ) and an excitation wavelength of 435 nm. The peak level of the PSI fluorescence at 730 nm was compared with the fluorescence maximum of PSII at 680 nm.

## 2.10 Immunoprecipitation analysis

For co-immunoprecipitation, total proteins were extracted with RIPA buffer (50 mM Tris HCl, 150 mM NaCl, 1% NP-40, 0.5% sodium deoxycholate, 0.1% SDS) with complete protease inhibitor (Roche). Magnetic separation was performed using  $\mu$ MACS GFP beads (Macs Miltenyi Biotec) according to manufacturer's protocol. The eluates were then used for RNA extraction and sequencing or run on a SDS-PAGE gel (12% polyacrylamide) and stained with colloidal coomassie for mass spectrometry analyses.

## 2.11 Size exclusion chromatography (SEC) and sucrose gradient

Chloroplasts were isolated from 2-week-old plants as described previously (Stoppel et al. 2012). Chloroplasts were lysed in extraction buffer (10 mM HEPES-KOH, pH 8.0, 5 mM

MgCl<sub>2</sub>, and protease inhibitor cocktail (Roche, Basel, Switzerland) by passing the suspension 20 times through a 0.5 mm needle. Membranes were pelleted by centrifugation at 45,000 g for 30 min at 4 °C. SEC of WT stroma extracts was performed as described recently (Meurer et al. 2017) with minor changes. Three milligrams of stroma were used. Extracts were centrifuged for 10 min at 4 °C / 16000 g after treatment with 300 µg RNase A to pellet precipitates prior SEC.

### 2.12 In vivo protein labeling

In vivo labeling of newly synthesized chloroplast proteins with [<sup>35</sup>S]methionine was essentially performed as described recently (Meurer et al. 2017) with some modifications. Plants were grown on sucrose-containing MS plates at 4 °C under long-day conditions (16 h light/8 h dark, 100 µmol photons m<sup>2</sup> s<sup>-1</sup>) for six weeks and subsequently transferred to 22 °C under same long-day conditions for 3 days. Labeling was performed for 15 min at ambient light. Soluble and insoluble fractions were prepared as described previously (Torabi et al. 2014) and proteins were loaded onto 12% SDS PAGE gels according to the calculated total counts (100% corresponds to 100,000 cpm for insoluble and 1,000,000 for soluble proteins, respectively). Gels were stained for 1 h with Roti-Blue quick (Carl Roth, Karlsruhe, Germany) and dried.

### 2.13 Polysome analyses

Polysome loading analyses were carried out as described previously (Barkan, 1993). The *psaA* probe was amplified with following primers Fw: AAAGTGTGGAAGCCTAGAAATATACA; Rev: ACTCACATTGGACCTAGTGC. For *rbcL*, an 80-mer oligonucleotide was used as a probe. Labeling was performed as described (Manavski et al. 2015).

### 2.14 Mass spectrometry

The in-gel tryptic digestion was done according to (Shevchenko et al. 2007). The peptides were resolubilized in 2.5% Acetonitrile and 0.5% Trifluoroacetic acid. They were desalted in the nano RSLC Ultimate 3000 system from Dionex via a Acclaim PepMap C18 500 mm length particle size 3 µm nano viper fingertight and separated with a Acclaim PepMap C18

150 mm length particle size 2  $\mu\text{m}$  using the following gradient linear gradient with the following solvents: solvent A: 0.1% Formic acid in water; solvent B: 0.1% Formic acid in 90%, acetonitrile and 10% water. The gradient went from 2% B to 45% B in 30 min. For eluting and washing the column the C was increased to 90% in one minute and hold for 5 min. A 15 min re-equilibration step followed. The connected ion trap AmZon ETD instrument (Bruker) measured the peptides with the factory proteomics AutoMS/MS CID method (Capillary voltage 1300, temperature 180 °C, mode Ultrascan for parental masses, Xtreme Scan for fragmented masses with Smart fragmentation on, top4 fragmentation, dynamic exclusion 0.2 min). 5,000 compound spectra with a TIC intensity higher than 10,000 were converted by the DataAnalysis software (Bruker) to mgf files and searched against the TAIR10 peptide database including contaminants with the Mascot Daemon 2.5.1. An error of 0.5 Da was allowed for the parental mass and the fragmented masses. Carbamidomethylation was set as a fixed modification and oxidation as a variable one. Peptides were taken as identified with a Score above 21. Proteins were taken as identified with two peptides for one protein or one reproducible peptide between the experiments with a Score above 60. As significance threshold ( $P < 0.01$ ) was used.

#### 2.15 RNA gel blot analysis and polysome loading

RNA extraction, electrophoresis, transfer, and probe labeling were performed as described recently (Manavski et al. 2015). Blots were stripped and reprobed. For primer information see supplemental Table 6.3. rRNA quantification was performed on Nanodrop (Thermo Scientific) using 1  $\mu\text{g}$  of total RNA. Polysome loading experiments were performed as described (Barkan 1993).

#### 2.16 RNA sequencing, mapping and slot-blot analysis

Total RNA was extracted as previously described from 3-weeks-old plants grown in long day conditions. Samples from two independent experiments using *oeCRASS#1* line were subjected to strand-specific transcriptome sequencing without mRNA enrichment (without polyT oligos) and without rRNA depletion (Beijing Genomics Institute). The RNA was fragmented to 160-180 nt, reverse transcribed, dATP was added, the fragments were size selected by gel electrophoresis and the selected fragments were PCR amplified. The sequencing was done using a paired-end 100 nt protocol on a Illumina HiSeq<sup>TM</sup> 4000. Paired-end reads were

mapped to the TAIR10 Arabidopsis genome (version 31) using STAR aligner 2.5.0 (Dobin et al., 2013) with the following options: -alignIntronMax 5000 - outFilterMismatchNmax 4 - outSAMmultNmax 1 - outMultimapperOrder Random. Next, the bam file was loaded into R and reads were counted with the summarizeOverlaps function from GenomicAlignments package (Lawrence et al., 2013). For further analysis, genes with at least 10 mapped reads were used. FPKM values (fragments per kilobase per million mapped fragments) were calculated using fpkm function from DEseq2 package (Love et al. 2014). Slot-blot experiments were performed as recently described (Manavski et al. 2015). Primers for PCR probes are listed in Supplemental Table 6.3.

### 2.17 Yeast two-hybrid analysis

The coding sequence of CRASS, PRPS5 and PRPS8 excluding the transit peptide were cloned into pGKBT7 (CRASS) and pGADT7 (PRPS5, PRPS8) vectors (Clontech). Interactions in yeast were analysed as previously described (DalCorso et al. 2008)

### 2.18 In vivo translation assay

The *in vivo* translation assay was performed as previously described (Paieri et al. 2017). In brief, to block cytosolic translation, ten seedlings growing for 6 weeks at 4 °C and recovered for 3 days at 22 °C were incubated in the presence of 20 µg/mL cycloheximide, 1 mM K<sub>2</sub>HP0<sub>4</sub>/KH<sub>2</sub>PO<sub>4</sub> (pH 6.3), and 0.1% (w/v) Tween-20. After labeled [<sup>35</sup>S]-methionine was supplemented (0.1 mCi mL<sup>-1</sup>), vacuum was applied under low light (20 µmol photons m<sup>2</sup> s<sup>-1</sup>) for 15 min. After protein extraction and SDS-PAGE protein separation, signals were detected using a PhosphoImager (GE Healthcare).

### 2.19 Confocal microscopy

Transgenic 7-day-old plants were analyzed for YFP fluorescence by confocal laser scanning microscopy using a Leica TCS SP2 (Leica, www.leica-microsystems.com). Samples were excited at 514 nm and fluorescence detected in the range 550-600 for YFP and 600-700 nm for Chl emission.

## 2.20 Accession numbers

Data used to create Figure 3.1B can be retrieved under the following accession numbers: AT5G14910 CRASS *Arabidopsis thaliana*, XP\_006286392 *Capsella rubella*, XP\_002871636 *Arabidopsis lyrata*, XP\_010453619 *Camelina sativa*, CDX85578 *Brassica napus*, XP\_009131426 *Brassica rapa*, XP\_008341487 *Malus domestica*, KDO72385 *Citrus sinensis*, XP\_002275276 *Vitis vinifera*, KNA24776 *Spinacia oleracea*, XP\_008443474 *Cucumis melo*, XP\_004147445 *Cucumis sativus*, XP\_006338529 *Solanum tuberosum*, KMZ72790 *Zostera marina*, AFK34041 *Lotus japonicus*, XP\_004232276 *Solanum lycopersicum*, XP\_009786795 *Nicotiana sylvestris*, KRH18591 *Glycine max*, XP\_013450869 *Medicago truncatula*, EEE63302 *Oryza sativa*, NP\_001143959 *Zea mays*, BAJ98599 *Hordeum vulgare*, ABK23791 *Picea sitchensis*, XP\_001772064 *Physcomitrella patens*, XP\_002968622 *Selaginella moellendorffii*, XP\_001758023 *Physcomitrella patens*, XP\_001763071 *Physcomitrella patens*. Data used to create the sequence alignment of CRASS with heavy metal associated (HMA) proteins (Supplemental Figure 6.2) can be retrieved under the following accession numbers: AT5G14910 CRASS *Arabidopsis thaliana*, XP\_002275276 *Vitis vinifera*, XP\_002968622 *Selaginella moellendorffii*, WP\_003720172 *Listeria ivanovii*, WP\_014093194 *Listeria ivanovii*, WP\_051872593 *Chryseobacterium haifense*, WP\_059344219 *Elizabethkingia genomosp. 2*, WP\_007292244 *Delta proteobacterium MLMS-1*, ANC24349 *Streptococcus pyogenes*.

---

### 3. Results CRASS

#### 3.1 CRASS is coregulated with plastidial ribosomal proteins

With the help of transcriptomics, it is possible to investigate protein expression in different tissues and growth conditions for thousands of genes. When a gene is expressed in the same conditions, tissues and amounts, it is likely that this co-expression has a functional reason. For example, genes coding for the photosynthetic apparatus tend to be highly coexpressed, because the availability of correct amounts of different components is crucial for an efficient assembly of the photosystem. In previous guilt-by-association studies, 101 conditions have been selected to modulate gene expression (Biehl et al. 2005). The resulting 23 coexpression groups were named regulons and provided useful hints for identifying new proteins involved in different pathways. Interestingly, regulon 2 contains mostly ribosomal proteins or components of the RNA metabolism. Among them our interest was drawn to a protein of unknown function, *AT5G14910*. In order to create a coexpression network, we selected all the known plastid ribosomal proteins encoded in the nucleus as bait and run a condition independent coexpression analysis. We found genes involved in RNA metabolism such as the 31-kDa RNA binding protein CP31A (Tillich et al. 2009), the ribosome recycling factor (RRF) (Wang et al. 2010) and several with unknown function. Among these *AT5G14910* was highly coexpressed with ribosomal proteins and at the centre of this wide network (Supplemental Figure 6.1). Furthermore, selecting *AT5G14910* as bait almost all its predicted interaction partners are also chloroplastic ribosomal subunits (Figure 3.1A). Thus we renamed *AT5G14910* as CRASS (CHLOROPLAST RIBOSOME ASSOCIATED).

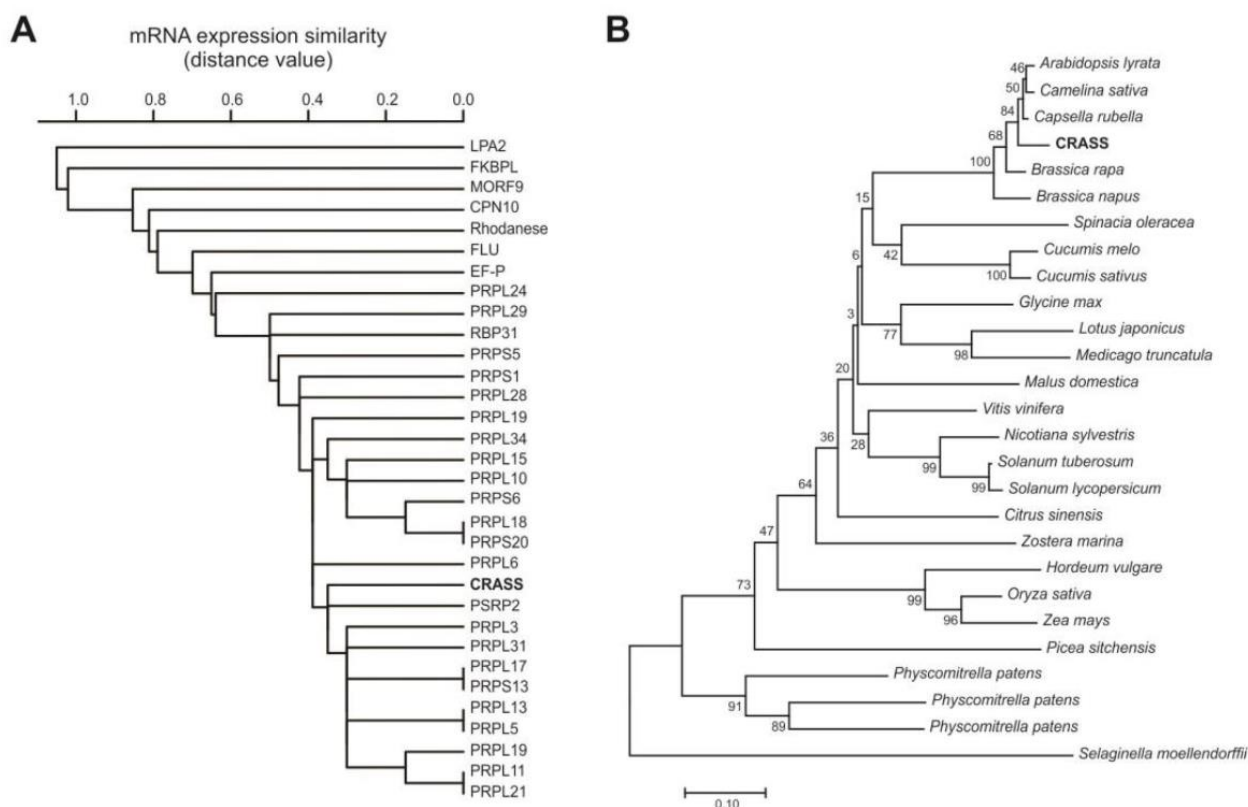


**Figure 3.1 Coexpression and phylogeny of CRASS**

(A) Coexpression of *CRASS* transcripts was analyzed using hierarchical clustering with single linkage method provided by the HCluster tool (<http://atted.jp>). (B) Phylogenetic tree made with the full sequences of Arabidopsis *CRASS* and orthologues from other species. The tree was rooted at midpoint using the neighbor-joining method in MEGA6. Bootstrap values (as a percentage of 2,000 replicates) are indicated at the branches. Accession numbers are reported in “Materials and Methods”.

### 3.2 CRASS is present in green plants but not in Charophyta or Chlorophyta

The *CRASS* sequence has no clear homology with any conserved domain or known motif. The only exception is a weak homology with a bacterial Heavy Metal Associated domain (HMA) (Supplemental Figure 6.2). This 25 residues domain, present across all kingdoms, especially in bacteria, usually indicates an involvement in metal ion transport and detoxification. However, the two cysteines responsible for this cation binding (Lutsenko et al. 1997) are not conserved in *CRASS* (Supplemental Figure 6.2). Therefore, it is likely that during the course of evolution this protein has lost its catalytic activity and gained a different function. The sequence of *CRASS* is exclusively found in Embryophyta and is not present in

yeast or photosynthetic bacteria or algae (Figure 3.1B). These results suggest a plant specific function for CRASS.

### 3.3 CRASS is a non-essential protein localized in the chloroplast stroma

Two mutant lines from the “Koncz collection” (Ríos et al. 2002) were selected for the T-DNA insertion on the CRASS first exon (*crass-1*) and third intron (*crass-2*) in order to investigate the effect of the absence or reduced amounts of CRASS on plant fitness (Figure 3.2A). In addition, to analyse overexpression and subcellular localisation, two CRASS-YFP overexpressing lines (*oeCRASS-YFP#1* and *oeCRASS-YFP#2*) were generated. In order to verify that the T-DNA lines were knock out alleles, we performed qPCR which confirmed that *crass-1* is a null allele while *crass-2* accumulates about 20% of WT amounts of CRASS. Transgenic overexpressor YFP-tagged lines displayed approximately double levels of CRASS compared to WT plants (Figure 3.2B). Plants grown for three weeks in long day conditions showed a slight growth impairment with a significant reduction of fresh weight in *crass-1* and *crass-2* plants (approx. 15%) compared to WT or to YFP lines (Figures 3.2B and 3.2C). When testing photosynthesis efficiency with the Imaging PAM, the mutants yielded the same  $F_v/F_m$  (maximum quantum yield of PSII) compared to WT and *oeCRASS-YFP* lines (Supplemental figure 6.3).

A chloroplast transit peptide is predicted in the CRASS N-terminus (ChloroP). In fact, CRASS has been found in chloroplast fractions in proteomic studies (Friso et al. 2004; Zybailov et al. 2008). Confocal microscopy experiments demonstrate that the YFP fluorescence of the *oeCRASS-YFP* line clearly overlaps with the chlorophyll autofluorescence of the chloroplasts (Figure 3.2D). Accordingly, experiments of subcellular localisation using fractionated chloroplasts in stroma and thylakoids, allowed to localize CRASS exclusively in the stroma fractions of chloroplasts (Figure 3.2E).

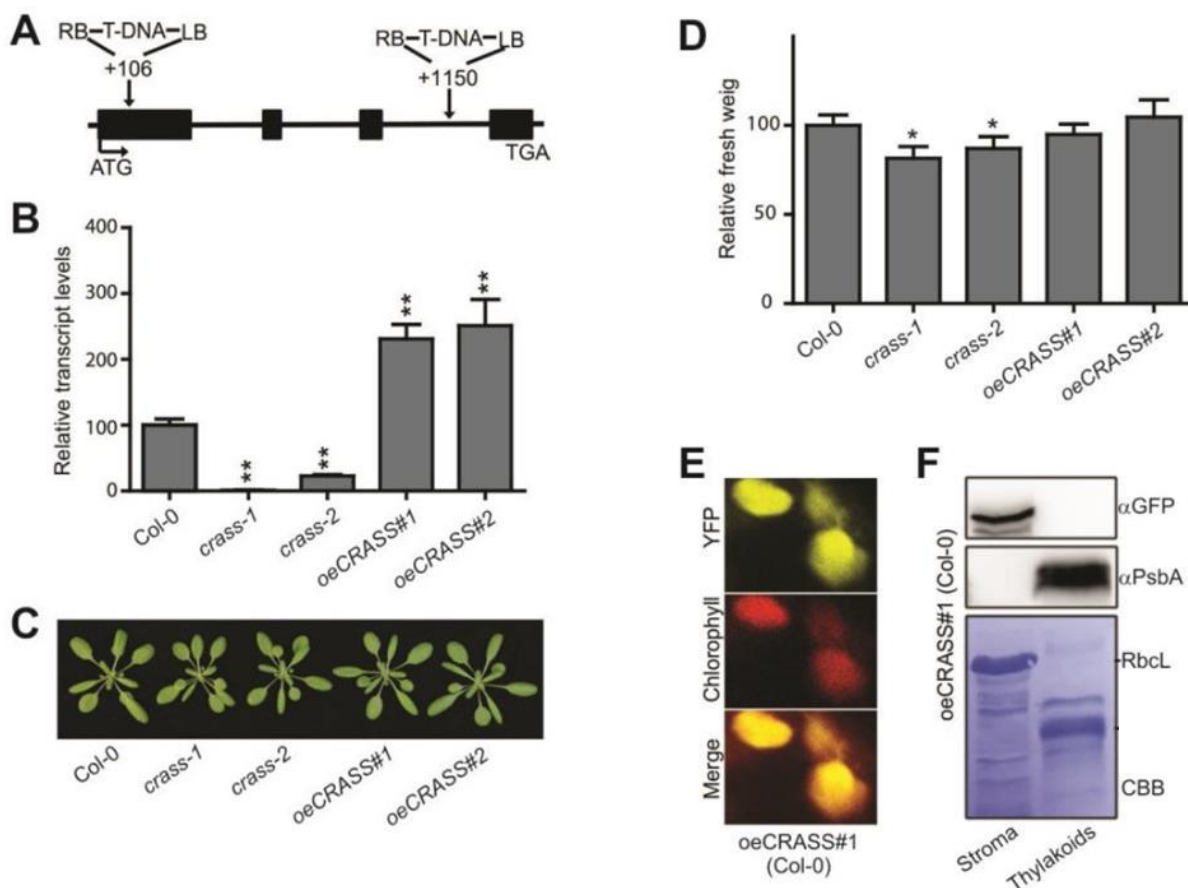


**Figure 3.2 Characterization of CRASS mutants and analysis of subcellular localization.**

(A) Gene model of CRASS (AT5G14910). Exons are shown as black boxes, introns as lines. Position of T-DNA insertions are indicated. (B), Transcript levels of *CRASS* were analyzed in the mutants and transgenic lines using *UBIQUITIN10* gene as control (see “Materials and Methods”). (C) Representative images of 3-week-old T-DNA insertion lines (*crass-1*, *crass-2*) wild-type (Col-0) and YFP-tagged overexpressor lines (*oeCRASS#1* and *oeCRASS#2*). (D) Fresh weight data correspond to the mean percentage of the WT and values of  $n \geq 6$  independent experiments with  $\geq 15$  plants grown for 3 weeks in long day (Student’s t-test: \* $P < 0.05$ ). (E) Mesophyll cells of *oeCRASS#1* plants analysed with a laser scanning confocal microscope. The merging of the YFP signal and the chloroplast autofluorescence (chlorophyll) demonstrated colocalization. F, Subcellular localization of CRASS using isolated chloroplast and subsequent fractioning into stroma and thylakoids fractions as described in “Materials and Methods” confirmed that CRASS is a stromal protein. The core protein from the photosystem II PsbA served as control for thylakoid membrane, absent in the stroma fraction in the Coomassie Brilliant Blue (C.B.B.) gel

### 3.4 CRASS does not alter rRNA accumulation under control conditions

Plants lacking ribosomal subunits or assembly factors often display severe phenotypes due to an impairment in rRNA processing. We analyzed the rRNA abundance and detected no significant differences between CRASS mutants, WT and CRASS overexpressing lines (Figure 3.3A). Alternatively, chloroplastic ribosomal subunits could be directly affected but we found no evident alteration of the protein levels of PRPS1, PRPS5, plastidial chaperones (HSP70, CPN60 $\alpha$ 1) or Rubisco large subunit (RbcL) in any of the lines tested (Figure 3.3B). Similarly, *psaA* and *rbcL* RNA association to polysomes did not result in clear differences in sucrose gradients between WT and CRASS mutant plants (Supplemental figure 6.4)

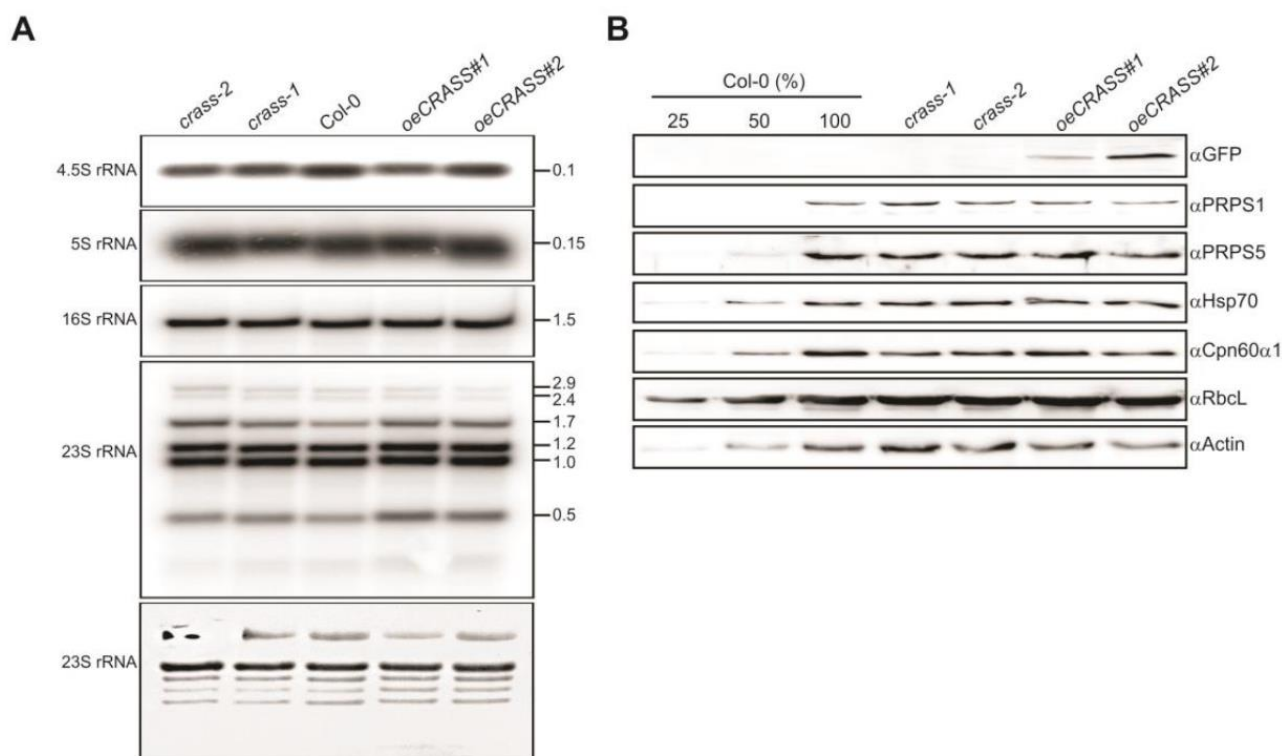


**Figure 3.3. Analysis of the effect of CRASS on the accumulation of plastid rRNA and protein levels.**

(A) RNA gel-blot analysis of 10  $\mu$ g of total RNA samples from 3-week-old plants with probes specific for plastid rRNAs (23S, 16S, 5S and 4.5S). The sizes of the transcripts are given in kilobases on the right. (B) The accumulation of chloroplastic proteins was analyzed by western blotting of samples from 3-week-old plants. Representative images of immunoblot analyses with the indicated antibodies are shown. Total protein extracts from wild-type (Col-0), CRASS mutants and transgenic lines were examined, together with a dilution series of the Col-0 sample as indicated.

### 3.5 The absence of CRASS triggers a reduced translational activity

In order to trigger an evident phenotype in mutant plants, we tested the growth on MS media supplemented with increasing amounts of lincomycin (LIN), a chloroplast translation inhibitor, at sublethal concentrations. LIN targets specifically plastid protein synthesis by binding the 50S ribosome thus reducing translation rate and protein biosynthesis (Liao et al. 2016). After one week of growth under long day conditions and in presence of LIN, both CRASS mutants were paler than the WT (Figure 3.4A). Statistical significance was confirmed by chlorophyll and pigment quantification (Figure 3.4B and 3.4C). Moreover the recombinant CRASS-YFP construct efficiently complemented the *crass-1* mutant (Supplemental Figure 6.6), reinforcing the hypothesis that CRASS has a role in ribosome function.

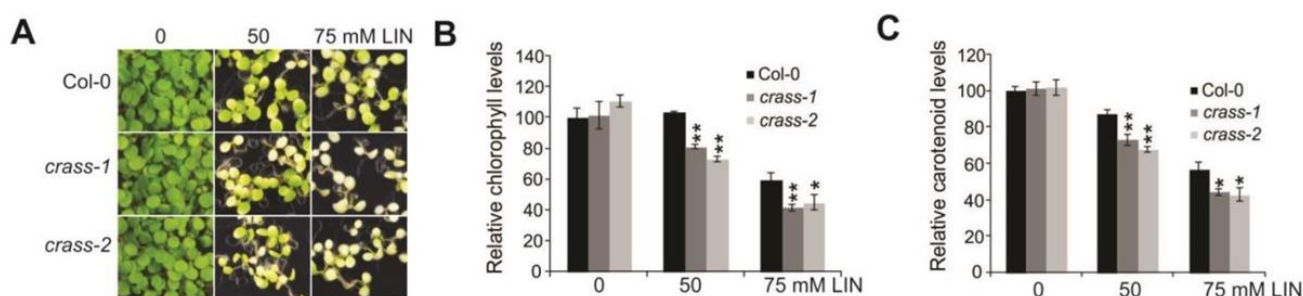


**Figure 3.4. Effects of the inhibition of chloroplast translation by lincomycin on CRASS mutants.**

(A) Representative images of 10-day-old wild-type (Col-0) and *crass-1* and *crass-2* mutant plants germinated on MS medium containing the indicated concentrations of lincomycin (LIN) are shown. Quantification of total chlorophyll (B) and carotenoid (C) levels demonstrate significant differences between wild-type and mutant plants in the presence of LIN. Relative data are shown (wild-type plants grown in the absence of LIN = 100%). Average and SE values (n = 4) are provided. Student's t-test (\*P < 0.05 and \*\*P < 0.01) was used for statistical analysis.

### 3.6 CRASS is necessary for cold stress tolerance

As discussed in the introduction, several mutants lacking ribosomal subunits show an increased sensitivity to cold stress. This is caused by a cold induced slower translation rate summed to an incomplete ribosome assembly (Rogalski et al. 2008; Kupsch et al. 2012). Moreover, a general impairment of the plastid ribosome induces a retrograde signaling which pleiotropically alter plant fitness (Zhang et al. 2016; Leister 2012). To test whether CRASS is

---

involved in cold tolerance, 2 week old plants were grown in standard long day condition and then transferred to a chamber set at 4 °C for 4 weeks (see Methods). After the cold treatment, plants were immediately measured with an Imaging PAM and the younger leaves of *crass-1* and *crass-2* showed lower  $F_v/F_m$  values compared to WT or complemented lines *crass-1 oeCRASS:YFP* (Figure 3.5A). We observed the same behaviour also when germinating and growing seedlings for 6 weeks at 4 °C (Figure 3.5C). The recovery appeared significantly slower in plants lacking CRASS and was further verified by in vivo [<sup>35</sup>S]-methionine labelling (Figure 3.5D). RNA gel-blot analysis of soluble RBCL and membrane PSBA/PSBD (PSII core proteins D1/D2) showed that incorporation of radioactively labelled methionine was reduced in *crass-1* mutant compared to WT or *oeCRASS-YFP#1* line. Protein levels were analysed after three days of recovery at 22 °C (Figure 3.5E) and a clear reduction is present regarding the ribosome small subunit proteins tested (PRPS1 and PRPS5) and chloroplast encoded proteins (PSAD, CYTf, CYTb6, ATPβ, RBCL). Interestingly also nuclear encoded photosynthetic proteins were affected (PSBR, PSAL, LHCA1, LHCB2) probably as an effect of a retrograde signalling from a defective chloroplast to the nucleus (Romani et al. 2012; Tadini et al. 2016). Levels of a 50S ribosomal subunit (PRPL2) and chaperones (HSP70, CLPC, CLPB3, CPN60α1) were unaffected, thus confirming the activity of CRASS in the small ribosome subunit.

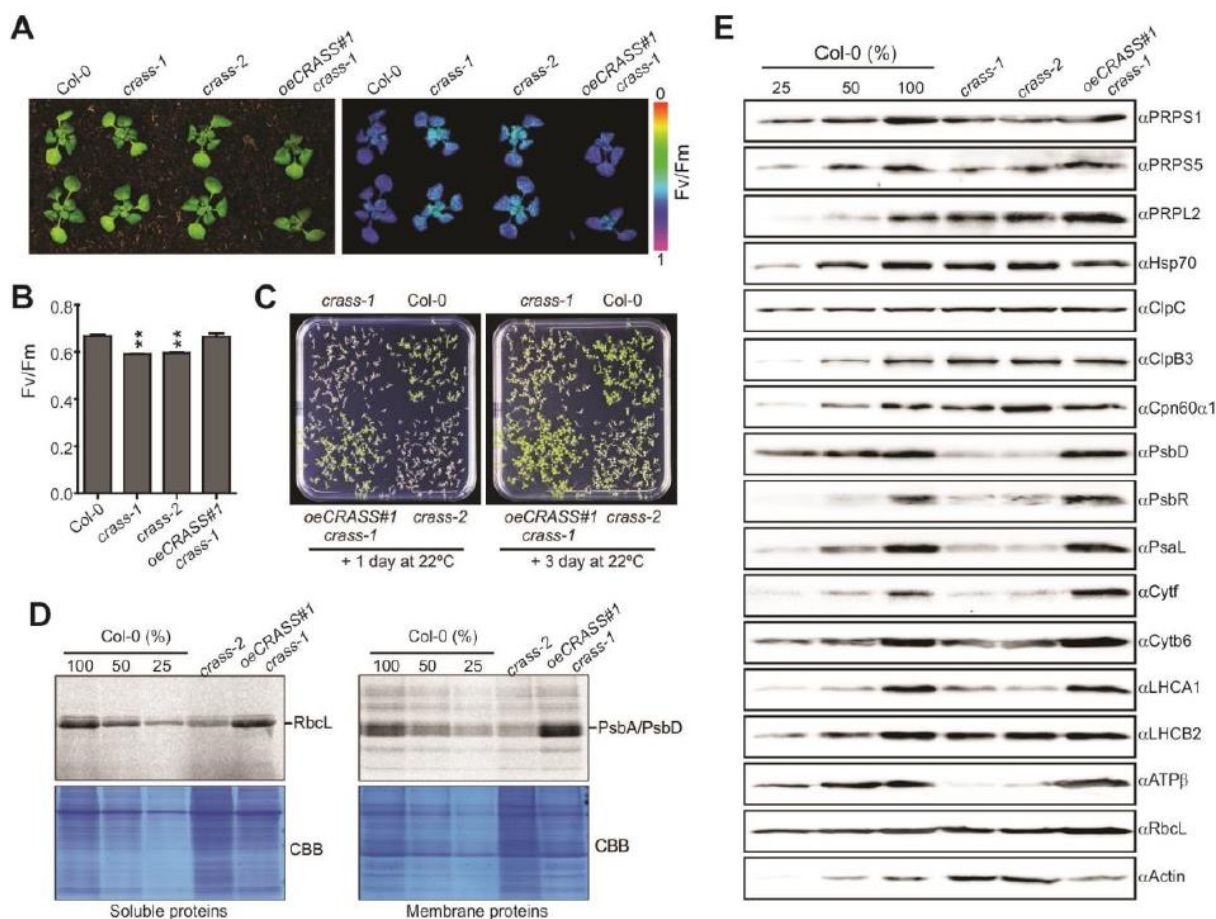


**Figure 3.5. CRASS is required for cold stress tolerance.**

**(A)** Representative images and Imaging PAM images of wild-type (Col-0), *crass-1* and *crass-2* mutants, and overexpressor line *oeCRASS#1 crass-1* grown on soil for 2 weeks at 22° C, followed by 5 weeks at 4°C. **(B)** Quantification of  $F_v/F_m$  demonstrated that both *crass-1* and *crass-2* show reduced efficiency of PSII after the cold treatment (Student's t-test: \*\*P < 0.01). **(C)** Representative images of wild-type (WT), *crass-1* and *crass-2* mutant plant grown on MS plates for 6 weeks at 22°C followed by 1 or 3 days at 22°C. **(D)**, Translation analysis Seedlings from the cold treatments were treated with [<sup>35</sup>S]methionine under low-level illumination (20 μmol photons m<sup>2</sup> s<sup>-1</sup>) for 15 minutes in the presence of cycloheximide (to inhibit cytosolic protein synthesis). The Coomassie Brilliant Blue (C.B.B.) gel of total proteins analyzed by SDS-PAGE and detected by autoradiography is showed. **(E)** Total protein extracts were analysed by western blot using material from cold treatments in MS plates. Representative images of immunoblot analyses with the indicated antibodies are shown.

### 3.7 Chloroplast 16S rRNA specifically coimmunoprecipitates with CRASS

To confirm the interaction with ribosomal subunits we performed RNA co-immunoprecipitation using GFP antibody with the *oeCRASS-YFP#1* line and WT as negative control. We then isolated the RNA for deep sequencing (RIP-seq). The majority of RNA

extracted from the CRASS-YFP lines resulted to be 16S ribosomal RNA while only traces of RNA were pulled down in the WT control (Figure 3.6A and Supplemental Table 6.2). We further confirmed this by hybridizing the immunoprecipitated RNA to rRNA probes and we obtained again a clear enrichment with the 16S probe (Figure 3.6B).

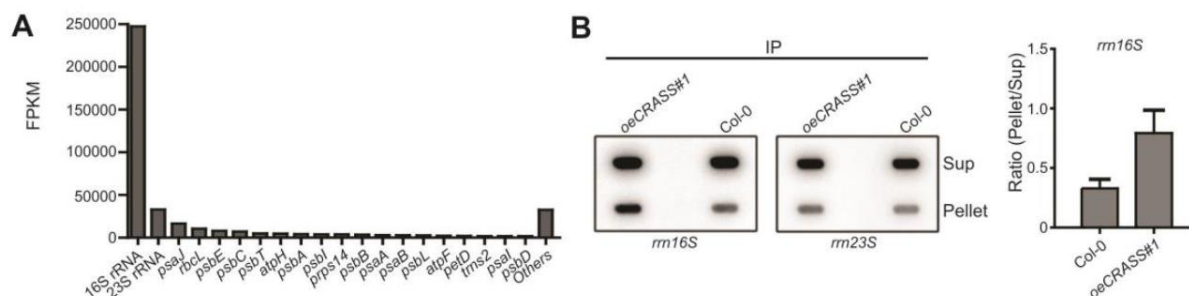


**Figure 3.6. RNA coimmunoprecipitation with CRASS.**

(A) The identification of RNA species associated with CRASS was performed by RNA immunoprecipitation in combination with high throughput RNA sequencing (RIP-seq) using plants overexpressing CRASS-YFP (*oeCRASS#1*). Fragments per kilobase of exon per million reads mapped (FPKM) values of the 20 most abundant immunoprecipitated RNAs among two independent RIP-seq experiments on transgenic line *oeCRASS#1* are shown. The remaining 153 genes with less than 1500 FPKMs are combined into “Others”. Trace amounts of RNA from the wild-type (Col-0) control are not shown in the chart. (B), Coprecipitated RNAs of the supernatant (Sup) and the pellet were applied to slot-blot. Filters were hybridized with the *rrn16S* and *rrn23S*-region-specific probes. The quantification of the signal showed a specific enrichment of *rrn16S* was found when overexpressing CRASS.

### CRASS interacts preferentially with ribosomal small subunit isoforms

In addition to RIP-seq analysis, for the identification of interaction partners, CRASS was overexpressed fused to YFP and epitope-based affinity purification with a monoclonal GFP antibody was carried out. The samples were analysed by LC-MS/MS. The results show a strong signal of the CRASS bait protein and evidence a clear enrichment of plastidial ribosomal proteins (Table 3.1). 87 proteins were identified with high confidence from two independent experiments, of which the 10 strongest hits after the bait (CRASS) were all chloroplast ribosomal subunits (Table 3.1). In comparison, CRASS-GFP fusion protein and plastidial ribosomal proteins were absent in the WT control sample plant. A repeat of the experiment confirmed the result. To validate this result, we attempted a reciprocal immunoprecipitation experiments with *oePRPS17-YFP* plants, which also pulled down

CRASS among its putative interaction partners (Supplemental Table 6.1). This is an indication that CRASS interacts or is part of the small subunit of the chloroplast ribosomes.

To verify the direct interaction with specific targets, we performed western blot analysis on the immunoprecipitation eluates with antibodies raised against ribosomal subunits from the small and large ribosomal subunit. The elution fractions showed a strong signal from small subunit proteins (PRPS1 and PRPS5) while no signal came from large subunit ones (PRPL11 and PRPL2). Interestingly, CRASS was also found in a PRPS5 immunoprecipitation (Zhang et al. 2016 supplementary information), supporting the hypothesis that the CRASS protein is able to interact with the ribosome in chloroplasts.

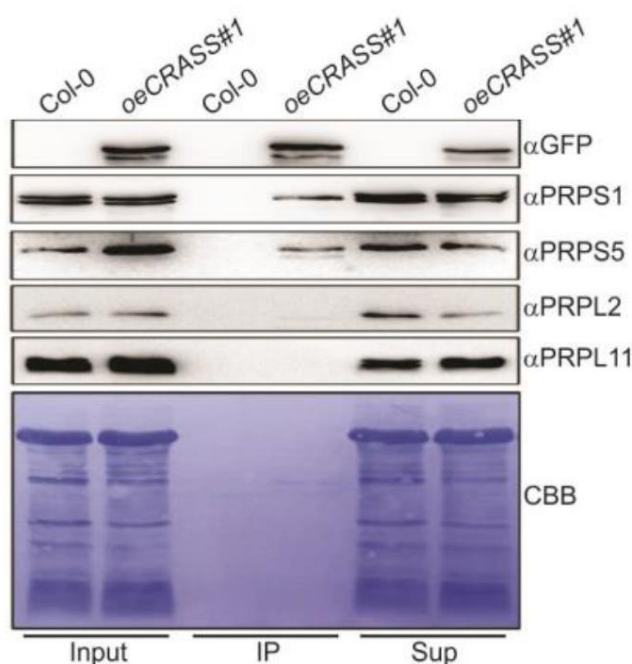


**Figure 3.7. Crass coimmunoprecipitation analysis**

Coimmunoprecipitation experiments were performed using 3-week-old wild-type (Col-0) and plants overexpressing CRASS-YFP (*oeCRASS#1*). Western blot analysis of input, supernatant and elution fractions confirmed the interaction of CRASS with the 30S proteins PRPS1 and PRPS5.

### 3.8 CRASS interacts with PRPS1 in a RNA-independent manner

At this stage, to further unravel the interaction CRASS – ribosome, we performed size exclusion chromatography (SEC) experiments aimed at clarifying if CRASS interacts with RNA during assembly or with fully assembled ribosomes (Figure 3.8). We fractionated native stroma in 20 fractions by SEC according to their molecular weight and ran those on SDS\_PAGE. We then performed western blot analysis of the distribution of CRASS-YFP and selected ribosomal proteins with and without RNase A treatment. RNase is expected to disassemble ribosomes and actually the same shift from high molecular weight to low molecular weight fractions due to the RNA degradation happening in ribosomal proteins was obtained also in CRASS-YFP (Figure 3.8A). This supports the hypothesis that CRASS is associated to fully mature ribosomes in vivo. In order to understand if the association occurs via RNA or not we carried out another immunoprecipitation after RNase treatment. The addition of RNase did not affect the pulling down of PRPS1 (Figure 3.8B), indicating that CRASS interacts with the 30S subunits via protein-protein interaction. Therefore, the presence of 16S RNA in the RIP-seq experiments was probably due to the immunoprecipitation of the native ribosomal complex, comprising ribosomal proteins and rRNAs. Direct protein interaction with PRPS1 and PRPS5 is not shown by yeast two-hybrid analysis supposedly because it happens in a multimeric binding or via another ribosomal subunit (Supplemental figure 6.5).

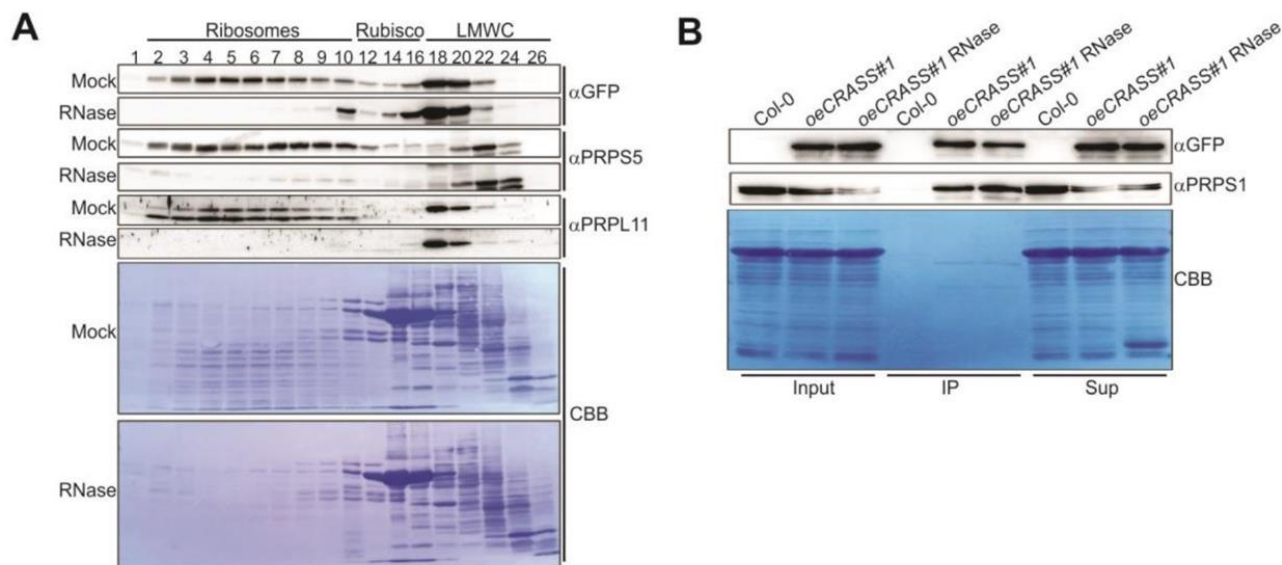


**Figure 3.8. Analysis of RNA-dependency of CRASS interaction with ribosomal proteins.**

(A) Size exclusion chromatography (SEC) analysis was performed as described in “Materials and Methods” with native stroma extracts from 3-week-old *oeCRASS#1* transgenic lines. Western blot analysis show that YFP-tagged CRASS co-migrates with ribosomal proteins, typically present in the first higher molecular weight fractions (ribosomal complexes) but also in the lower molecular weight complexes (LMWC) fractions. Treatments of samples with RNase A cause the shift of CRASS, PRPS5 and PRPL11 to LMWC fractions, presumably by the disassembly of the ribosomal complexes. (B) Coimmunoprecipitation experiments were performed using 3-week-old wild-type (WT) and transgenic line *oeCRASS#1* plants. Western blot analysis of input, supernatant and elution fractions demonstrated that CRASS interacts with PRPS1 independently of the presence or absence of RNase A. Experiments performed under technical assistance of Dr. Nikolay Manavski.

### 3.9 Synergistic effect between CRASS and PRPS17

In order to verify the interaction at a genetic level, we characterized the effects of the absence of CRASS in the background of other ribosomal mutants. We successfully generated viable double mutants crossing *crass-1* with *prps17* and *prpl11*. Interestingly, a synergistic effect was present with an evident phenotype when the small subunit was affected (as in *prps17*) rather than the large one (as in *prpl11*) where differences were not significant (figure 3.9). In adult plants the double mutant *crass prps17* was clearly retarded in growth (Figure 3.9A) and displayed significantly lower  $F_v/F_m$  values (Figure 3.9B) under both long and short day conditions (Supplemental Figures 6.7A and 6.7B). All these results together point to a role of CRASS in biogenesis and/or stabilization of the 30S subunit of the chloroplast ribosome.

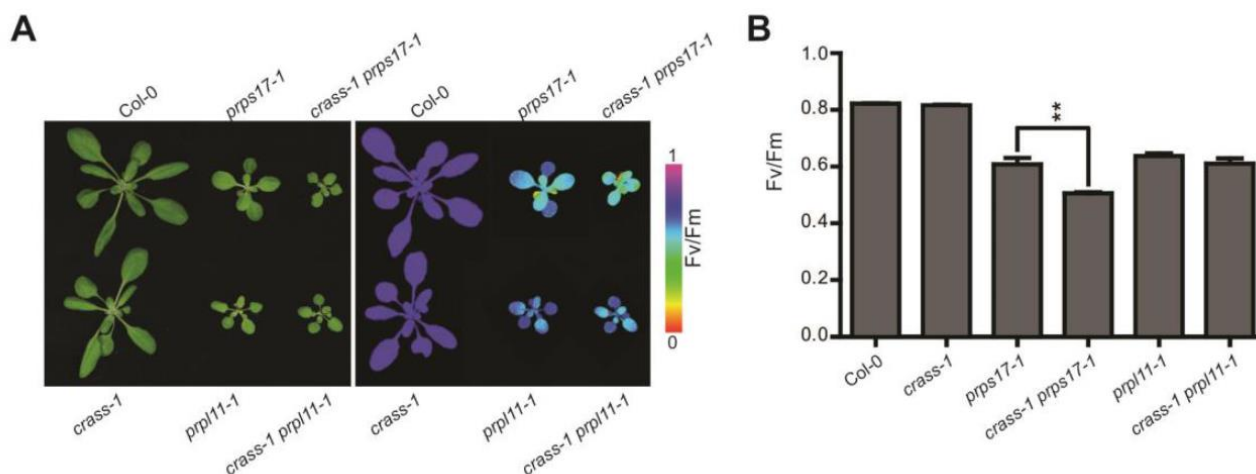


**Figure 3.9. Genetic interactions between CRASS and ribosomal proteins.**

(A) Representative image of the indicated genotypes after 21 days in long day conditions (left panel). The photosynthetic parameter  $F_v/F_m$  (maximum quantum yield of PSII) was measured using an Imaging PAM system as described in “Materials and Methods” (right panel). (B) Quantification of  $F_v/F_m$  measures demonstrated an additive effect in the double mutant *crass-1 prps17-1* but not in *crass-1 prpl11-1*. Average and SE (n = 20) are provided. Student’s t-test (\*\*P < 0.01) was used for statistical analysis.

AGI code	ID	Protein MW (kDa)	Score Exp 1	Score Exp 2	Coverage Exp 1 (%)	Coverage Exp 2 (%)	Most abundant peptide
AT5G14910	CRASS	19.1	3023	2303	27.5	27.5	ALQDIDGVSNLK
ATCG00770	PRPS8	15.5	560	492	33.6	43.3	DTIADIITSIR
AT1G07320	PRPL4	30.5	541	223	25.5	20.6	TLNLFDILNADK
AT2G33800	PRPS5	32.7	426	300	10.9	4.6	IVLEMAGVENALGK
AT5G30510	PRPS1	45.3	410	466	26.4	34.1	GGLVALVEGLR
AT1G05190	PRPL6	24.7	409	296	31.8	31.8	GPLGELALTYPR
AT1G74970	PRPS9	22.6	379	188	16.3	16.3	EYLQGNPLWLQYVK
AT3G44890	PRPL9	22.2	331	289	17.8	17.8	LIFGSVTAQDLVDIHK
AT5G14320	PRPS13	19.4	305	243	17.8	19.5	DMAEEELIILR
AT2G43030	PRPL3	29.3	295	155	13.7	8.1	TLATDGYDAVQIGYR
AT1G32990	PRPL11	23.3	209	254	16.2	25.2	AGYIIPVEITVFDDK

**Table 3-1 CRASS coimmunoprecipitates with plastid ribosomal proteins.**

Proteins immunoprecipitated with an antibody against GFP from the transgenic line *oeCRASS#1* were separated by SDS-PAGE. Gel fractions were analysed by MALDI TOF mass spectrometry in order to identify CRASS bound proteins. To check for unspecific contaminants the output has been compared to the immunoprecipitation of wild-type plants as described in “Materials and Methods.” Analysis has been performed on two independent biological replicates. For these two biological replicates, the 10 best candidates are shown. Dr. Lars Scharff supervised the immunoprecipitation experiments, Dr. Piotr Gawronsky performed bioinformatic analysis and Dr. Annemarie Matthes produced the mass spectrometry data.

## 4. Results SCO2

### 4.1 Absence of SCO2 results in leaf variegation in *L. japonicus*

*Lotus japonicus* is a model legume, for which mutant lines based on the endogenous retrotransposon LORE1 have been made publicly available (Fukai et al. 2012; Urbański et al. 2012). New mutants were recently released, some of which display albino or variegated phenotypes (Małolepszy et al. 2016). In this work, we identified three different mutant lines, *ljSCO2-1* (30096086), *ljSCO2-2* (30099994) and *ljSCO2-3* (30006602), in which the coding region of the SCO2 gene (LjSCO2; Lj3g3v0537380) is disrupted (Supplemental Figure 6.8). The open reading frame of LjSCO2 consists of three exons, coding for a protein of 190 amino acids. In *Arabidopsis thaliana*, loss of SCO2 (*atsCO2*) results in pale/albino cotyledons, but normal true leaves (Albrecht et al. 2008; Shimada et al. 2007). Similarly, *ljSCO2* mutants displayed paler cotyledons with lower  $F_v/F_m$ , indicating functional impairment of PSII (Figure 4.1A). However, the defects in chloroplast development in *ljSCO2* mutants also extended to true leaves, which exhibit a variegated phenotype and lower maximum quantum yield of PSII ( $F_v/F_m$ ) in the white areas (Figure 4.1B). Among 48 *ljSCO2-1* and 70 *ljSCO2-2* plants obtained by selfing of plants hemizygous for the respective LORE1 insertion in the LjSCO2 gene, we identified 15 and 17 variegated plants, respectively, which were all homozygous for the LORE1 insertion, demonstrating perfect linkage between disruption of the LjSCO2 gene and the leaf phenotype. The analysis of *LjSCO2* expression demonstrated that all three mutants are knockouts for the LjSCO2 gene (Supplemental Figure 6.8B). Interestingly, transcript expression of LjSCO2 is higher in cotyledons compared to true leaves, similarly to as described in *Arabidopsis* (Shimada et al. 2007) with higher transcript and protein levels in 5-day-old seedlings compared to rosette or cauline leaves. Mutants are also characterized by stunted root and shoot growth (Supplemental Figure 6.8D) and reduced size (Supplemental Figure 6.8E). Variegation in leaves is independent of developmental stage. Therefore, these results indicate that SCO2 is involved in leaf variegation in *Lotus*. The different phenotypes observed in *Arabidopsis* and *Lotus sco2* mutants raised the question whether the function of the protein is conserved. An alignment with orthologous protein sequences from various plant species revealed that, in all species investigated, SCO2 has a C-terminal DNAJ-related zinc-finger domain, which contains two pairs of cysteines (CXXC) and three additional, highly conserved Cys residues (Supplemental Figure 6.9A). These cysteines have been proposed to play an important role in the interaction with AtSCO2 substrates (Muranaka et al. 2012).

---

Phylogenetic analysis of AtSCO2 orthologues and other reported DNAJ-related proteins from Arabidopsis demonstrated that all SCO2 proteins belong to the same clade (Supplemental Figure 6.9B). These results suggest that SCO2 from Arabidopsis and Lotus may be true functional orthologues.

SCO2 function is conserved between *A. thaliana* and *L. japonicus*

In order to test whether the SCO2 function is indeed conserved in *L. japonicus*, we performed greening experiments. Seedlings kept in darkness for 8 days were exposed to light for 1 or 8 days (Figure 4.2A). Like the Arabidopsis mutant (Albrecht et al. 2008), plants lacking LjSCO2 failed to accumulate pigments upon exposure to light. Quantification of total chlorophyll clearly showed a reduction in chlorophyll accumulation (Figure 4.2B). To further investigate photosystem functionality, we carried out measurements of the 77K fluorescence emission spectra, which allowed us to quantify PSI (peak at 737 nm) and PSII (peak at 693 nm) levels in Lotus cotyledons and true leaves. As previously reported for Arabidopsis (Albrecht et al. 2008), in the *ljSCO2-1* mutant, the height of the PSI-specific peak was markedly reduced in both cotyledons and true leaves (Figure 4.2C). Analysis of isolated chloroplasts using the same amount of chlorophyll confirmed the results obtained directly on true leaves (Supplemental Figure 6.10). Although variegation in the Arabidopsis *atsco2* mutant has not been observed in photosynthetically competent leaves, we measured the effects of different light regimes on growth. Strikingly, under short-day conditions, *atsco2* plants showed a decrease in growth, as well as paler coloration (Figure 4.2D).  $F_v/F_m$  values were lower in true leaves in *atsco2* mutant compared with WT plants, in particular under short day conditions (Figure 4.2D). We thus conclude that, as in *ljSCO2* plants, cotyledons and true leaves are affected in *atsco2* mutants. Moreover, we found that *atsco2* cotyledons are not only paler in plants grown under short-day conditions, but also under continuous light (Supplemental Figure 6.11A). Quantification of chlorophylls and carotenoids showed that levels of both pigments are higher in *atsco2* plants, under the long-day regime, whereas in WT seedlings pigment levels were maximized in continuous light (Supplemental Figures 6.11B and 4C). To study the effects of growth conditions and light intensity on leaf variegation of Lotus mutants, we grew WT and *ljSCO2-1* mutant under different light regimes (see Methods). Similar to the Arabidopsis mutant, *ljSCO2-1* is paler and smaller under short day conditions (Figure 4.3A). Accordingly, quantification of chlorophylls and carotenoids showed that *ljSCO2-1* accumulates less than 50% of WT pigment levels (Figures 4.3B and 4.3C). Interestingly, although true leaves are variegated in all conditions tested, this

phenotype is less pronounced when plants were grown under high light, resulting in lower differences in pigment levels between WT and *ljSCO2-1* plants.

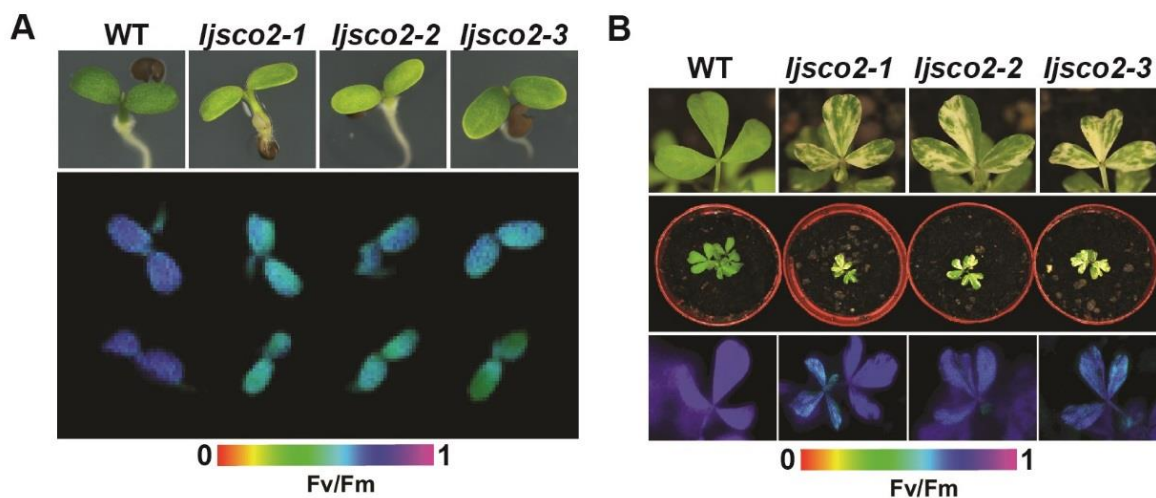


**Figure 4.1** Mutation of LjSCO2 impairs chloroplast development in cotyledons and true leaves in *Lotus japonicus*.

Representative pictures of 4-day-old cotyledons (A) and 3-week-old (B) *Lotus* wild-type (WT) plants and *ljSCO2* mutants are shown (top panels). The photosynthetic parameter  $F_v/F_m$  (maximum quantum yield of PSII) was measured using an Imaging PAM system as described in Methods (lower panels). Signal intensities for  $F_v/F_m$  are indicated in accordance with the color scale (right bar).

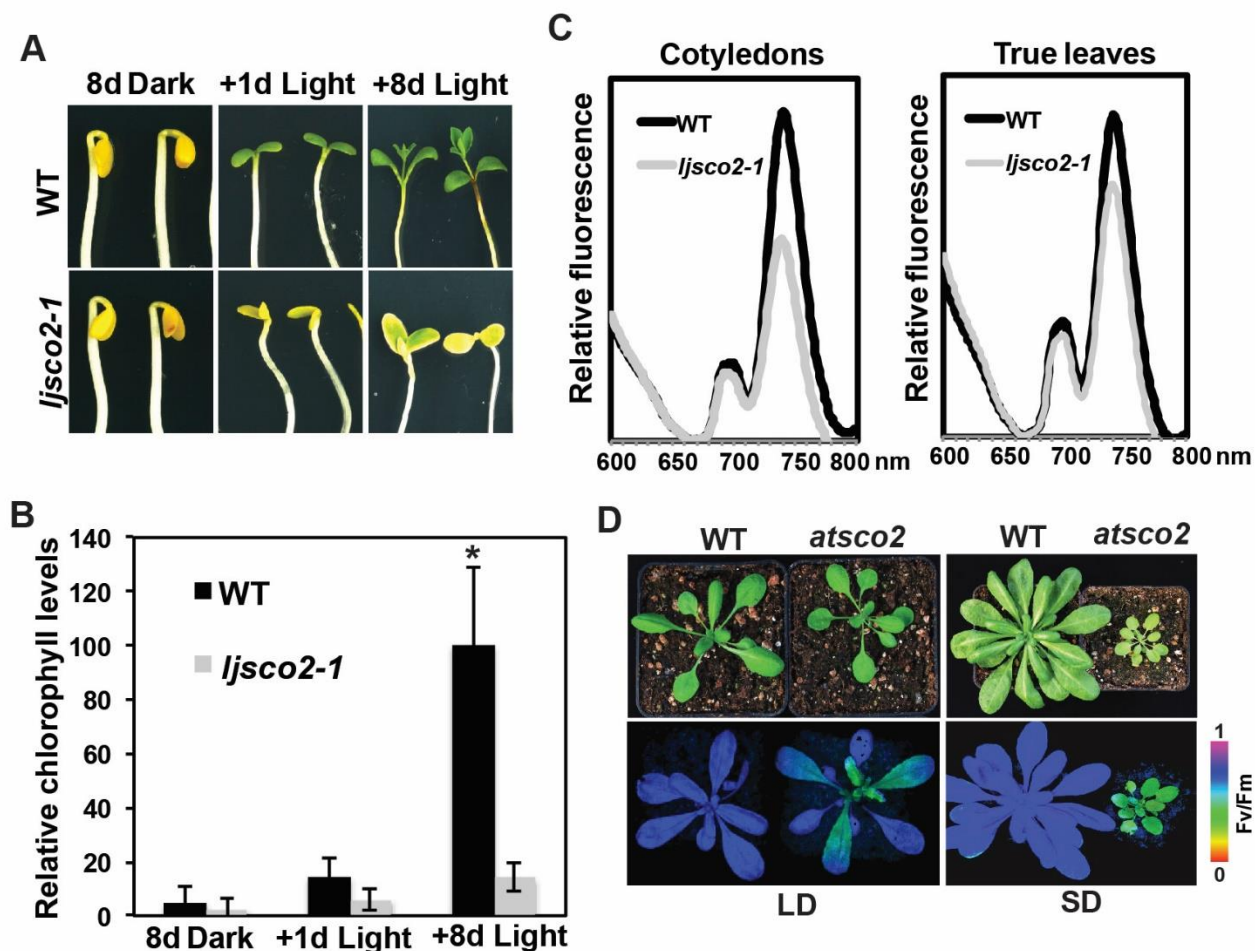


**Figure 4.2** Greening and photosynthetic measures confirm conserved roles of SCO2 between *A. thaliana* and *L. japonicus*.

(A) In the greening experiments, Lotus wild-type (WT) and *ljSCO2-1* were grown in darkness for 8 days and then exposed to light for 1 or 8 days. (B) Quantification of total chlorophyll accumulation during the greening experiments was carried out as described in Methods. Data correspond to the mean and SD values of 3 independent experiments and are expressed as relative levels (WT plants after 8 days of light = 100%). Statistically significant differences relative to WT in darkness are indicated ( $*P < 0.05$ , t-test). (C) The 77K fluorescence emission spectrum was analyzed for Lotus cotyledons and true leaves. The fluorescence emission signals were normalized to the minimum at 670 nm. Representative experiments are shown for the WT (black lines) and the *ljSCO2-1* mutant (gray lines). (D) Phenotype of 24-day-old (long day) and 8-week-old (short day) Arabidopsis WT and the *atsCO2* mutant. Signal intensities for  $F_v/F_m$  are indicated in accordance with the color scale (right bar).

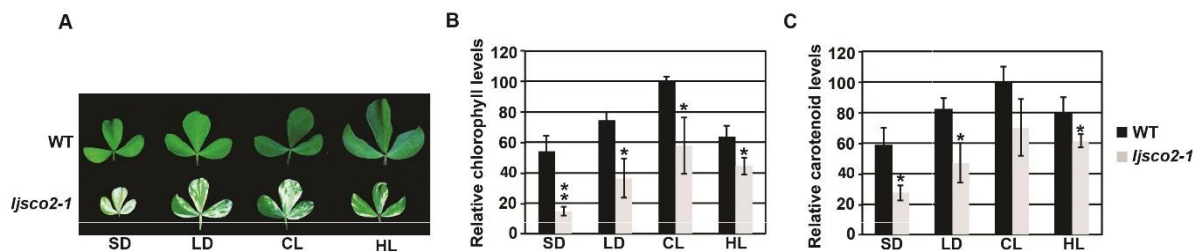


**Figure 4.3 Analysis of the leaf phenotype of the *ljSCO2-1* mutant under different growth conditions.**

(A) Phenotypes of representative leaves of 45-day-old Lotus wild-type (WT) and *ljSCO2-1* mutant grown under short-day (SD), long-day (LD), continuous light (CL) or high light (HL) conditions. Plant material was collected and standard pigment amounts were determined as described in Methods. Relative values of total chlorophyll (B) and carotenoids (C) are provided (WT grown in CL = 100%). Data correspond to the mean and SD values of n=4 independent experiments (Student's t test: \*P < 0.05 and \*\*P < 0.01).

#### 4.2 LjSCO2 is essential for photosynthetic activity in *L. japonicus*

Changes in 77-K fluorescence emission demonstrated that PSI is affected in the *ljSCO2-1* mutant. Furthermore, measurements of  $F_v/F_m$  in plants that had been dark-adapted for 30 min showed that PSII photosynthetic efficiency is also reduced in *ljSCO2-1* leaves ( $0.64 \pm 0.07$ ) compared with WT ( $0.76 \pm 0.02$ ), similarly to cotyledons (Figure 4.1A). Light-response experiments using increasing light intensities confirmed lower electron transport rates for PSII (ETR II) in the *ljSCO2-1* mutant compared to WT (Figure 4.4A). The *ljSCO2-1* mutant also differs from the WT with respect to the kinetics of transient NPQ (non-photochemical quenching) induction (Figure 4.4B). NPQ was analyzed in dark-adapted plants by exposing them to high light levels ( $830 \mu\text{mol photons m}^{-2} \text{s}^{-1}$ ) for 30 min, followed by 15 min of darkness. At the beginning of the light period, NPQ was higher in the *ljSCO2-1* mutant than in WT, whereas after 10 min NPQ levels decreased in the WT. In the subsequent dark period (relaxation), values of NPQ dropped in both genotypes, but remained higher in the mutant. The faster NPQ induction in the mutant suggested a pre-accumulation of zeaxanthin in the mutant. Indeed, HPLC experiments confirmed that zeaxanthin highly accumulates in the *ljSCO2-1* mutant under low light conditions, whereas it is only detected in WT plants when grown under high light (Figure 4.4C and Supplemental Figure 6.12). Interestingly,

tocopherols were also present at higher levels in the mutant suggesting a constitutive up-regulation of antioxidant metabolism. NPQ includes several components, one of which may involve LHC antenna proteins (Niyogi and Truong, 2013). Because SCO2 interacts with LHCB1 (Tanz et al. 2012), it was not surprising to find that absence of SCO2 can affect NPQ formation. However, while antisense lines for LHCB1 are compromised in NPQ, the kinetics of NPQ has been shown to be similar to WT (Pietrzykowska et al. 2014). Therefore, SCO2 might have additional roles in modulating photosynthesis.

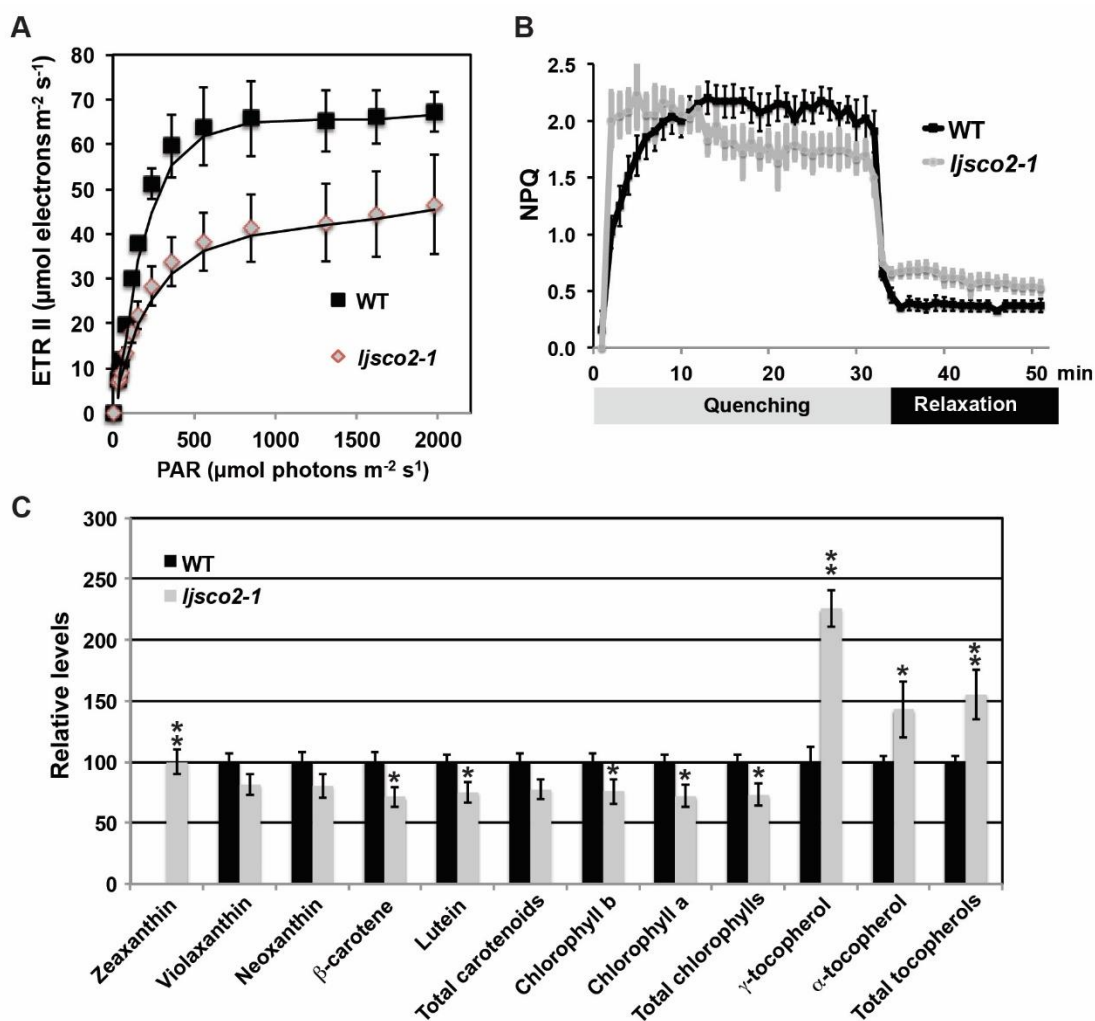


**Figure 4.4** *L. japonicus ljSCO2-1* mutant displays impaired photosynthesis.

Chlorophyll fluorescence parameters of 6-week-old *Lotus* WT and *ljSCO2-1* mutant grown under long-day conditions were analyzed using a DUAL PAM system as described in Methods. (A) Electron transport rate of photosystem II (ETR<sub>II</sub>) was calculated at different light intensities in light response curve. (B) For non-photochemical quenching (NPQ) analysis, plants were kept in the dark overnight prior to measurements. Gray and black bars indicate periods of illumination with actinic light and intervals in the dark, respectively. Data in (A) and (B) are representative of at least 3 independent experiments. Means and SD values are for  $n \geq 5$  different plants. (C) Metabolite analyses by HPLC was performed with the *L. japonicus* plants as described in Methods. Except in the case of zeaxanthin, relative values to the WT plants are provided (absolute values in Supplemental Figure 6.12). Data correspond to the mean and SD values of  $n=4$  independent experiments (Student's *t* test: \* $P < 0.05$  and \*\* $P < 0.01$ ). HPLC analyses (C) performed by the laboratory of Prof. Dr. Manuel Rodriguez-Concepcion

### 4.3 Variegated leaves display altered protein profiles in *L. japonicus*

In order to compare the effects of the absence of LjSCO2 in cotyledons and variegated true leaves, several chloroplastic pathways were analyzed by immunoblotting using specific antibodies (see Methods). Since SCO2 is a DNAJ-related protein, with potential chaperone/protein disulphide isomerase activity (Albrecht et al. 2008; Muranaka et al. 2012; Shimada et al. 2007), we first looked at components of the protein quality control system, including chaperones and proteases (Figure 4.5). Although there is no clear difference between mutant and WT cotyledons, chaperones and proteases levels are increased in variegated true leaves in the *ljSCO2-1* mutant. These results, together with zeaxanthin and tocopherol accumulation, appear to confirm the up-regulation of the anti-stress machinery in the true leaves in the *ljSCO2-1* mutant. Less LHCB1 was detected in the mutant than in the wild-type (WT) (Figure 4.5), as reported for the *atsCO2* mutant of Arabidopsis (Albrecht et al. 2008; Shimada et al. 2007; Tanz et al. 2012). The down-regulation of LHCB1 was confirmed in the other two *ljSCO2* mutants (in contrast to higher levels of Hsp70) (Supplemental Figure 6.13A). The up-regulation of LHCB4 in *ljSCO2-1* suggests the activation of compensatory mechanisms, while amounts of the PSI and PSII components PsaB, PsaL, PsbD, PsbC were lower than in WT, in agreement with previous reports for the *atsCO2* mutant. However, accumulation of PsbQ and PsbO was enhanced in variegated *ljSCO2-1* leaves. Both proteins form part of the oxygen-evolving complex and play a role in the supramolecular organization of PSII (Allahverdiyeva et al. 2013). Similarly, SUPPRESSOR OF VARIATION4 (SVR4) and its homologue SVR4L are both also overexpressed in variegated *ljSCO2-1* leaves. Interestingly, ATPB is clearly downregulated in both cotyledons and true leaves, whereas other chloroplastic proteins like FNR and RBCL were slightly down-regulated in the *ljSCO2-1* mutant and mitochondrial COXII and cytosolic ACT was virtually unchanged. In conclusion, absence of LjSCO2 causes mild responses in cotyledons but has more marked effects in true leaves.

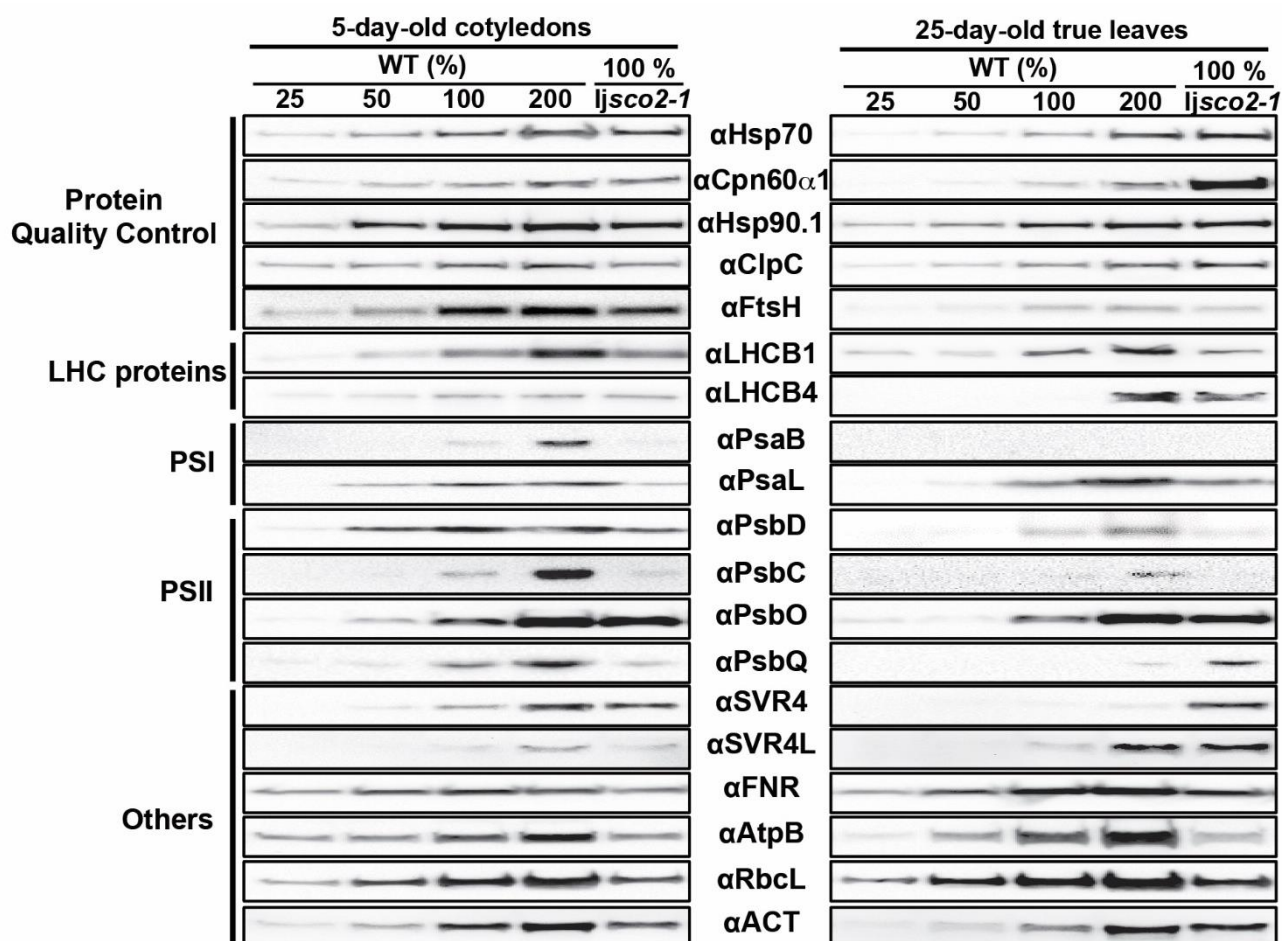


**Figure 4.5** Western-blot analyses of cotyledons and true leaves in *L. japonicus*.

The accumulation of proteins involved in protein quality control, photosynthesis and other processes was analysed by western blotting of samples from 5-day-old cotyledons and 25-day-old true leaves of Lotus. Representative images of immunoblot analyses with the indicated antibodies are shown. Total protein extracts (10 µg of protein) from WT and the *ljsco2-1* mutant were examined, together with a dilution series of the WT sample as indicated.

#### 4.4 SCO2 is involved in the assembly or repair of PSII complexes

We next performed lpBN-PAGE (large-pore blue-native PAGE) on thylakoid samples isolated from true leaves of Arabidopsis (Figure 4.6A) and Lotus (Figure 4.6B), using as detergent either digitonin (left panels) or dodecyl-β-D-maltoside (β-DM, right panels). Digitonin facilitates the analysis of the labile PSI–LHCII megacomplexes, while β-DM permits efficient solubilization without disassembling PSII–LHCII supercomplexes (Järvi et al. 2011). In order to address the impact of lower levels of LHCB1 or PSBD (D2), samples containing equal amounts of chlorophyll were loaded, to compensate for the quantitative differences in the latter between WT and *sco2* mutants (Supplemental Figure 6.13B). After denaturation of the

IpBN gels, immunoblot experiments using a specific antibody directed against the PSBD (D2) protein from the PSII reaction center permitted the detection of all PSII complexes (Figure 4.6A and 4.6B, Supplemental Figure 6.13C). In particular, when digitonin was used as detergent, a reduction in PSII-LHCII super- and megacomplexes, together with a general increase in the PSII assembly complexes reaction centers RC, RC47, RCC1 and RCC2, was observed in *sco2* mutants of both plant species. This suggests that the formation of super- and megacomplexes may be especially impaired in the absence of SCO2. Silver staining of the second-dimension gels corroborated that *sco2* mutants in both species proportionally accumulate less high-molecular complexes than smaller intermediate-sized complexes compared to WT plants (Supplemental Figure 6.14). In addition, an over-accumulation of LHCII trimers was noted in *sco2* mutants, which is compatible with the involvement of SCO2 in the assembly of LHCs into the photosystems (Figures 4.6A and 4.6B). Because SCO2 was found in complexes compatible in size with PSI-LHCII and PSII-LHCII (Shimada et al. 2007), our results indicate that SCO2 has a role in the assembly or repair of PSII.

To determine whether loss of SCO2 can affect state transitions, we determined the maximum fluorescence in state 2 (plants under red light) or state 1 (plants exposed to red and far-red light) (Bellafiore et al. 2005; Pribil et al. 2010). Although *ljSCO2-1* mutant plants generally displayed lower chlorophyll fluorescence (accordingly to the decrease in chlorophyll levels), they showed a WT-like response during the transition between state 2 and state 1 (Supplemental Figure 6.15). The degree of quenching of chlorophyll fluorescence can be quantified by calculating the parameter qT (Pribil et al. 2010; Ruban & Johnson 2009). The qT values obtained for WT ( $0.083 \pm 0.008$ ) and *ljSCO2-1* mutant ( $0.084 \pm 0.008$ ) plants were almost identical, indicating that in the absence of LjSCO2 the plants are still able to undergo reversible state transitions. Inhibition of protein synthesis in the chloroplast does not suppress variegation in *ljSCO2* mutants. The widely accepted threshold model for variegation postulates that an imbalance in the levels of chloroplast and nucleus-encoded photosynthetic proteins is responsible for the impairments in chloroplast development (Liu et al. 2010b; Putarjunan et al. 2013). In line with this, the variegated phenotype of several mutants defective for nucleus-encoded proteins can be suppressed by mutations that reduce rates of protein synthesis in the chloroplast (Hu et al. 2015; Liu et al. 2010a; Liu et al. 2010c). Sub-lethal concentrations of chloroplast translation inhibitors are also able to suppress variegation (Yu et al. 2008). Therefore, we tested whether the chloroplast translation inhibitor lincomycin (LIN) suppresses variegation in *ljSCO2* mutants. Surprisingly, none of the concentrations tested restored normal chloroplast development (Figures 7A and Supplemental Figure 6.16A). In

fact, the *ljSCO2* mutant is hypersensitive to LIN, unlike variegated Arabidopsis mutants such as *var1* (*ftsh5*) and *var2* (*ftsh2*) (Figure 4.7B) (Yu et al. 2008). Chloramphenicol (CAP), an alternative chloroplast translation inhibitor, was similarly unable to suppress leaf variegation in *ljSCO2* mutants (Supplemental Figures 6.16B and 6.16C), implying that the molecular mechanism underlying *ljSCO2* variegation might differ substantially from that responsible for other instances of variegation.

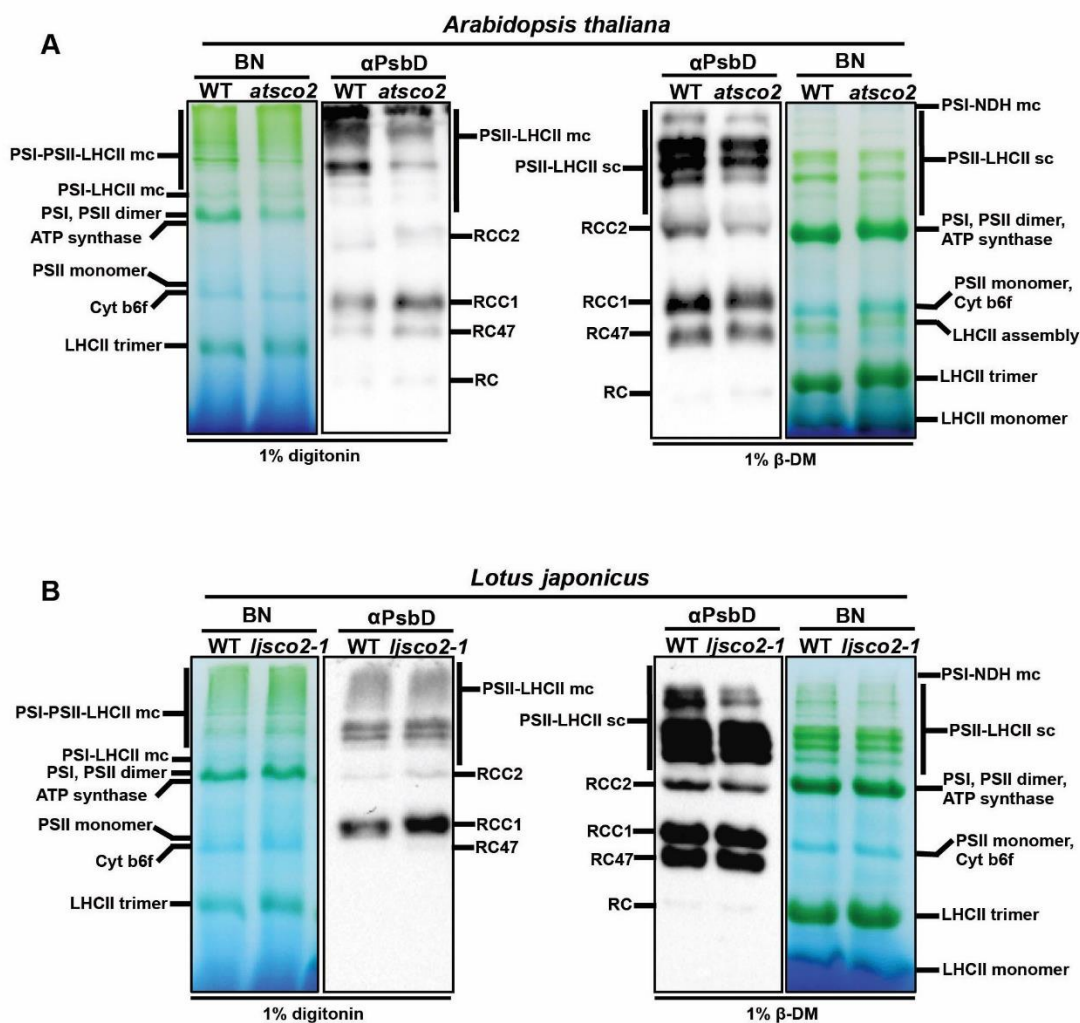


**Figure 4.6** SCO2 is required for PSII supercomplex and megacomplex accumulation.

Thylakoid membranes from Arabidopsis (**A**) and Lotus (**B**) were solubilized in 1% digitonin (w/v) (left panels) or 1%  $\beta$ -DM (w/v) (right panels). Samples were fractionated by 5 to 12% 1pBN-PAGE as described in Methods. Subsequent denaturation and immunoblot analysis with a PsbD-specific antibody allows to compare PSII complex pattern in WT and *sco2* mutants in both Arabidopsis and Lotus. The major protein complexes were assigned to individual bands as described (Järvi et al. 2011). Supercomplexes (sc) and megacomplexes (mc) are indicated.

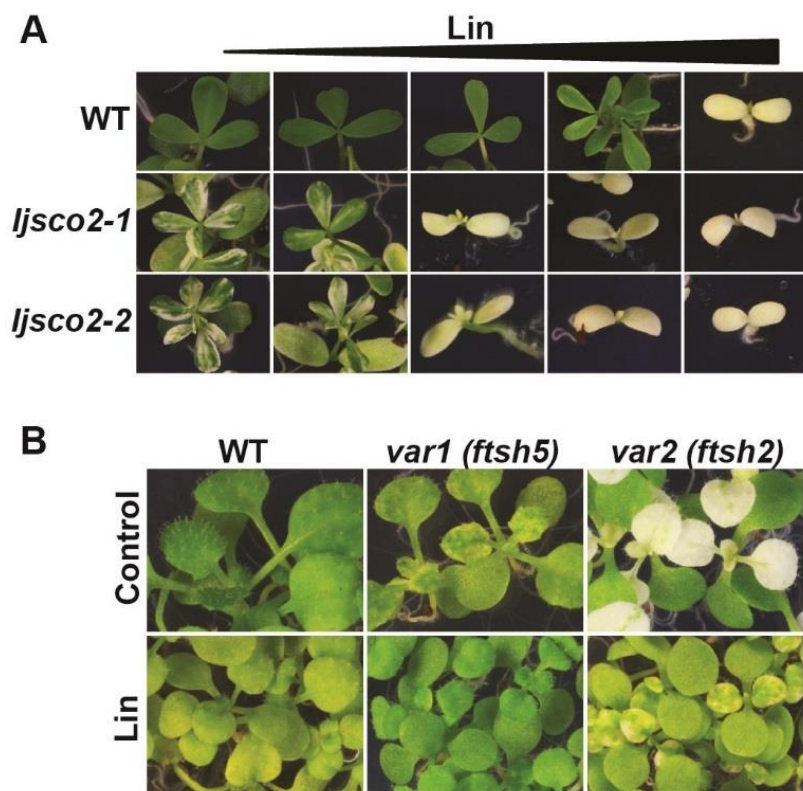


**Figure 4.7 Inhibition of translation in the chloroplast does not suppress variegation in *ljSCO2* mutants**

(A) Representative examples of Lotus WT, and *ljSCO2-1* and *ljSCO2-2* mutant plants germinated and grown for 20 days on MS medium supplemented with increasing concentrations (from left to right: 0, 10, 50, 250 and 2500 µM) of lincomycin (LIN). None of the concentrations tested suppressed leaf variegation in the *ljSCO2* mutants. On the contrary, the mutants proved to be abnormally sensitive to LIN-induced bleaching. (B) Representative examples of *A. thaliana* WT, *var1 (ftsh5)* and *var2 (ftsh2)* mutants grown in the presence or absence of 10 µM LIN. The variegation of true leaves in *ftsh* mutants is suppressed in the presence of LIN.

#### 4.5 SCO2 has also a role in variegation in *A. thaliana*

The finding that *atsco2* leaves are smaller and paler than their WT counterparts under short-day conditions (Figure 4.2D), and that assembly of PSII complexes is impaired in the mutant (Figure 4.6A), demonstrates that the AtSCO2 function also extends beyond the cotyledon stage in Arabidopsis. The enhanced sensitivity of *ljSCO2* mutants to lincomycin (LIN) suggests a link between SCO2 and protein synthesis in the chloroplast. Therefore, a double mutant was generated in Arabidopsis by crossing *atsco2* with the *atclpr1* mutant (also named *svr2*) (Supplemental Figure 6.17), which was previously shown to suppress the variegation phenotype of the *var2* (*ftsh2*) mutant (Yu et al. 2008). In fact, *atclpr1* is impaired in chloroplast rRNA processing, a feature shared by several suppressors of variegation (Yu et al. 2008). As a consequence, chloroplast translation is inhibited in *atclpr1* and several representative plastid genes display normal levels of transcripts but reduced protein accumulation (Koussevitzky et al. 2007). Strikingly, the double mutant *atsco2 atclpr1* exhibited very pale and variegated true leaves (Figure 4.8A), which supports a function for AtSCO2 in photosynthetically competent leaves in Arabidopsis. The additive phenotype in the double mutant already becomes manifest at the seedling stage (Figure 4.8B). This is in striking contrast to the variegated mutants *var2* (Yu et al. 2008) and *thf1* (Ma et al. 2015), which display reduced leaf variegation when the corresponding mutations are introduced into a background in which protein synthesis in chloroplasts is compromised. Taken together, these results point to a distinct mechanism of action for SCO2.

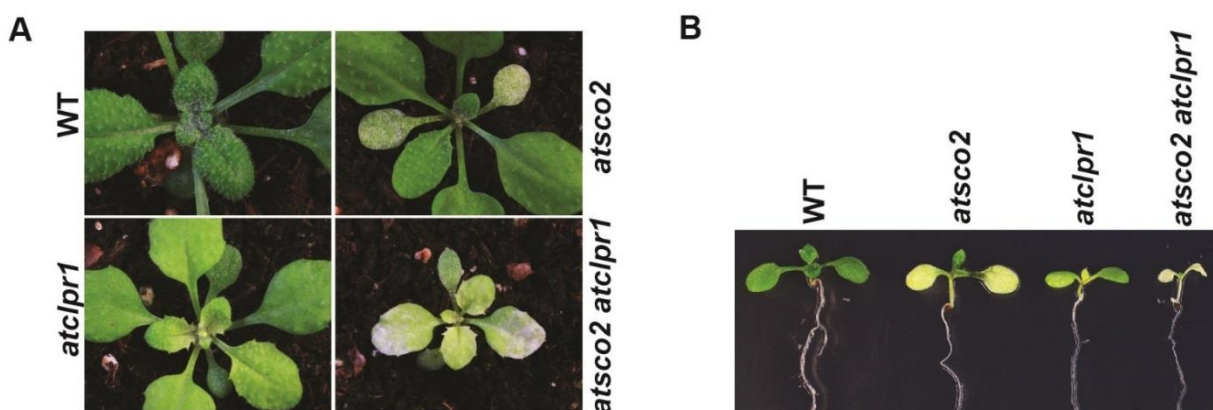


**Figure 4.8** *Arabidopsis thaliana* double mutant *atsco2 atclpr1* displays a variegated phenotype.

Representative 3-week-old Arabidopsis plants (A) and 10-day-old seedlings (B) grown in long-day conditions. Genotypes: WT, *atsco2*, *atclpr1* and *atsco2 atclpr1*.

## 5. Discussion

### 5.1 CRASS is located in the stroma of *Arabidopsis thaliana* chloroplasts

In this study we have identified the *Arabidopsis thaliana* protein CRASS as an important factor involved in the stability and activity of the 30S subunit of the chloroplast ribosome. We have demonstrated that the lack of CRASS leads to a lower fitness under optimal growth conditions and to severe phenotypes when ribosome activity is challenged (Figures 3.4 and 3.5). Chloroplast development is characterized by a very high demand for *de novo* protein synthesis since the crucial photosynthetic machinery has to be built rapidly to sustain plant growth. Defects in the translational machinery generally lead to evident phenotypes especially in young tissues. The lack of any obvious phenotype among CRASS knockout plants even in developing leaves indicates that CRASS does not play any essential role for ribosome biogenesis, stability or activity under optimal growth conditions. A guilt-by-association approach helped us identifying this protein which was probably overlooked by previous studies even if it was found from different groups in mass spectrometry of chloroplast ribosomes (Friso et al. 2004; J. Wang et al. 2016; Zybailov et al. 2008) and it is evident from databases search that it is also strongly coexpressed with ribosomal proteins (Figure 4.1A). The predicted chloroplast localization was suggested by its cTP and several groups reported CRASS in the stroma fraction with abundance levels comparable to those of chloroplastic ribosome proteins (Olinares et al. 2010; Zybailov et al. 2008; Zhang et al. 2016). We confirmed its localization by confocal microscopy with a recombinant CRASS-YFP line. Stroma localization was confirmed also by western blot and it is in agreement with the localization of most ribosomal proteins which often form aggregates around the nucleoid fractions. CRASS has not been identified so far in nucleoid co-immunoprecipitation experiments even if YFP aggregates in the chloroplast were often found during preliminary confocal microscopy analysis. This might suggest a transient binding with proteins that can be easily broken during nucleoid extraction. Sporadic observations of CRASS-YFP within chloroplast stromules further suggests that the binding to the nucleoids is not permanent since so far nucleoids are not known to be present in stromule fractions (Newell et al. 2012). At this stage of the work though, we consider the presence of punctuate patterns of YFP expression in the chloroplasts as an artefact due to the excess of recombinant protein induced by the strong 35S promoter leading to the formation of non functional YFP aggregates within the chloroplasts (Llamas et al. 2017).

## 5.2 The HMA domain of CRASS lost its function during evolution

CRASS is present in land plants and generally in Embryophytae but it is absent in *Chlamydomonas* and other photosynthetic organisms. However, we found no CRASS homolog in bacteria, algae or yeast, with the exception of bacterial HMA proteins with only partial homology. Therefore, it is likely that CRASS protein might have evolved from a HMA protein, after a gene transfer from bacteria occurred millions of years ago.

The lack of the essential cysteines makes the domain unable to bind the metals and perform any transport or detoxification activity. Probably, CRASS gained during evolution a completely different function in the binding of specific ribosomal proteins or assisting the assembly of the ribosome. Examples of similar conserved domains with lost or changed function can be found in several proteins. One example is the group of glutaredoxin-like domain proteins lacking the essential cysteine in the active site and thus seems to have lost glutaredoxin activity (Pulido and Leister, 2017). An alternative RNA related predicted function has been described showing a strong similarity between the RNA recognition motif (RRM) and HMA domains since both are composed of tandem repeats with an oligomeric structure that is usually associated with the binding of single stranded RNA (Aloy et al. 2002).

## 5.3 CRASS assists ribosome assembly when stress is applied

In order to challenge our mutants, we looked for conditions in which translation is reduced. Several ribosomal subunit mutants show evident phenotypes only in cold stress conditions (Zhang et al. 2016; Rogalski et al. 2008). Two main reasons have been proposed to explain this sensitivity to cold stress. First, in these conditions, molecules trafficking within the chloroplast is slowed down so that an unstable structure caused by a missing subunit ends up in an impaired rRNA folding and processing that in turn will delay plant growth (Ehrnthaler et al. 2014). Secondly, an unstable ribosome induces a retrograde signaling from chloroplast to nucleus further reducing plant fitness (Leister 2012). Knocking out a retrograde signaling modulator like GUN1, in fact, leads to a milder phenotype in a *prps1* mutant background (Tadini et al. 2016). In this regard, we tested cold stress at both seedling and adult stage and in each of the two cases the mutant phenotype was clearly distinct from the WT one. Mutant seedlings after 6 weeks of growth at 4 °C almost lost their ability to sustain chloroplast biogenesis when transferred to 22 °C. Young leaves of adult mutant plants transferred to cold chamber showed a lower photosynthetic efficiency compared to WT leaves. This was less

evident in older leaves, where translational capacity decreases and the unpaired machinery manages to produce anyway wild type like amounts of proteins (Fleischmann et al. 2011). Thus, the lower  $F_v/F_m$  in young leaves is presumably the effect of a limited translational capacity which in turn slows down chloroplast biogenesis. Complementation with the recombinant YFP fusion gene restores WT levels of photosynthesis efficiency. It would be interesting to characterize double knockouts *crass* x *gun1* in order to investigate or rule out a potential retrograde signaling function of CRASS as occurs in other ribosomal components.

An additional layer of evidence for CRASS involvement with ribosomal activity was given by tests with lincomycin, a specific chloroplast translation inhibitor (Tenson et al. 2003; Llamas et al. 2017). Growing mutants and WT on MS supplemented with lincomycin yielded a decrease in seedling vitality more critical where CRASS was knocked out (Figure 3.4). Chlorophyll and carotenoid levels were significantly different and genetic complementation also in this case evidenced the hypersensitivity directly caused by the absence of the CRASS protein (Supplemental Figure 6.6). On the other hand, similarly to ribosomal mutants with very mild phenotype as *psrp2* and *psrp6* which show no differences on polysome loading (Tiller et al. 2012) we found no reliable difference between WT and *crass* mutants.

#### 5.4 CRASS interacts with chloroplastic small ribosomal proteins

The YFP tagged *oeCRASS#1* line has been used for phenotype complementation by crossing it with *crass-1*, demonstrating that the recombinant CRASS-YFP is active *in vivo* (Figure 3.2). Therefore, it was also analysed in coimmunoprecipitation experiments that pulled down both proteins and RNA which we investigated by mass spectrometry and deep sequencing (Table 3.1 and Figure 3.6). RNA extraction from the WT control using GFP beads rescued only traces amounts of RNA. The RNA in the eluate of the transgenic line instead was composed almost exclusively by chloroplastic ribosomal RNA, mainly 16S (Figure 3.6A and Supplemental Table 6.2). Slot blot analysis further confirmed that 16S rRNA was pulled down significantly in higher amounts compared to WT or other RNAs tested (Figure 3.6B).

The eluates were also used for protein identification yielding a great abundance of chloroplastic ribosomal proteins. In order to verify the actual presence of the ribosomal proteins we run a western blot with antibodies raised against ribosomal proteins and strikingly only those from the 30S subunit gave a clear signal. Additionally the PRPS1 interaction remained stable even after RNase treatment pointing more toward a direct protein-protein

interaction rather than a CRASS-RNA interaction. The RNA that was isolated is very likely the effect of pulling down native 30S ribosomal complexes.

Size exclusion chromatography has been used to detect binding with assembled ribosomes (Figure 3.8A). Looking at the accumulation of PRPS5 and PRPL11 there is an indication that after RNase treatment most of the ribosomes were degraded but a strong CRASS GFP band larger than Rubisco is present. This suggests that CRASS binding to the ribosomes is direct and not dependent on mRNA or rRNA.

### 5.5 CRASS is directly involved in ribosome functionality

A final proof for an interaction between ribosomal proteins and CRASS comes from the double mutants *crass-1 prps17* and *crass-1 prpl11* where the genetic interaction leads to a clear synergistic phenotype.

PRPL11 is a nonessential subunit whose mutant phenotype is characterized by a mild impairment in growth and photosynthesis efficiency (Pesaresi et al. 2001). When in this background also CRASS is missing, the additive phenotype is only visible in young leaves where the  $F_v/F_m$  is slightly decreased while the rest of growth parameters are unchanged. The double mutant *crass prps17* is instead strongly delayed in growth, photosynthesis efficiency and seed viability, especially in short day where plants have less time per day to build up photosynthetic machinery and the genetic interaction leads to a clear synergistic phenotype. (Figure 3.9 and Supplemental Figure 6.7).

More experiments are required to elucidate the exact molecular mechanism that makes CRASS vital for the plant during cold stress or translation inhibition. One hypothesis is that the CRASS mutation affects directly the translation rate, already reduced at chilling temperature causing the impaired protein synthesis and photosynthesis capacity. Alternatively, instead of affecting the entire translation process by itself, it might alter the folding or structural localization of a ribosomal subunit, e.g. PRPS1, inducing a more severe defect in translation and ribosome assembly.

## 5.6 SCO2 is a DNAJ-related protein involved in chloroplast biogenesis

The group of SNOWY COTYLEDON mutants is composed by several mutants whose role is supposed to be exclusive for cotyledon biogenesis and greening with a rather unaltered growth of the rest of the plant. In this study, we showed that SNOWY COTYLEDON 2, (SCO2), previously characterized as a cotyledon specific factor (Albrecht et al., 2008; Shimada et al., 2007), is indeed playing a key role when the plant is forming cotyledons, but differently to what was reported previously, we found that SCO2 is also crucial in true leaves since its lack leads to stunted growth in short day conditions. In addition, we here reported three *Lotus japonicus* mutant lines with knocked out expression of SCO2, all of them clearly characterized by pale cotyledons and variegated true leaves (Figure 4.1 and Supplemental Figure 6.8). *Ljsco2* mutants are also affected during the transition from dark (etioplast) to light (chloroplast) and in the accumulation of PSI (Figure 4.2A). These findings reveal a new role in leaf development for SCO2, and support the hypothesis that it has a deeper importance than previously expected.

The SCO2 gene shows some similarities to the DNA-J clade, a group of molecular chaperone proteins, but lacks the central J-domain needed for direct interaction with the Hsp70 chaperones. It maintained instead the CXXCXGXG zinc finger domain which is needed for protein binding and allows conformational changes by oxidizing thiol groups (Shimada et al. 2007; Muranaka et al. 2012; Rajan & D'Silva 2009). The closest paralogue to SCO2 is LOW QUANTUM YIELD 1 (LQY1), the mutant of which does not display either albino cotyledons or an obvious defect in chloroplast biogenesis (Lu et al. 2011).

## 5.7 SCO2 is required for the assembly or repair of LHC

Chaperones and proteases act co-ordinately as constituents of the protein quality control system that is essential for plant survival (Lee et al. 2009; Pulido et al. 2016). In chloroplasts, it is well known that the chaperone Hsp70 post-translationally regulates PSII assembly and repair, and contributes to the heat-shock response and protein import into the chloroplast (Schroda 1999; Shi & Theg 2010; Su & Li 2010; Su & Li 2008). The specificity of Hsp70 is known to be determined by its DNAJ partners, which act as adaptors that recognize unfolded substrates and transfer them to the chaperone for refolding. In classical A-type DNAJ proteins, the J-domain is responsible for the interaction with Hsp70, while the zinc finger interacts with the substrate (Kampinga & Craig 2010; Miernyk 2001; Rajan & D'Silva 2009).

In the absence of a conserved J-domain, DNAJ-related proteins are assumed to exhibit a chaperone-like activity independently of Hsp70, interacting with and stabilizing client substrates, such as the ORANGE (OR) proteins required for accumulation of phytoene synthase (PSY) and the biosynthesis of carotenoids (Zhou et al. 2015). Interestingly, the closest homolog of SCO2, LOW QUANTUM YIELD OF PHOTOSYSTEM III (LQY1), shows disulphide isomerase activity and interacts with the PSII core complex (Lu et al. 2011). Indeed, AtSCO2 itself reduces cysteines in artificial substrates in vitro (Muranaka et al. 2012; Shimada et al. 2007). Both LQY1 and AtSCO2 participate in the assembly or repair of PSII complexes, but they differ in the number of pairs of cysteines conserved (only 2 in SCO2, Supplemental Figure 6.9), and in their interaction partners, as revealed by BN-PAGE analyses (Lu et al., 2011; Shimada et al., 2007). LQY1 was found to comigrate with the PSII core monomer (RCC1) and the CP43-less PSII monomer (RC47) after exposure to high light levels, which suggests a role in repair and reassembly of PSII complexes (Lu et al., 2011). AtSCO2 associates with PSI-LHCII and PSII-LHCII complexes, but further experiments are required to characterise these complexes. We have demonstrated that *sco2* mutants in both Arabidopsis and Lotus not only accumulate reduced amounts of PSII components, but are defective in the biogenesis or repair of the PSII complexes in true leaves (Figure 4.6, Supplemental Figure 6.13C and 6.14). Thus, there is a general increase of the levels of intermediate complexes RC, RC47, RCC1 and RCC2, with a concomitant build-up of LHCII trimers in *sco2* mutants. Accordingly, maximum quantum yield and electron transport rate of PSII are both reduced in *ljSCO2* mutants (Figure 4.4A). However, PSI accumulation is also affected, as can be deduced from 77K fluorescence emission experiments (Figure 4.2A) and previous reports (Figure 4.5) (Albrecht et al., 2008; Shimada et al., 2007). Additionally, the levels of the ATP synthase subunit AtpB are decreased in the absence of LjSCO2 (Figure 4.5) such that other roles of LjSCO2 in thylakoid biogenesis and functioning, in addition to photosystem-related processes, cannot be ruled out. Although the only substrate known to interact with AtSCO2 in vivo is LHCB1 (Tanz et al., 2012), other putative targets have been proposed. Thus analysis with the split-ubiquitin system has suggested the interaction of AtSCO2 with PSI (A1 and A2 subunits), as well as PSII (CP43 and CP47 subunits) (Muranaka et al., 2012). However, the in vivo relevance of these interactions remains to be studied. The effects on NPQ noted in *sco2* mutants might result from these complex interactions. The Lotus *ljSCO2-1* mutant displays a rapid increase in NPQ values upon illumination, but the values remain below the WT average until the situation is reversed in the relaxation phase (Figure 4.4B). Faster NPQ induction may be linked to pre-accumulation of

zeaxanthin in the *ljSCO2-1* mutant (Figure 4.4C), which is only detected in WT plants under high light conditions (Supplemental Figure 6.12). Given that AtSCO2 interacts with LHCB1, it is not surprising that LjSCO2 has a role in the regulation of NPQ. LHCB1 is involved in thermal dissipation of the excess light energy absorbed during photosynthesis (Niyogi and Truong, 2013) and the down-regulation of LHCB1 produces a decrease in NPQ values (Pietrzykowska et al. 2014). Interestingly, wild-type plants also show an increase in NPQ at higher temperatures (Bilger & Bjorkman 1991) and after heat shock (Marutani et al. 2014). Moreover, paraquat treatment causes NPQ to peak at the beginning of the quenching phase (Moustaka et al. 2015), as in the *ljSCO2-1* mutant. Therefore, maybe other stress situations can also induce zeaxanthin levels. The fact that the *ljSCO2-1* mutant is under constitutive stress, as indicated by the accumulation of zeaxanthin and tocopherols (Figure 4.4C and Supplemental Figure 6.12) and higher levels of chaperones and proteases (Figure 4.5), might contribute to the observed alterations in NPQ.

## 5.8 SCO2 constitutes a novel factor involved in leaf variegation

Multiple factors have been reported to control leaf variegation. In Arabidopsis, *immutans* (*im*) and *variegated 2* (*var2*) mutants, which are defective in plastid terminal oxidase (PTOX) and the thylakoid protease FtsH2, respectively, are the best characterized chloroplast biogenesis mutants (Foudree et al. 2012; Aluru et al. 2006; Putarjunan et al. 2013). Loss of PTOX impairs the activity of phytoene desaturase (PDS), an enzyme in the carotenoid biosynthesis pathway (Ruiz-Sola & Rodríguez-Concepción 2012). PTOX is a central regulator of thylakoid redox and PSII excitation pressure, modulating the redox state of the PQ pool. Thus the variegation seen in the absence of PTOX has been attributed to a redox imbalance in Arabidopsis (Rosso et al. 2009). Mutational inactivation of PROTON GRADIENT REGULATION5 (PGR5) or CHLORORESPIRATORY REDUCTION2 (CRR2) suppresses variegation in *im* mutants by reducing the excitation pressure (Hashimoto et al. 2003; Munekage et al. 2002; Okegawa et al. 2010). The suppression of variegation in *var2* mutants has uncovered a link with protein biosynthesis in the chloroplast. Several mutations affecting chloroplast translation or chloroplast RNA processing have been reported to suppress variegation in plants lacking FtsH2 (Liu et al., 2010a; Miura et al., 2007; Park and Rodermel, 2004; Yu et al., 2008; Yu et al., 2011). Furthermore, the variegated phenotype of a mutant named *thylakoid formation 1* (*thf1*) is also suppressed when chloroplast protein biosynthesis is impaired (Hu et al. 2015; Ma et al. 2015). Interestingly, THF1, like AtSCO2, interacts with

LHCB1. However, the inhibition of chloroplast translation (Figure 4.7 and Supplemental Figure 6.16) does not suppress the variegation in *ljsc2*. Furthermore, the clearly additive effect seen in variegated true leaves in *atsco2 atclpr1* plants demonstrates that reducing rates of protein biosynthesis in the chloroplast actually exacerbates the defect in chloroplast biogenesis observed in the absence of SCO2 alone. Hence, we suggest that variegation in *ljsc2* mutants is controlled by a distinct molecular mechanism.

Since the variegation phenotype is based on the incorrect balance of quantity and type of FtsH subunits, it is possible that SCO2 acts as a helper in delivering the required FtsHs from stroma-exposed lamellae to grana margins where D1 degradation takes place (Adam et al. 2005; Järvi et al. 2016). The zinc finger domain might have a cochaperone activity similar to DNAJ proteins assisting the precise assembly and activity of the FtsHs. The carrier activity hypothesis is supported by the previously reported vesicle formation in *sc2* cotyledons (Tanz et al. 2012) where the lack of SCO2 affects strongly the transport of proteins toward the interior of the chloroplast.

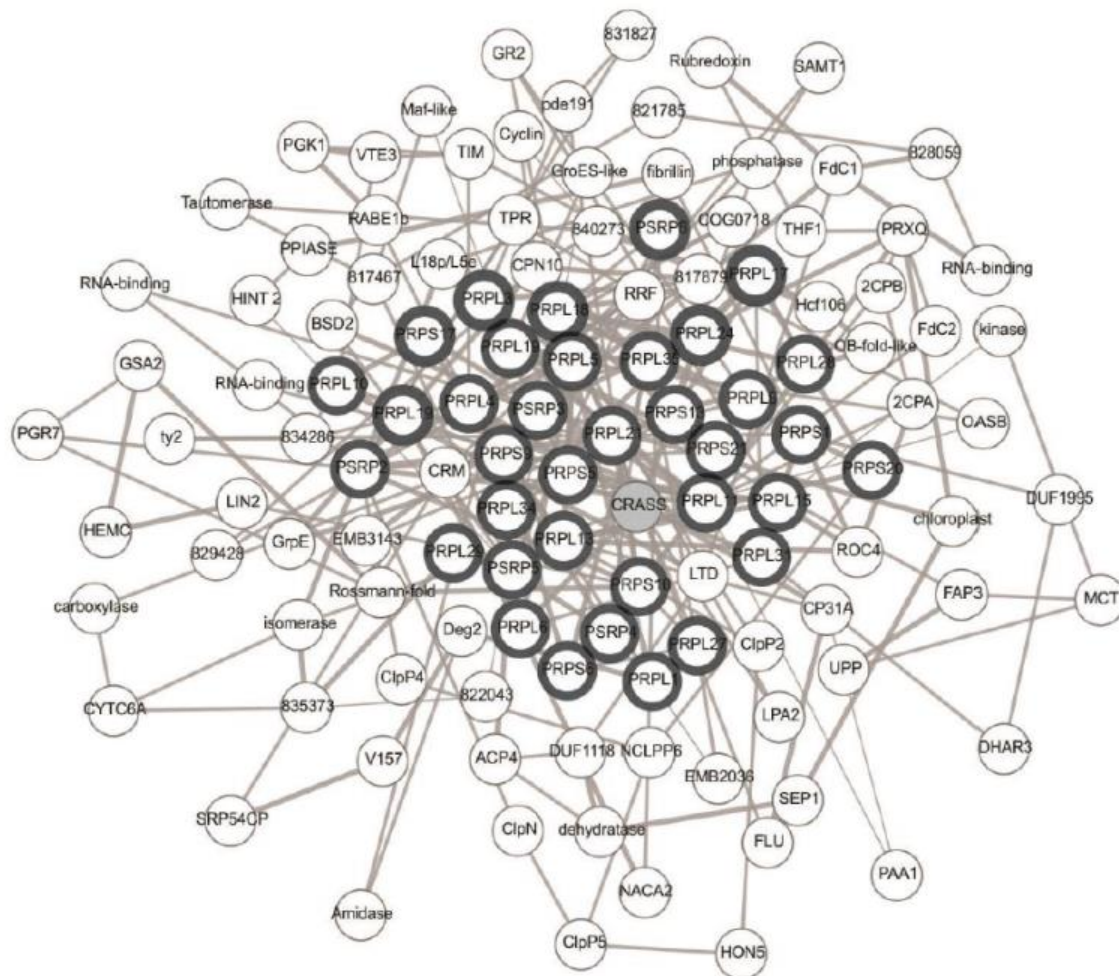
Interestingly *FtsH4* mutants, defective for a mitochondrial targeted protease, (Gibala et al. 2009) show several characteristics in common with *sc2* phenotypes. Namely, a short day specific phenotype, chloroplast defect and an overexpression of HSP70. In the model proposed here (Figure 4.8C), THF1 and FtsH affect the accumulation of LHCS and the PSII reaction-center protein D1, respectively. In both cases, the balance required for the assembly of photosynthetic mega-complexes is disrupted, hence producing variegation. Decreasing protein biosynthesis in the chloroplast (by deleting ClpR1 or applying inhibitors of chloroplast translation such as LIN) reduces the levels of chloroplast-encoded components of the photosynthetic machinery, partially restoring the stoichiometry required for complex assembly and suppressing variegation. However, the absence of SCO2 impaired the attachment of LHCS to PSI and PSII. In this genetic situation, the reduction of chloroplast translation with inhibitors or the introduction of the *atclpr1* mutation further aggravates the perturbation in the assembly of the photosystems with the antenna complexes (Figure 4.8C).

## 5.9 Stressful environmental conditions facilitate protein characterization

In conclusion, this thesis puts the emphasis on the possibility to discover new gene functions by artificially altering plant growth conditions. Under optimal greenhouse conditions *crass* mutants would be undistinguishable from the WT and, except for the pale cotyledons, the

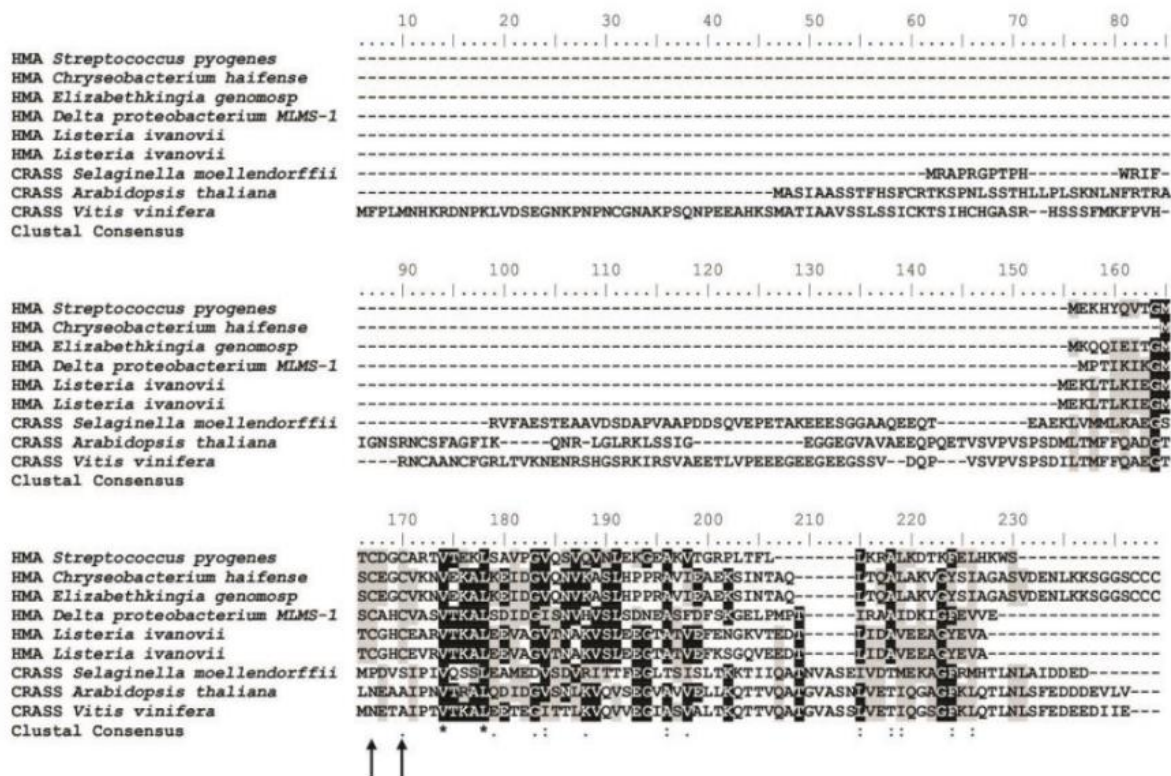
same holds true for *scd2* plants. Both CRASS and SCO2 have been characterized by inducing stresses that enhanced otherwise undetectable phenotypes. Especially for those proteins that interact transiently, or only under a specific stress, with their targets, such an approach extends the likelihood of correctly identifying interaction partners and protein function. In this regard, the guilt-by-association approach we used is crucial to select candidate genes whose function can be partially predicted but which has never been demonstrated and which can potentially be characterized at molecular level with the available expertise. Further co-immunoprecipitation and biochemical studies are necessary to finalize the understanding of the precise function of these proteins and their mechanism of action, being now clear that their presence in the chloroplast is not as disposable as previously thought.

## 6. Appendix



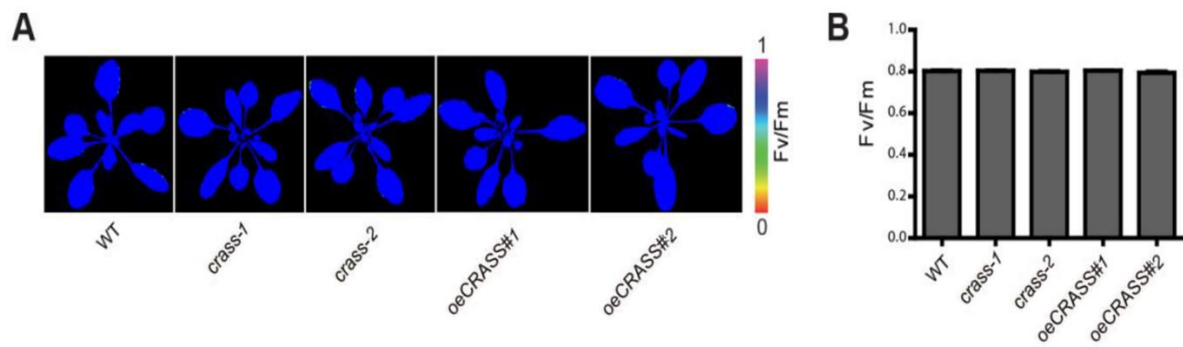
**Supplemental Figure 6.1 The coexpression regulon of plastid ribosomal proteins.**

Nuclear encoded plastid ribosomal proteins (PRPs) and plastid specific ribosomal proteins (PSRPs) genes (Tiller and Bock, 2014) were selected for “guilt-by-association” analysis: PRPS1 (AT5G30510), PRPS5 (AT2G33800), PRPS6 (AT1G64510), PRPS7 (AT5G30510), PRPS9 (AT1G74970), PRPS10 (AT3G13120), PRPS13 (AT5G14320), PRPS17 (AT1G79850), PRPS20 (AT3G15190), PRPS21 (AT3G27160), PRPL1 (AT3G63490), PRPL3 (AT2G43030), PRPL4 (AT1G07320), PRPL5 (AT4G01310), PRPL6 (AT1G05190), PRPL9 (AT3G44890), PRPL10 (AT5G13510), PRPL11 (AT1G32990), PRPL13 (AT1G78630), PRPL15 (AT3G25920), PRPL17 (AT3G54210), PRPL18 (AT1G48350), PRPL19 (AT5G47190, AT4G17560), PRPL21 (AT1G35680), PRPL24 (AT5G54600), PRPL27 (AT5G40950), PRPL28 (AT2G33450), PRPL29 (AT5G65220), PRPL31 (AT1G75350), PRPL34 (AT1G29070), PRPL35 (AT2G24090), PSRP2 (AT3G52150), PSRP3 (AT1G68590), PSRP4 (AT2G38140), PSRP5 (AT3G56910) and PSRP6 (AT5G17870). The co-regulation gene network derived from condition-independent co-expression analysis was generated using the ATTED-II tool ([www.atted.jp](http://www.atted.jp)). Input genes are marked with a thicker line. CRASS protein target is highlighted in grey.



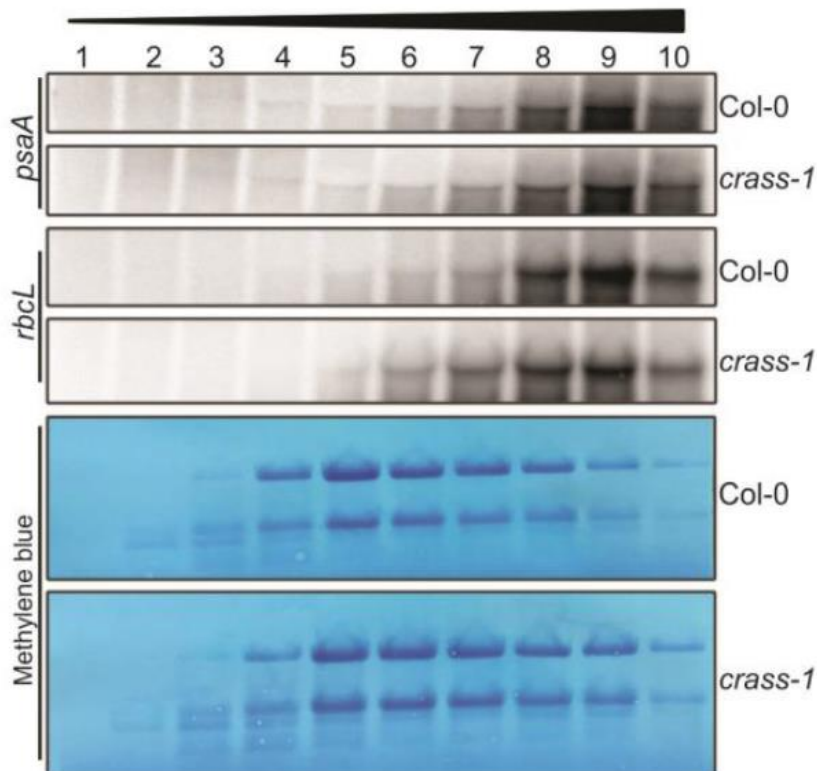
Supplemental Figure 6.2 Sequence alignment of CRASS and bacterial heavy metal associated (HMA) proteins.

An alignment of the full sequence of CRASS proteins and HMA proteins is shown. The sequences were aligned using MUSCLE (<http://www.ebi.ac.uk/Tools/msa/muscle>) and Bioedit editor (see “Materials and Methods”). The consensus sequence is indicated with identical residues marked by asterisks. Arrows mark the two cysteines conserved in the active site of HMA domain, absent in CRASS proteins.



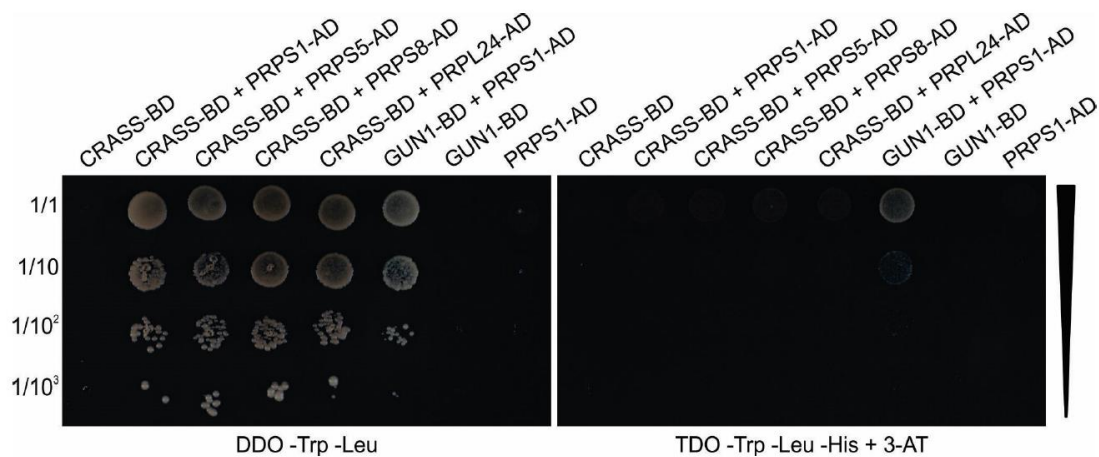
**Supplemental Figure 6.3 Altered CRASS levels do not affect to photosynthetic efficiency.**

(A) Representative picture of 21-days-old wild-type (WT), *crass-1*, *crass-2*, *oeCRASS#1* and *oeCRASS#2* plants grown in long day conditions were analyzed using an Imaging PAM system as described in “Materials and Methods.” The photosynthetic parameter  $F_v/F_m$  (maximum quantum yield of PSII) was measured as indicated by the color scale (bar on the right). (B) Quantification of  $F_v/F_m$  values confirmed that the different lines do not exhibit differences growing in control conditions.



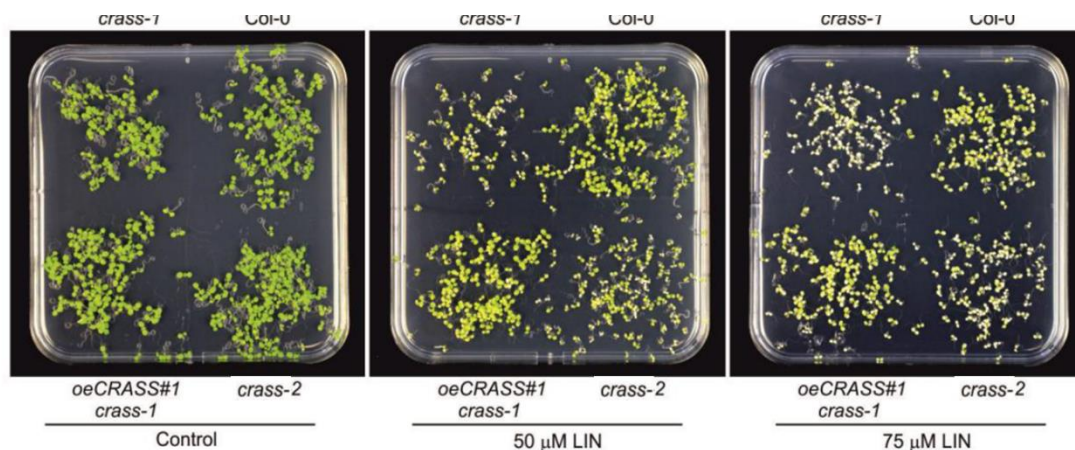
**Supplemental Figure 6.4 Analysis of the effect of CRASS on polysome loading of *psaA* and *rbcL*.**

RNA gel blot analysis of polysome fractions from a 15 to 55% sucrose gradient of the wild-type (Col-0) and *crass-1* plants as indicated in “Materials and Methods.” rRNA was stained with methylene blue.



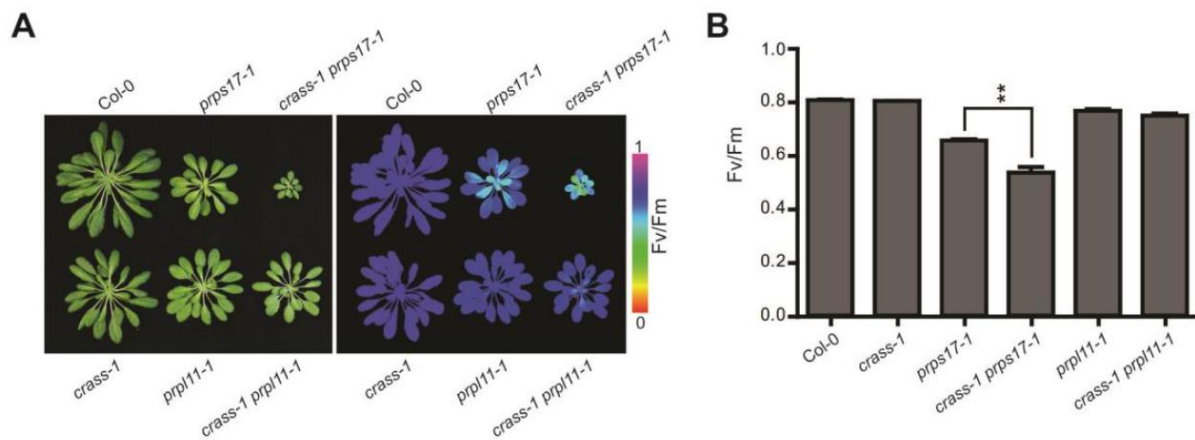
**Supplemental Figure 6.6** Yeast two hybrid analysis of CRASS and ribosomal proteins.

Yeast cells were cotransformed with a plasmid expressing mature CRASS-BD as bait protein and plasmids expressing ribosomal proteins PRPS1-AD, PRPS5-AD and PRPL24-AD as prey proteins. Interaction was tested on media double drop out (DDO) lacking tryptophane (Trp) and leucine (Leu) and quadruple drop out (QDO) additionally lacking histidine (his) and adenine (ade) with a dilution series 1:10 starting with an  $OD_{600}$  of 2. Although the presence of both plasmids allowed the yeast to grow in DDO media, none of the combinations survived on QDO media. Although the presence of both plasmids allowed the yeast to grow except for GUN1-BD/PRPS1-AD, which served as the positive control. GUN1 was previously shown to interact with PRPS1 in yeast-two-hybrid experiments (Tadini et al., 2016). Therefore, direct interactions between CRASS and the ribosomal proteins could not be demonstrated by yeast two hybrid analysis.



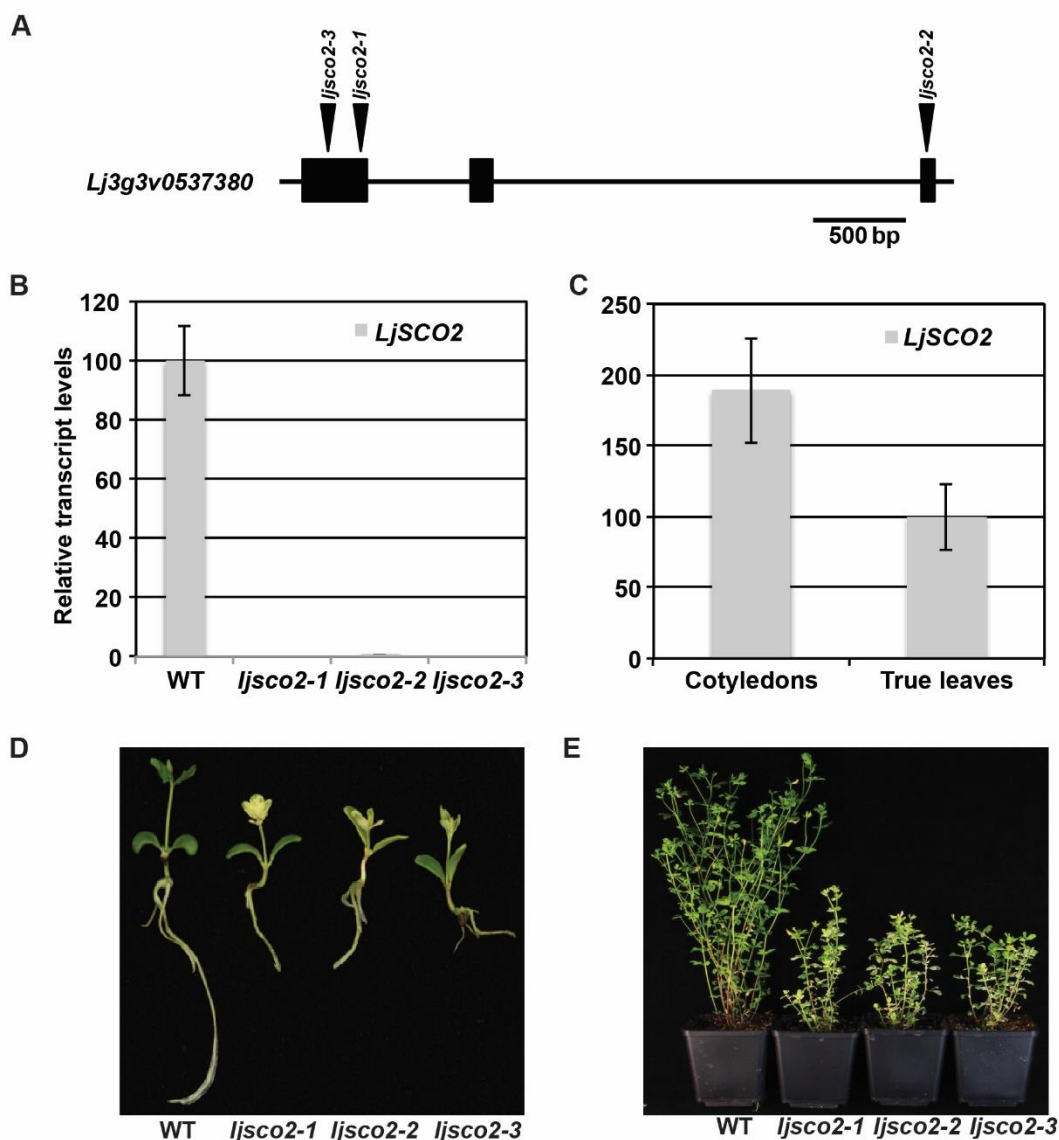
**Supplemental Figure 6.5** Analysis of the inhibition of chloroplast translation in overexpressor lines.

Representative pictures of wild-type (Col-0), *crass-1*, *crass-2* and overexpressor lines *oeCRASS#1 crass-1* growing in plates for 10 days in control conditions or under lincomycin treatments as indicated. Significantly the overexpression of CRASS-YFP suppress the hypersensitivity of *crass-1* to LIN-induced bleaching, confirming the activity of the fusion protein in the transgenic line.



**Supplemental Figure 6.7 Analysis of plant development in short day conditions in the absence of plastidial ribosomal proteins.**

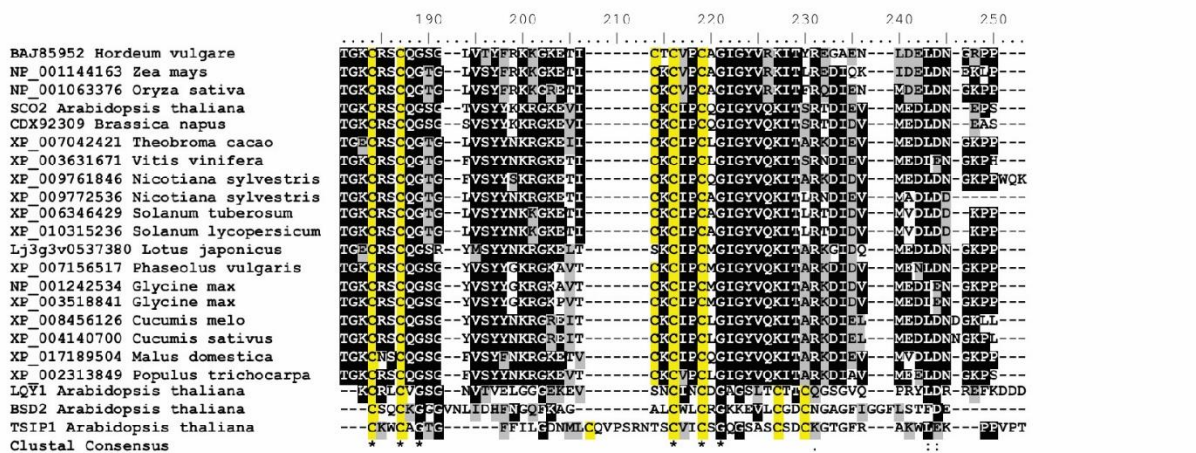
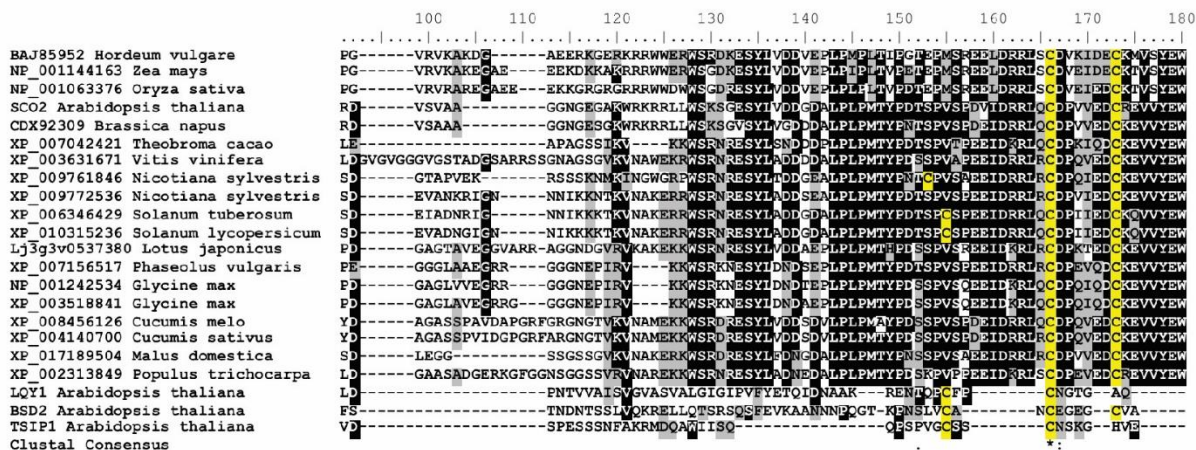
(A) Representative picture of the indicated backgrounds after 60 days in short day conditions (left panel). The photosynthetic parameter  $F_v/F_m$  (maximum quantum yield of PSII) was measured using an Imaging PAM system as described in “Materials and Methods” (right panel). (B) Quantification of  $F_v/F_m$  measures demonstrated an additive effect in the double mutant *crass-1 prps17-1* but not in *crass-1 prpl11-1*. Average and SE (n = 20) are provided. Student’s t-test (\*\*P < 0.01) was used for statistical analysis.



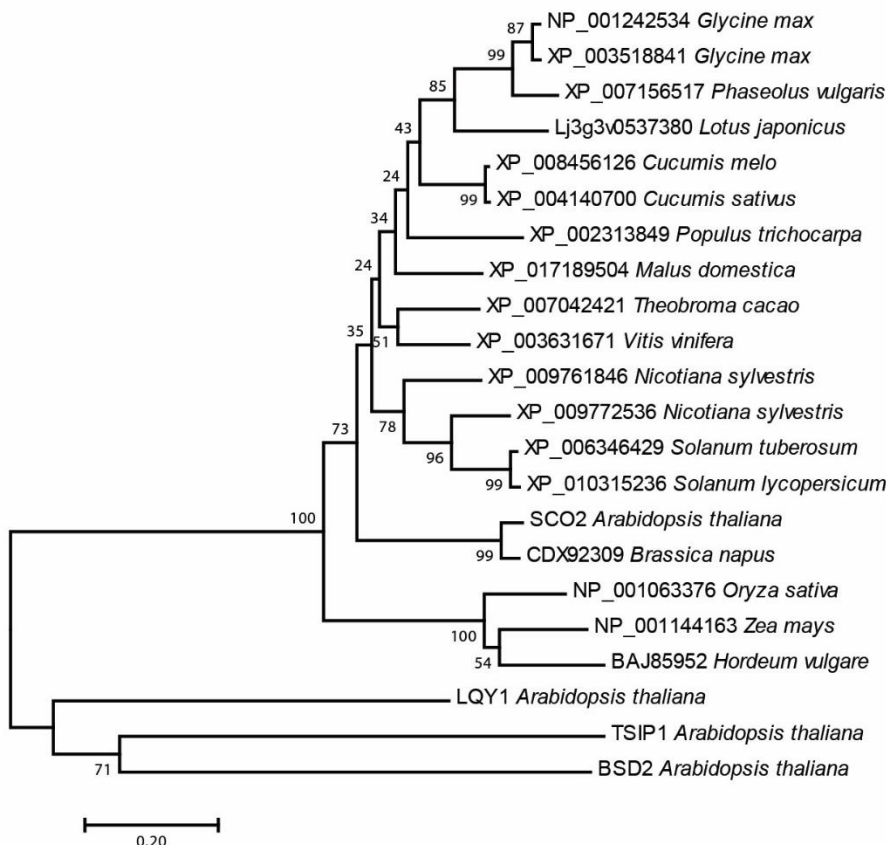
**Supplemental Figure 6.8 Characterization of three independent mutant lines for SCO2 in *Lotus japonicus*.**

(A) Schematic representation of the structure of the *LjSCO2* gene (*Lj3g3v0537380*) showing the positions of the *LORE1* retrotransposon in the lines *ljsco2-1* (30096086), *ljsco2-2* (30099994) and *ljsco2-3* (30006602). All mutations disrupt the *LjSCO2* ORF. (B) RNA samples from WT and *ljsco2* mutants were used for quantitative PCR analysis of *LjSCO2* transcript levels using the *LjUBQ* gene as a control (see Methods). (C) Transcript levels of *LjSCO2* was compared between 4-days-old cotyledons and 25-days-old true leaves for WT plants. The graphs show mean and SD values of n=4 independent experiments. Phenotypes of representative *Lotus* wild-type (WT), *ljsco2-1*, *ljsco2-2* and *ljsco2-3* mutants are shown at the ages of 14 days (D) and 60 days (E). In addition to the variegation phenotype, *ljsco2* mutants display stunted root and shoot growth.

A

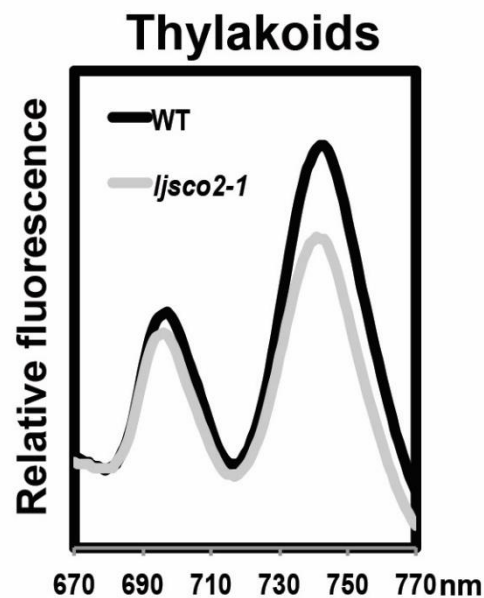


B

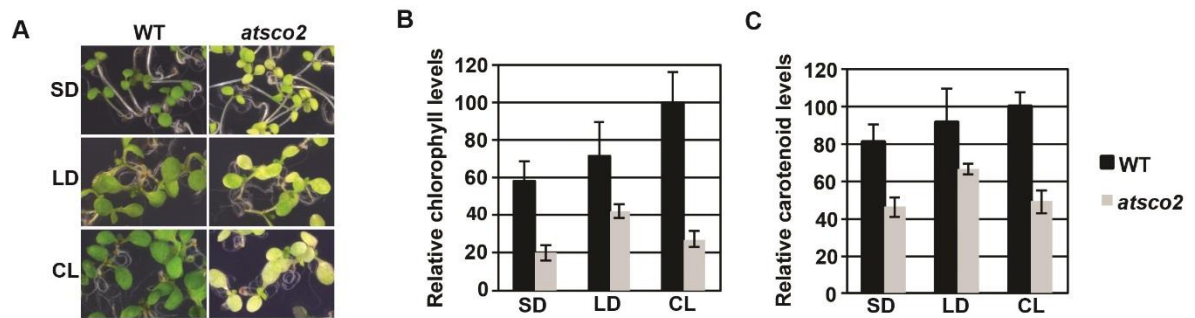


**Supplemental Figure 6.9 Sequence and phylogenetic analysis of SCO2.**

(A) The sequence of the C-terminal zinc finger of LjSCO2 from *L. japonicus* was compared with related sequences from *A. thaliana* and other plants. The sequences were aligned using MUSCLE and Bioedit (see Methods). The consensus sequence is indicated with identical residues marked by asterisks. Cysteines are highlighted in yellow. (B) Phylogenetic tree based on the complete sequences of the SCO2 proteins shown in (A), together with those of other DNAJ-like proteins reported from Arabidopsis: BSD2 (Brutnell 1999), LQY1 (Lu et al., 2011) and TSIP1 (Ham et al. 2006). The tree was rooted at midpoint using the neighbor-joining method in MEGA6. Bootstrap values (as a percentage of 2,000 replicates) are indicated at the branches.

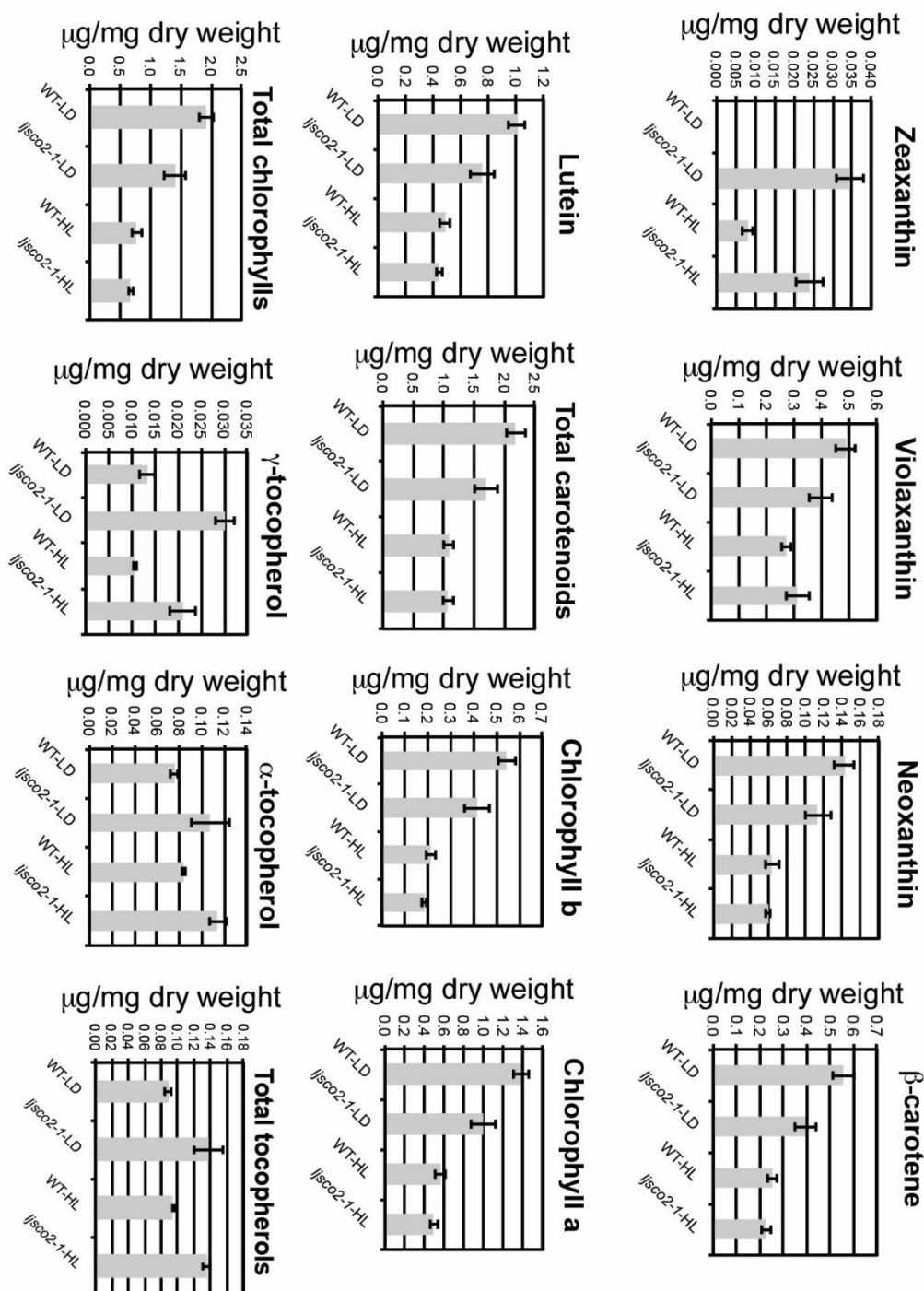
**Supplemental Figure 6.10 77K fluorescence emission spectra of thylakoid samples.**

The 77K fluorescence emission spectrum was analyzed for isolated thylakoids of Lotus true leaves. The fluorescence emission signals were normalized to the minimum at 670 nm. Representative experiments are shown for the WT (black lines) and the *ljSCO2-1* mutant (grey lines). Experiments performed with technical assistance of Dr. Chiara Gandini.



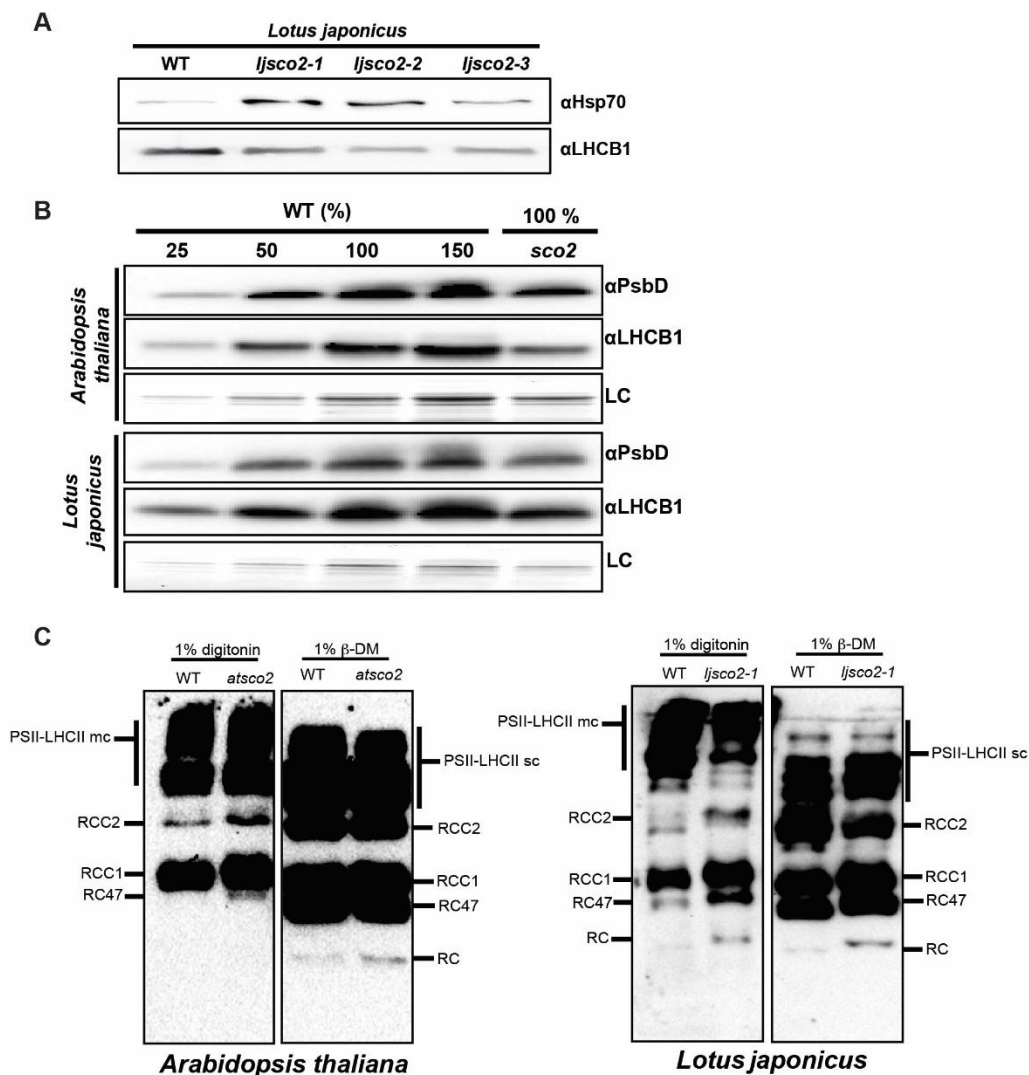
**Supplemental Figure 6.11 Analysis of the cotyledon phenotype of the *atSCO2* mutant under different light regimes.**

(A) Phenotypes of representative 7-day-old *Arabidopsis* wild-type (WT) and *atSCO2* mutant seedlings grown on MS plates under short-day (SD) or long-day (LD) conditions or in continuous light (CL). Plant material was collected and standard pigment amounts were determined as described in Methods. Relative values of total chlorophyll (B) and carotenoids (C) are provided (WT grown in CL = 100%). Data correspond to the mean and SEM values of  $n=3$  independent experiments. Although both chlorophyll and carotenoid levels increase in WT proportionally to the hours of light, maximum pigment accumulation in the *atSCO2* mutant is observed under LD conditions.



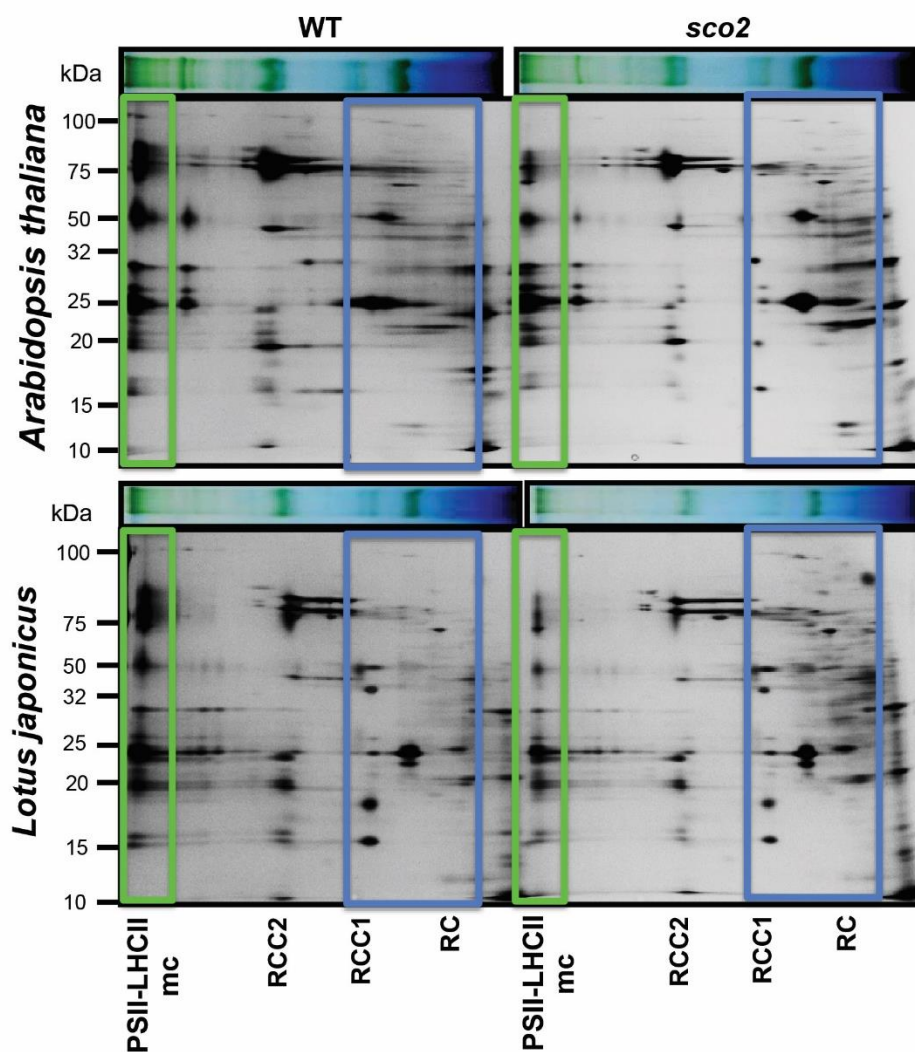
**Supplemental Figure 6.12** Metabolic analyses of *L. japonicus* plants.

Metabolite analyses by HPLC was performed with 45-day-old *L. japonicus* plants as described in Methods. Absolute values are referred to dry tissue. Data correspond to the mean and SD values of  $n=4$  independent experiments (Student's t test: \* $P < 0.05$  and \*\* $P < 0.01$ ). Experiments performed by the lab of Prof. Dr. Manuel Rodriguez-Concepcion.



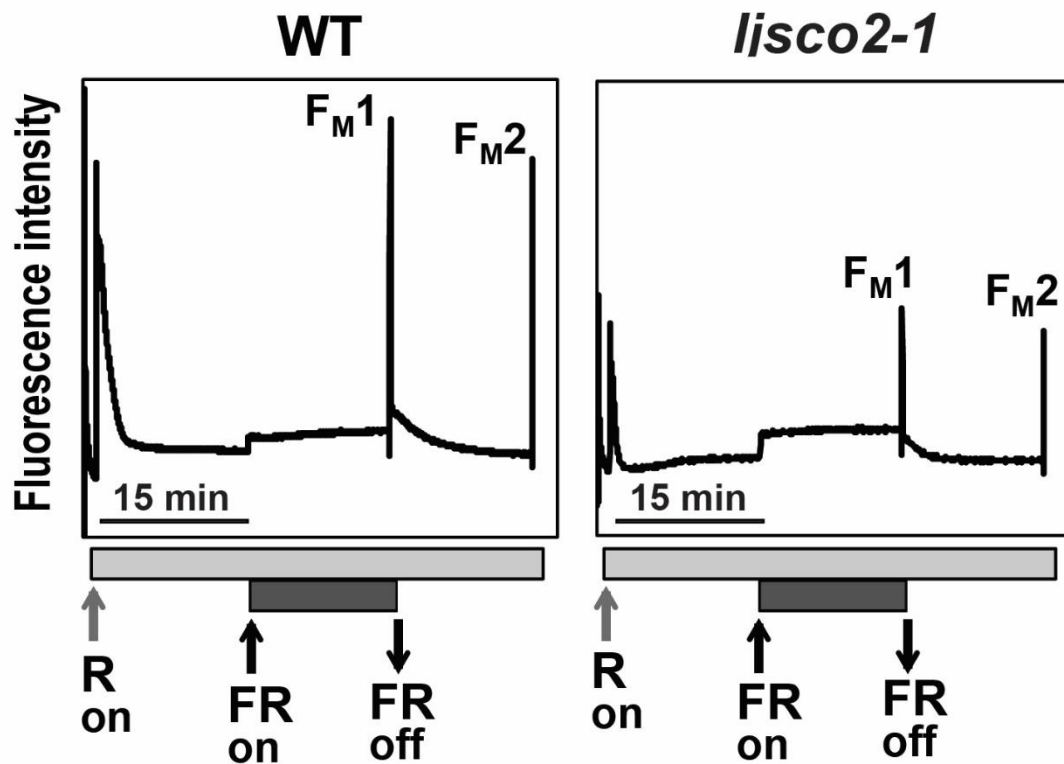
**Supplemental Figure 6.13 PsbD and LHCb1 accumulation in *L. japonicus* true leaves.**

(A) Levels of LHCb1 and Hsp70 were analysed in total extracts from true leaves of WT and the three *ljsco2* mutants. (B) Thylakoid membranes from *Arabidopsis* and *Lotus* were submitted to immunoblot analyses with specific antibodies against the D2 protein from PSII and LHCb1. Coomassie blue-stained gels were used as loading control (LC) showing the representative RbcL band. Samples containing 2 and 0.4  $\mu\text{g}$  of chlorophyll were loaded for *atsco2* and *ljsco2-1* mutants, respectively. In addition, a dilution series of the wild-type sample was loaded as indicated. (C) Thylakoid membranes from *Arabidopsis* and *Lotus* were solubilized in 1% digitonin (w/v) (left panels) or 1%  $\beta$ -DM (w/v) (right panels). Samples were fractionated by 5 to 12% lpBN-PAGE similarly to Figure 4.6. Membranes were over-exposed to visualize the smaller complexes (RCC1, RC47 and RC). Experiments performed with technical assistance of Dr. Omar Sandoval-Ibanez.



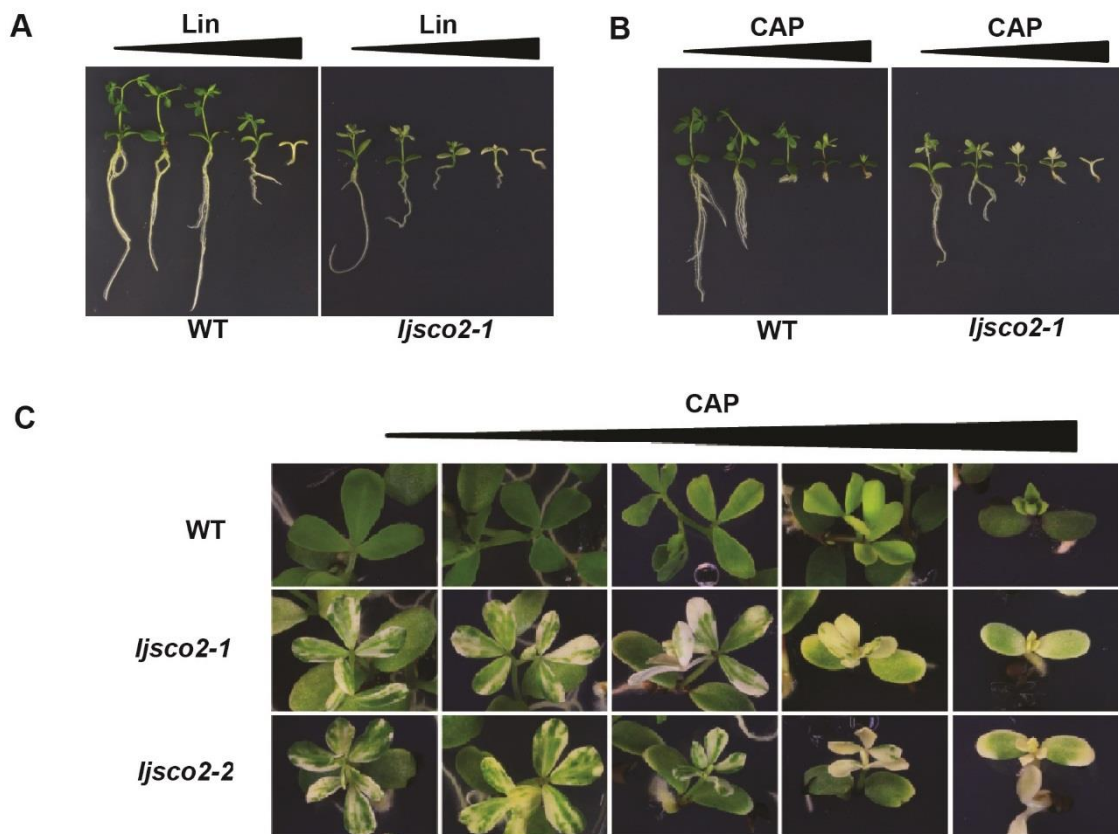
**Supplemental Figure 6.14 SCO2 is required for PSII megacomplex accumulation.**

Thylakoid membranes from *Arabidopsis* and *Lotus* were solubilized in 1% digitonin (w/v). Samples were fractionated by 5 to 12% IpBN-PAGE as described in Methods. Subsequent second dimension gel electrophoresis and silver staining was performed. PSII-LHCII mega complexes are marked in green, whereas small intermediate-sized complexes are marked in blue.



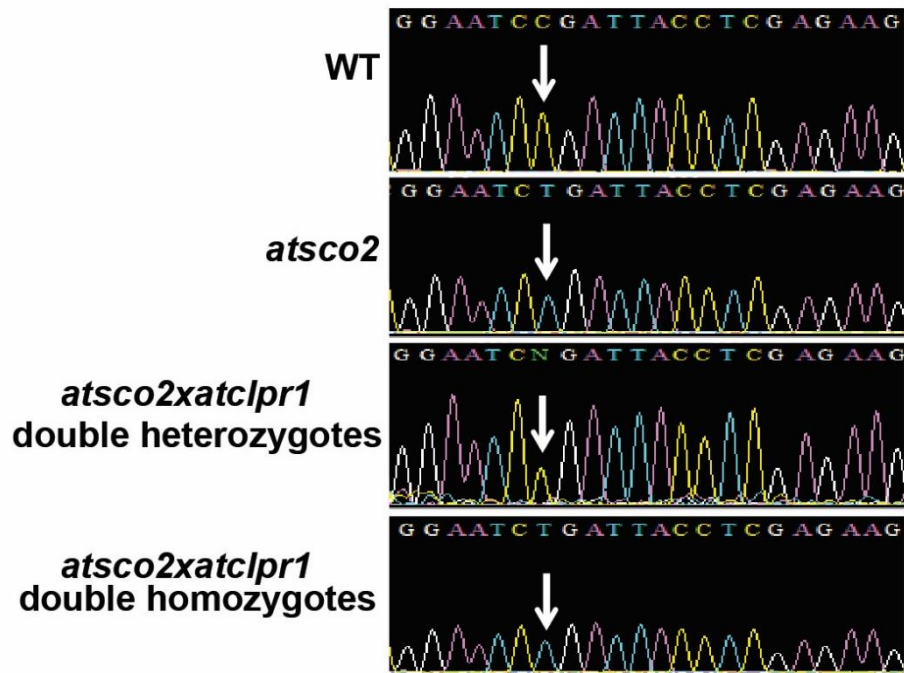
Supplemental Figure 6.15 *LjSCO2* is not required for state transitions.

Red light (R) and red light supplemented with far-red (FR) were used to induce transitions to state 2 and state 1, respectively.  $F_{M1}$  and  $F_{M2}$  represent maximal chlorophyll fluorescence levels in states 1 and 2, respectively. Horizontal bars indicate the length of illumination. Data correspond to the mean values of  $n \geq 4$  independent experiments.



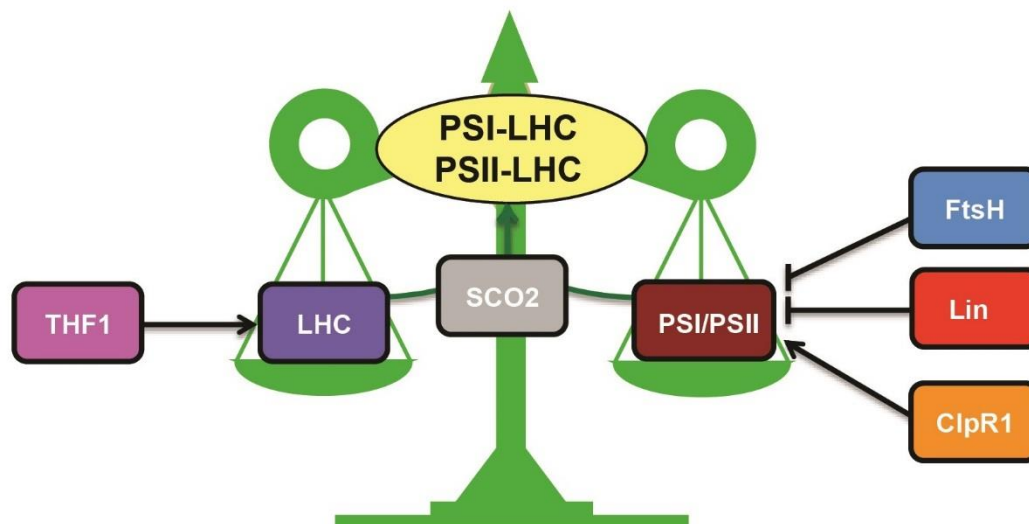
**Supplemental Figure 6.16 Chloroplast translation inhibitors do not suppress variegation in *ljSCO2* mutants.**

(A) Lotus wild-type (WT) and *ljSCO2-1* mutant plants were germinated and grown for 20 days on MS medium supplemented with increasing concentrations (from left to right: 0, 10, 50, 250 and 2500  $\mu\text{M}$ ) of lincomycin (LIN). Note the reduction in root length and pigment concentration with increasing amounts of LIN. Similarly, none of the different concentrations (from left to right: 0, 15, 50, 100 and 300  $\mu\text{M}$ ) of chloramphenicol (CAP) tested could suppress the variegation seen in the *SCO2* mutants. Representative images of plants (B) and close-ups of the leaf phenotype (C) show that LIN and CAP have similar effects.



**Supplemental Figure 6.17** The *Arabidopsis thaliana* double mutant *atsco2 atclpr1* contains the same point mutation as the *sco2* single mutant.

The *Arabidopsis atsco2* mutant was obtained by ethyl-methylsulfonate (EMS) mutagenesis (Albrecht et al., 2008). Comparison of wild-type (WT) and *atsco2* mutant sequences revealed the replacement of a C by a T in the DNA sequence of the *SCO2* gene. After crossing *atsco2* and *atclpr1* mutants, F1 double heterozygous plants sequence showed a peak that could not be assigned to any nucleotide, likely due to the overlapping of the signals of both C and T. However, F2 double homozygous *atsco2 atclpr1* plants displayed a clear single peak corresponding to T, like homozygous *atsco2* single mutants.



**Supplemental Figure 6.18 Model of SCO2 function in the assembly or repair of photosynthetic complexes.**

In the proposed model, THF1 and FtsH affect the accumulation of LHC (PSI and PSII) and the reaction center protein D1 (PSII), respectively. In both cases the balance required for the assembly of photosynthetic complexes is disrupted, hence producing variegation. Decreasing protein biosynthesis in the chloroplast (absence of ClpR1 or applying LIN) reduce the levels of several chloroplast-encoded photosynthetic proteins, partially restoring the proper ratio for complexes assembly and suppressing variegation. However, SCO2 acts in a later step of the pathway, assisting to the assembly or repair of LHC with PSI and PSII. Therefore, the role in variegation of SCO2 cannot be suppressed by the downregulation of protein biosynthesis in the chloroplast.

Ranking	Name	Description	Score	Mass	Coverage	Peptide
1	PRPS17-venus	S17-venusYFP	1833	44926	41,5	TFVAVPVPPR
49	AT5G14910.1	CRASS	184	19059	29,8	QTTVQATGVASNLVETIQGAGFK

**Supplemental Table 6-1 Data set of protein coimmunoprecipitation experiments.**

Wild-type (Col-0) and PRPS17-YFP were used in coimmunoprecipitation experiments. Proteins immunoprecipitated with an antibody against YFP from the transgenic line PRPS17-YFP were separated by SDS-PAGE. Gel fractions were analysed by MALDI TOF mass spectrometry in order to identify PRPS17 bound proteins (see “Materials and Methods”). To check for unspecific contaminants the output has been compared to the wild-type immunoprecipitation. Partial data from PRPS17-YFP immunoprecipitation demonstrates that CRASS was identified as a putative interactor of PRPS17. Dr. Lars Scharff performed the immunoprecipitation experiments, Dr. Piotr Gawronsky performed bioinformatic analysis and Dr. Annemarie Matthes produced the mass spectrometry data.

Ranking	AGI	Name	Average	Ranking	AGI	Name	Average	Ranking	AGI	Name	Average
1	ATCG01210	RRN16S	494502	38	ATCG00780	RPL14	582	75	ATCG00180	RPOC1	138
2	ATCG01180	RRN23S	65412	39	ATCG01310	RPL2	571	76	ATCG01250	NDHB	133
3	ATCG00630	PSAJ	16562	40	ATCG00420	NDHJ	545	77	ATCG00620	TRNP	131
4	ATCG00490	RBCL	10558	41	ATCG00770	RPS8	535	78	ATCG00750	RPS11	130
5	ATCG00580	PSBE	7949	42	ATCG00210	YCF6	512	79	ATCG01110	NDHH	127
6	ATCG00280	PSBC	7181	43	ATCG01080	NDHG	511	80	ATCG00030	TRNK	125
7	ATCG00690	PSBT	4960	44	ATCG01020	RPL32	498	81	ATCG00170	RPOC2	88
8	ATCG00140	ATPH	4625	45	ATCG00090	TRNS.1	492	82	ATCG01010	NDHF	85
9	ATCG00020	PSBA	4000	46	ATCG00220	PSBM	468	83	ATCG01040	YCF5	82
10	ATCG00080	PSBI	3944	47	ATCG01060	PSAC	410	84	ATCG00930	TRNI.2	76
11	ATCG00330	RPS14	3795	48	ATCG00900	RPS7	380	85	ATCG00570	PSBF	69
12	ATCG00680	PSBB	3487	49	ATCG00760	RPL36	373	86	AT2G01021	unknown	69
13	ATCG00350	PSAA	2927	50	ATCG00790	RPL16	372	87	ATCG01200	TRNI.3	66
14	ATCG00340	PSAB	2900	51	ATCG00160	RPS2	354	88	AT2G01020	5.8S rRNA	63
15	ATCG00560	PSBL	2595	52	ATCG00670	CLPP1	350	89	ATCG00400	TRNL.1	62
16	ATCG00130	ATPF	2163	53	ATCG01070	NDHE	336	90	ATCG00610	TRNW	56
17	ATCG00730	PETD	2061	54	ATCG01300	RPL23	336	91	ATCG01170	RRN4.5S	55
18	ATCG00290	TRNS.2	1710	55	ATCG01050	NDHD	324	92	ATCG01160	RRN5S	55
19	ATCG00510	PSAI	1708	56	ATCG00640	RPL33	312	93	ATCG00040	MATK	54
20	ATCG00270	PSBD	1676	57	ATCG00820	RPS19	304	94	ATCG00190	RPOB	44
21	ATCG00150	ATPI	1620	58	ATCG00940	TRNA.1	297	95	ATCG01000	YCF1.1	42
22	ATCG00070	PSBK	1369	59	ATCG00600	PETG	288	96	ATCG00200	TRNC	39
23	ATCG00430	PSBG	1369	60	ATCG00110	TRNR.1	281	97	ATCG01130	TIC2.14	37
24	ATCG00550	PSBJ	1328	61	ATCG00800	RPS3	247	98	ATCG00500	ACCD	36
25	ATCG00720	PETB	1273	62	ATCG01100	NDHA	246	99	ATCG00010	TRNH	30
26	ATCG00100	TRNG.1	1254	63	ATCG00530	YCF10	244	100	ATCG00870	ORF77	30
27	ATCG00905	RPS12	1244	64	ATCG00360	YCF3	238	101	ATCG01220	TRNV.3	28
28	ATCG00300	YCF9	1242	65	ATCG00650	RPS18	224	102	ATCG00460	TRNM	25
29	ATCG00120	ATPA	1205	66	ATCG00370	TRNS.3	221	103	ATCG00860	YCF2.1	25
30	ATCG00440	NDHC	1087	67	AT2G01010	18S rRNA	217	104	ATCG00240	TRNY	22
31	ATCG00700	PSBN	1079	68	ATCG00380	RPS4	202	105	ATCG00410	TRNF	20
32	ATCG00660	RPL20	946	69	ATCG00740	RPOA	201	106	ATCG01290	TRNI.4	18
33	ATCG00480	ATPB	944	70	ATCG01120	RPS15	183	107	ATCG00820	TRNFM	17
34	ATCG00540	PETA	911	71	ATCG00450	TRNV.1	162	108	ATCG00850	TRNI.1	17
35	ATCG00520	YCF4	833	72	ATCG00810	RPL22	157	109	ATCG00910	TRNV.2	16
36	ATCG00470	ATPE	765	73	ATCG00590	ORF31	154	110	AT1G67090	RBCS1A	14
37	ATCG00710	PSBH	708	74	ATCG01090	NDHI	142	111	ATMG01390	RRN18	13

### Supplemental Table 6-2 Data set of RNA coimmunoprecipitation with CRASS.

Transgenic line *oeCRASS#1* overexpressing the recombinant protein CRASS-YFP was used for RNA coimmunoprecipitation experiments with a specific antibody (see “Materials and Methods”). Fragments per kilobase of exon per million reads mapped (FPKM) values of two independent experiments of high throughput RNA sequencing (RIP-seq) were analyzed and exclusion of duplicated genes was performed. Average of both experiments was calculated and the 20 most abundant immunoprecipitated RNAs were selected for presentation in Figure 3.6A. Dr. Lars Scharff supervised the immunoprecipitation experiments, Dr. Piotr Gawronsky performed bioinformatic analysis and Dr. Annemarie Matthes produced the mass spectrometry data.

Locus (allele)	Sense primer (SP)	Antisense primer (ASP)	Primer combination	Vector
<b>T-DNA primers</b>				
Lb3	ATGGTTCACCGTAGTGGCCATCG			
Lb5	CTGGGAATGGCGAAATCAAGGCATC			
Ds-4	TACGATAACGGGTCCGTACGG			
<b>Mutant lines</b>				
<i>CRASS (crass-1)</i>	GTCAGAACTGTGTTTGCAAGG	ATTCCGATAGCTCTGGTCC	Lb5/SP	
<i>CRASS (crass-2)</i>	GATATTGATGGAGTTTCCAAT	CCACTCCTGTTGCTTGAACC	Lb5/SP	
<b>qPCR</b>				
<i>CRASS</i> (AT5G14910)	CCAGGCTGATGGAACTTTG	GCTCAACGACCGGCAACACC	SP/ASP	
<i>UBQ10</i> (AT4G05320)	GAAGTTCATGTTTCGTTTCATGT	GGATTATACAAAGGCCCAAAA	SP/ASP	
<b>Northern blot</b>				
16S rRNA	AGTCATCATGCCCTTATGC	CAGTCACTAGCCCTGCCTTC	SP/ASP	
23S rRNA	GTTGAGTACCAGGCGCTAC	CGGAGACCTGTGTTTTGGT	SP/ASP	
5S rRNA	TATTCTGGTGTCTAGGCGTAG	ATCCTGGCGTCGAGCTATTTTCC	SP/ASP	
4.5S rRNA	GAAGGTCACGGCGAGACGAGCC	GTTCAAGTCTACCGGTCCTGTTAGG	SP/ASP	
<b>Polysome analysis</b>				
<i>psa4</i>	AAACTGTGGAAGCCTAGAAATATACA	ACTCACATTGGACCTAGTGC	SP/ASP	
	TCCAGAGCTACTCGGTTGGCTACGGCA			
	CCCGGTGCATTTCCCAAGGGTGGCC			
	TAAAGTTCCTCCACCGAATTGTAGTAC			
<b>Gateway cloning</b>				
<i>rbcl</i>				
<i>CRASS</i>	CACCATGGCGTGGATTGCGAGCTTC	GACAAGAACCCTCATGTCATC	SP/ASP	pGWB641
<b>Yeast two hybrid</b>				
<i>CRASS</i>	GACTAGCATATGGCTATCGGAATAGCCCGC	GACTAGGAATTCCTAGACAAGAACCCTCAT	SP/ASP	pGBKT7
<i>PRP5</i>	GACTAGCATATGGCCCTCATCGACCGATAC	GACTAGGAATTCCTACACTCCAGAGTTCTTCC	SP/ASP	pGADT7
<i>PRP58</i>	GACTAGCATATGATGGGAAAGACACCAATTG	GACTAGGATCCTTACCATATATAACACAA AATTTCTCCG	SP/ASP	pGADT7

Supplemental Table 6-3 List of primers used in this work

Sense (SP) and antisense (ASP) primers (5'→3') were employed for the WT alleles, for RNA probes or for cloning, whereas T-DNA specific primers were used in combination with either with SP or ASP for the mutant alleles.

Mutant line	Forward Primer	Reverse Primer
<i>ljSCO2-1</i>	GCGGTTGGGTGATTTCCAGTTTGA	CTCTCCCCCTTCCCTCGCCTCTTC
<i>ljSCO2-2</i>	CAATAGACCGTGAATTCCCGATGTTAAGAA	GATCCTGCCGCCCTTCCTTGTA
<i>ljSCO2-3</i>	TTTCTTCACGCGAAACAGGCGAGG	TCCCCCTCAACTCTAACGCCTAACTCCA
<i>atclpr1</i>	CTTAGCGACCCATTTATCTGC	ACTGCAGGTACGATCTGCAAG
<i>atsCO2</i>	ATGTTCCGATTATACCCTA	TCAAGATGGTTCATTATCC
<i>LORE1 P2</i>	CCATGGCGGTTCCGTGAATCTTAGG	
<i>qPCR</i>	Forward Primer	Reverse Primer
<i>LjSCO2</i>	GCATTCCTTGCATGGGA	CACGGTGGTTTCCCATT
<i>LjUBQ</i>	ATGCAGATCTTCGTCAAGACCTTG	ACCTCCCCTCAGACGAAG

**Supplemental Table 6-4 List of primers used in this work**

Forward and reverse primers were employed for the WT alleles or for RNA probes whereas T-DNA specific primer LORE1 P2 was used in combination with either forward or reverse primers for the mutant alleles in *Lotus japonicus*.

## 7. References

- Adam, Z. et al., 2005. FtsH proteases in chloroplasts and cyanobacteria. *Physiologia Plantarum*, 123(4), pp.386–390.
- Albrecht, V., Ingenfeld, A. & Apel, K., 2006. Characterization of the snowy cotyledon 1 mutant of *Arabidopsis thaliana*: The impact of chloroplast elongation factor G on chloroplast development and plant vitality. *Plant Molecular Biology*, 60(4), pp.507–518.
- Albrecht, V., Ingenfeld, A. & Apel, K., 2008. Snowy cotyledon 2: The identification of a zinc finger domain protein essential for chloroplast development in cotyledons but not in true leaves. *Plant Molecular Biology*, 66, pp.599–608.
- Allahverdiyeva, Y. et al., 2013. *Arabidopsis* plants lacking PsbQ and PsbR subunits of the oxygen-evolving complex show altered PSII super-complex organization and short-term adaptive mechanisms. *Plant Journal*, 75(4), pp.671–684.
- Aloy, P. et al., 2002. Structural similarity to link sequence space : New potential superfamilies and implications for structural genomics. *Protein Science*, 11, pp.1101–1116.
- Aluru, M.R. et al., 2006. *Arabidopsis* variegation mutants: New insights into chloroplast biogenesis. *Journal of Experimental Botany*, 57(9), pp.1871–1881.
- Anderson, P. & Kedersha, N., 2006. RNA granules. *Journal of Cell Biology*, 172(6), pp.803–808.
- Arquier, N., Bourouis, M. & Leopold, P., 2005. *Drosophila* Lk6 Kinase Controls Phosphorylation of Eukaryotic Translation Initiation Factor 4E and Promotes Normal Growth and Development. *Current Biology*, 15, pp.19–23.
- Ban, N. et al., 1999. Placement of protein and RNA structures into a 5 Å-resolution map of the 50S ribosomal subunit. *Nature*, 400(6747), pp.841–847.
- Barbrook, A.C., Howe, C.J. & Purton, S., 2006. Why are plastid genomes retained in non-photosynthetic organisms? *Trends in Plant Science*, 11(2), pp.101–108.
- Barkan, A., 1993. Nuclear mutants of maize with defects in chloroplast polysome assembly have altered chloroplast RNA metabolism. *The Plant Cell*, 5(4), pp.389–402.
- Bellafiore, S. et al., 2005. State transitions and light adaptation require chloroplast thylakoid protein kinase STN7. *Nature*, 433(7028), pp.892–895.
- Biehl, A. et al., 2005. Analysis of 101 nuclear transcriptomes reveals 23 distinct regulons and their relationship to metabolism, chromosomal gene distribution and co-ordination of nuclear and plastid gene expression. *Gene*, 344, pp.33–41.
- Bilger, W. & Bjorkman, O., 1991. Temperature dependence of violaxanthin de-epoxidation and non-photochemical fluorescence quenching in intact leaves of *Gossypium hirsutum* L. and *Malva parviflora* L. *Planta*, 184(2), pp.226–234.

- Bock, R. & Timmis, J.N., 2008. Reconstructing evolution: Gene transfer from plastids to the nucleus. *BioEssays*, 30(6), pp.556–566.
- Brutnell, T.P., 1999. BUNDLE SHEATH DEFECTIVE2, a Novel Protein Required for Post-Translational Regulation of the *rbcL* Gene of Maize. *The Plant cell*, 11(5), pp.849–864.
- Chotewutmontri, P. & Barkan, A., 2016. Dynamics of Chloroplast Translation during Chloroplast Differentiation in Maize. *PLoS Genetics*, 12(7), pp.1–28.
- Colombo, M. et al., 2016. GUN1, a Jack-Of-All-Trades in Chloroplast Protein Homeostasis and Signaling. *Frontiers in Plant Science*, 7(September).
- DalCorso, G. et al., 2008. A Complex Containing PGRL1 and PGR5 Is Involved in the Switch between Linear and Cyclic Electron Flow in Arabidopsis. *Cell*, 132(2), pp.273–285.
- Delvillani, F. et al., 2011. S1 ribosomal protein and the interplay between translation and mRNA decay. *Nucleic Acids Research*, 39(17), pp.7702–7715.
- Dinman, J.D., 2009. The eukaryotic ribosome: Current status and challenges. *Journal of Biological Chemistry*, 284(18), pp.11761–11765.
- Edwards, K., Johnstone, C. & Thompson, C., 1991. A simple and rapid method for the preparation of plant genomic DNA for PCR analysis. *Nucleic Acids Research*, 19(6), p.1349.
- Ehrnthaler, M. et al., 2014. Synthetic lethality in the tobacco plastid ribosome and its rescue at elevated growth temperatures. *The Plant cell*, 26(2), pp.765–76.
- Fleischmann, T.T. et al., 2011. Nonessential Plastid-Encoded Ribosomal Proteins in Tobacco: A Developmental Role for Plastid Translation and Implications for Reductive Genome Evolution. *the Plant Cell*, 23(9), pp.3137–3155.
- Foudree, A. et al., 2012. The Mechanism of Variegation in *immutans* Provides Insight into Chloroplast Biogenesis. *Frontiers in Plant Science*, 3(November), pp.1–10.
- Friso, G. et al., 2004. In-Depth Analysis of the Thylakoid Membrane Proteome of *Arabidopsis thaliana*. *The Plant Cell*, 16(February), pp.478–499.
- Fristedt, R. et al., 2014. RBF1, a Plant Homolog of the Bacterial Ribosome-Binding Factor RbfA, Acts in Processing of the Chloroplast 16S Ribosomal RNA. *Plant Physiology*, 164(1), pp.201–215.
- Fukai, E. et al., 2012. Establishment of a *Lotus japonicus* gene tagging population using the exon-targeting endogenous retrotransposon LORE1. *Plant Journal*, 69(4), pp.720–730.
- Gibala, M. et al., 2009. The lack of mitochondrial AtFtsH4 protease alters *Arabidopsis* leaf morphology at the late stage of rosette development under short-day photoperiod. *Plant Journal*, 59(5), pp.685–699.
- Ham, B.-K. et al., 2006. Tobacco Tsi1, a DnaJ-type Zn finger protein, is recruited to and potentiates Tsi1-mediated transcriptional activation. *The Plant cell*, 18(8), pp.2005–20.

- Handberg, K. & Stougaard, J., 1992. Lotus japonicus, an autogamous, diploid legume species for Classical and Molecular Genetics. *The Plant Journal*, 2, pp.487–496.
- Hansen, M. et al., 2007. Lifespan extension by conditions that inhibit translation in *Caenorhabditis elegans*. *Aging Cell*, 6(1), pp.95–110.
- Harris, M.E. et al., 1994. Use of photoaffinity crosslinking and molecular modeling to analyze the global architecture of ribonuclease P RNA. *The EMBO journal*, 13(17), pp.3953–3963.
- Hashimoto, M. et al., 2003. A nucleus-encoded factor, CRR2, is essential for the expression of chloroplast *ndhB* in Arabidopsis. *The Plant Journal*, 36(4), pp.541–549.
- Hu, F. et al., 2015. Leaf Variegation of *Thylakoid Formation1* Is Suppressed by Mutations of Specific  $\sigma$ -Factors in Arabidopsis. *Plant Physiology*, 168(3), pp.1066–1075.
- Järvi, S. et al., 2016. FtsH facilitates proper biosynthesis of photosystem I in Arabidopsis thaliana. *Plant Physiology*, 171(June), p.pp.00200.2016.
- Järvi, S. et al., 2011. Optimized native gel systems for separation of thylakoid protein complexes: novel super- and mega-complexes. *Biochemical Journal*, 439(2), pp.207–214.
- Jarvis, P. & López-Juez, E., 2013. Biogenesis and homeostasis of chloroplasts and other plastids. *Nature Reviews Molecular Cell Biology*, 14(12), pp.787–802.
- Jones, P.G. & Inouye, M., 1996. *RbfA, a 30S ribosomal binding factor, is a cold shock protein whose absence triggers the cold shock response,*
- Kampinga, H.H. & Craig, E. a, 2010. The HSP70 chaperone machinery: J proteins as drivers of functional specificity. *Nature reviews. Molecular cell biology*, 11(8), pp.579–92.
- Kato, Y. et al., 2009. The Variegated Mutants Lacking Chloroplastic FtsHs Are Defective in D1 Degradation and Accumulate Reactive Oxygen Species. *Plant Physiology*, 151(4), pp.1790–1801.
- Kleine, T., Voigt, C. & Leister, D., 2009. Plastid signalling to the nucleus: messengers still lost in the mists? *Trends in Genetics*, 25(4), pp.185–192.
- Koussevitzky, S. et al., 2007. An Arabidopsis thaliana virescent mutant reveals a role for ClpR1 in plastid development. *Plant Molecular Biology*, 63, pp.85–96.
- Kupsch, C. et al., 2012. Arabidopsis chloroplast RNA binding proteins CP31A and CP29A associate with large transcript pools and confer cold stress tolerance by influencing multiple chloroplast RNA processing steps. *The Plant cell*, 24(10), pp.4266–80.
- Lee, S. et al., 2009. Heat Shock Protein Cognate 70-4 and an E3 Ubiquitin Ligase, CHIP, Mediate Plastid-Destined Precursor Degradation through the Ubiquitin-26S Proteasome System in Arabidopsis. *The Plant Cell*, 21(12), pp.3984–4001.
- Leister, D., 2012. Retrograde signaling in plants: from simple to complex scenarios. *Frontiers*

- in plant science*, 3(June), p.135.
- Liao, J.-C. et al., 2016. Dysfunctional chloroplasts up-regulate the expression of mitochondrial genes in Arabidopsis seedlings. *Photosynthesis Research*, 127(2), pp.151–159.
- Lichtenthaler, H. & Wellburn, A., 1983. Determinations of total carotenoids and chlorophylls b of leaf extracts in different solvents. *Biochemical Society Transactions*, 11(1955), pp.591–592.
- Liu, X., Rodermel, S.R. & Yu, F., 2010. A var2 leaf variegation suppressor locus, SUPPRESSOR OF VARIATION3, encodes a putative chloroplast translation elongation factor that is important for chloroplast development in the cold. *BMC plant biology*, 10(1), p.287.
- Liu, X., Yu, F. & Rodermel, S., 2010. An Arabidopsis Pentatricopeptide Repeat Protein, SUPPRESSOR OF VARIATION7, Is Required for FtsH-Mediated Chloroplast Biogenesis. *Plant Physiology*, 154(4), pp.1588–1601.
- Liu, X., Yu, F. & Rodermel, S., 2010. Arabidopsis Chloroplast FtsH, var2 and Suppressors of var2 Leaf Variegation: A Review. *Journal of Integrative Plant Biology*, 52(8), pp.750–761.
- Llamas, E., Pulido, P. & Rodriguez-Concepcion, M., 2017. Interference with plastome gene expression and Clp protease activity in Arabidopsis triggers a chloroplast unfolded protein response to restore protein homeostasis. *PLoS Genetics*, 13(9), pp.1–27.
- Lopez-Juez, E. & Pyke, K.A., 2005. Plastids unleashed: Their development and their integration in plant development. *International Journal of Developmental Biology*, 49(5–6), pp.557–577.
- Lorsch, J.R., 2002. RNA Chaperones Exist and DEAD Box Proteins Get a Life. *Cell*, 109, pp.797–800.
- Love, M.I., Huber, W. & Anders, S., 2014. Moderated estimation of fold change and dispersion for RNA-seq data with DESeq2. *Genome Biology*, 15(12), pp.1–21.
- Lu, Y., 2016. Identification and Roles of Photosystem II Assembly, Stability, and Repair Factors in Arabidopsis. *Frontiers in Plant Science*, 7(February), p.168.
- Lu, Y., Hall, D.A. & Last, R.L., 2011. A Small Zinc Finger Thylakoid Protein Plays a Role in Maintenance of Photosystem II in *Arabidopsis thaliana*. *The Plant Cell*, 23(5), pp.1861–1875.
- Lutsenko, S. et al., 1997. N-terminal domains of human copper-transporting adenosine triphosphatases (the Wilson's and Menkes Disease Proteins) bind copper selectively in vivo and in vitro with stoichiometry of one copper per metal-binding repeat. *Journal of Biological Chemistry*, 272(30), pp.18939–18944.
- Ma, Z. et al., 2015. Down-regulation of specific plastid ribosomal proteins suppresses thf1 leaf variegation, implying a role of THF1 in plastid gene expression. *Photosynthesis*

- Research*, 126(2–3), pp.301–310.
- Małolepszy, A. et al., 2016. The LORE1 insertion mutant resource. *Plant Journal*, 88(2), pp.306–317.
- Manavski, N. et al., 2015. HIGH CHLOROPHYLL FLUORESCENCE145 Binds to and Stabilizes the *psaA* 5' UTR via a Newly Defined Repeat Motif in Embryophyta. *The Plant Cell*, 27(9), pp.2600–2615.
- Marín-Navarro, J. et al., 2007. Chloroplast translation regulation. *Photosynthesis Research*, 94(2–3), pp.359–374.
- Marutani, Y. et al., 2014. Regulation of Photochemical Energy Transfer Accompanied by Structural Changes in Thylakoid Membranes of Heat-Stressed Wheat. *International Journal of Molecular Sciences*, 15(12), pp.23042–23058.
- Melonek, J., Oetke, S. & Krupinska, K., 2016. Multifunctionality of plastid nucleoids as revealed by proteome analyses. *Biochimica et Biophysica Acta (BBA) - Proteins and Proteomics*.
- Merendino, L., Falciatore, A. & Rochaix, J.-D., 2003. Expression and RNA binding properties of the chloroplast ribosomal protein S1 from *Chlamydomonas reinhardtii*. *Plant Molecular Biology*, 53(3), pp.371–382.
- Meurer, J. et al., 2017. PALE CRESS Binds to Plastid RNAs and Facilitates the Biogenesis of the 50S. , 12(10), pp.3218–3221.
- Miernyk, J. a., 2001. The J-domain proteins of *Arabidopsis thaliana*: an unexpectedly large and diverse family of chaperones. *Cell Stress & Chaperones*, 6(3), p.209.
- Miura, E. et al., 2007. The Balance between Protein Synthesis and Degradation in Chloroplasts Determines Leaf Variegation in *Arabidopsis* yellow variegated Mutants. *the Plant Cell*, 19(4), pp.1313–1328.
- Moreira, D., Le Guyader, H. & Philippe, H., 2000. The origin of red algae and the evolution of chloroplasts.[see comment]. *Nature*, 405(6782), pp.69–72.
- Moustaka, J. et al., 2015. Leaf Age-Dependent Photoprotective and Antioxidative Response Mechanisms to Paraquat-Induced Oxidative Stress in *Arabidopsis thaliana*. *International Journal of Molecular Sciences*, 16(12), pp.13989–14006.
- Munekage, Y. et al., 2002. PGR5 Is Involved in Cyclic Electron Flow around Photosystem I and Is Essential for Photoprotection in *Arabidopsis*. *Cell*, 110(3), pp.361–371.
- Muranaka, A. et al., 2012. *Arabidopsis* cotyledon chloroplast biogenesis factor CYO1 uses glutathione as an electron donor and interacts with PSI (A1 and A2) and PSII (CP43 and CP47) subunits. *Journal of Plant Physiology*, 169(12), pp.1212–1215.
- Newell, C.A. et al., 2012. Exclusion of plastid nucleoids and ribosomes from stromules in tobacco and *Arabidopsis*. *Plant Journal*, 69(3), pp.399–410.

- Okegawa, Y., Kobayashi, Y. & Shikanai, T., 2010. Physiological links among alternative electron transport pathways that reduce and oxidize plastoquinone in Arabidopsis. *The Plant Journal*, 63(3), pp.458–468.
- Olinares, P.D.B., Ponnala, L. & van Wijk, K.J., 2010. Megadalton complexes in the chloroplast stroma of Arabidopsis thaliana characterized by size exclusion chromatography, mass spectrometry, and hierarchical clustering. *Molecular & cellular proteomics : MCP*, 9(7), pp.1594–615.
- Oota, Y. & Takata, K., 1959. Changes in Microsomal Ribonucleoproteins in the Time Course of the Germination Stage as Revealed by Electrophoresis. *Physiologia Plantarum*, 12(3), pp.518–525.
- Paieri, F. et al., 2017. The DEAD-box RNA helicase RH50 is a 23S-4.5S rRNA maturation factor that functionally overlaps with the plastid signaling factor GUN1. *Plant Physiology*, 176(January), p.pp.01545.2017.
- Palade, G.E. & Siekevitz, P., 1956. Liver Microsomes. *The Journal of biophysical and biochemical cytology*, 2(2), pp.171–200.
- Pendle, A. et al., 2005. Proteomic Analysis of the Arabidopsis Nucleolus Suggests Novel Nucleolar Functions. *Molecular biology of the cell*, 16(1), pp.1–13.
- Pesaresi, P. et al., 2009. Arabidopsis STN7 Kinase Provides a Link between Short- and Long-Term Photosynthetic Acclimation. *the Plant Cell*, 21(8), pp.2402–2423.
- Pesaresi, P. et al., 2001. Knock-out of the plastid ribosomal protein L11 in Arabidopsis: Effects on mRNA translation and photosynthesis. *Plant Journal*, 27(3), pp.179–189.
- Pesaresi, P., 2006. Nuclear Photosynthetic Gene Expression Is Synergistically Modulated by Rates of Protein Synthesis in Chloroplasts and Mitochondria. *The Plant cell*, 18(4), pp.970–991.
- Pietrzykowska, M. et al., 2014. The Light-Harvesting Chlorophyll a/b Binding Proteins Lhcb1 and Lhcb2 Play Complementary Roles during State Transitions in Arabidopsis. *The Plant Cell*, 26(September), pp.3646–3660.
- Powikrowska, M. et al., 2014. Dynamic composition, shaping and organization of plastid nucleoids. *Frontiers in Plant Science*, 5(September), pp.1–14.
- Pribil, M. et al., 2010. Role of plastid protein phosphatase TAP38 in LHCII dephosphorylation and thylakoid electron flow. *PLoS Biology*, 8(1).
- Pulido, P. et al., 2013. Arabidopsis J-protein J20 delivers the first enzyme of the plastidial isoprenoid pathway to protein quality control. *The Plant cell*, 25(10), pp.4183–94.
- Pulido, P. et al., 2016. Specific Hsp100 Chaperones Determine the Fate of the First Enzyme of the Plastidial Isoprenoid Pathway for Either Refolding or Degradation by the Stromal Clp Protease in Arabidopsis. *PLoS Genetics*, 12(1), pp.1–19.
- Pulido, P. & Leister, D., 2018. Novel DNAJ-related proteins in Arabidopsis thaliana. *New*

- Phytologist*, 217(2), pp.480–490.
- Putarjunan, A. et al., 2013. Understanding chloroplast biogenesis using second-site suppressors of *immutans* and *var2*. *Photosynthesis Research*, 116(2–3), pp.437–453.
- Rajan, V.B. V & D’Silva, P., 2009. Arabidopsis thaliana J-class heat shock proteins: cellular stress sensors. *Functional & integrative genomics*, 9(4), pp.433–46.
- Richly, E. et al., 2003. Covariations in the nuclear chloroplast transcriptome reveal a regulatory master-switch. *EMBO Reports*, 4(5), pp.491–498.
- Ríos, G. et al., 2002. Rapid identification of Arabidopsis insertion mutants by non-radioactive detection of T-DNA tagged genes. *Plant Journal*, 32(2), pp.243–253.
- Rodriguez-Concepcion, M., 2004. Distinct Light-Mediated Pathways Regulate the Biosynthesis and Exchange of Isoprenoid Precursors during Arabidopsis Seedling Development. *the Plant Cell*, 16(1), pp.144–156.
- Rogalski, M. et al., 2008. Rpl33, a Nonessential Plastid-Encoded Ribosomal Protein in Tobacco, Is Required under Cold Stress Conditions. *the Plant Cell*, 20(8), pp.2221–2237.
- Romani, I. et al., 2012. Versatile roles of Arabidopsis plastid ribosomal proteins in plant growth and development. *The Plant Journal*, 72(6), pp.922–934.
- Rosso, D. et al., 2009. Photosynthetic Redox Imbalance Governs Leaf Sectoring in the Arabidopsis thaliana Variegation Mutants *immutans*, *spotty*, *var1*, and *var2*. *The Plant Cell*, 21(11), pp.3473–3492.
- Ruban, A. V. & Johnson, M.P., 2009. Dynamics of higher plant photosystem cross-section associated with state transitions. *Photosynthesis Research*, 99(3), pp.173–183.
- Ruckle, M.E. & Larkin, R.M., 2009. Plastid signals that affect photomorphogenesis in. *New Phytologist*, pp.367–379.
- Rühle, T. & Leister, D., 2016. Photosystem II Assembly from Scratch. *Frontiers in Plant Science*, 6(January), pp.1–5.
- Ruiz-Sola, M.Á. & Rodríguez-Concepción, M., 2012. Carotenoid biosynthesis in Arabidopsis: a colorful pathway. *The Arabidopsis book / American Society of Plant Biologists*, 10, p.e0158.
- Sakamoto, W., 2003. Leaf-variegated mutations and their responsible genes in Arabidopsis thaliana. *Genes & Genetic Systems*, 78, pp.1–9.
- Sakamoto, W., Miyagishima, S. & Jarvis, P., 2008. Chloroplast Biogenesis: Control of Plastid Development, Protein Import, Division and Inheritance. *The Arabidopsis Book*, 6, p.e0110.
- Salah, P. et al., 2009. Probing the relationship between gram-negative and gram-positive S1 proteins by sequence analysis. *Nucleic Acids Research*, 37(16), pp.5578–5588.

- Schroda, M., 1999. A Chloroplast-Targeted Heat Shock Protein 70 (HSP70) Contributes to the Photoprotection and Repair of Photosystem II during and after Photoinhibition. *the Plant Cell*, 11(6), pp.1165–1178.
- Shevchenko, A. et al., 2007. In-gel digestion for mass spectrometric characterization of proteins and proteomes. *Nature Protocols*, 1(6), pp.2856–2860.
- Shi, L.-X. & Theg, S.M., 2010. A Stromal Heat Shock Protein 70 System Functions in Protein Import into Chloroplasts in the Moss *Physcomitrella patens*. *The Plant Cell*, 22(1), pp.205–220.
- Shimada, H. et al., 2007. Arabidopsis cotyledon-specific chloroplast biogenesis factor CYO1 is a protein disulfide isomerase. *The Plant cell*, 19(October), pp.3157–3169.
- Sørensen, M.A., Fricke, J. & Pedersen, S., 1998. Ribosomal protein S1 is required for translation of most, if not all, natural mRNAs in *Escherichia coli* in vivo. *Journal of Molecular Biology*, 280(4), pp.561–569.
- Stark, M. & Cundliffe, E., 1979. On the biological role of ribosomal protein BM-L11 of *Bacillus megaterium*, homologous with *Escherichia coli* ribosomal protein L11. *Journal of Molecular Biology*, 134(4), pp.767–779.
- Stoppel, R. et al., 2012. RHON1 is a novel ribonucleic acid-binding protein that supports RNase e function in the Arabidopsis chloroplast. *Nucleic Acids Research*, 40(17), pp.8593–8606.
- Stoyanova-Bakalova, E. et al., 2004. Cell division and cell expansion in cotyledons of Arabidopsis seedlings. *New Phytologist*, 162(2), pp.471–479.
- Strittmatter, G. & Kossel, H., 1984. Nucleic Acids Research. *Nucleic Acids Research*, 12(22), pp.7633–7647.
- Su, P.-H. & Li, H. -m., 2010. Stromal Hsp70 Is Important for Protein Translocation into Pea and Arabidopsis Chloroplasts. *the Plant Cell*, 22(5), pp.1516–1531.
- Su, P.-H. & Li, H.-M., 2008. Arabidopsis stromal 70-kD heat shock proteins are essential for plant development and important for thermotolerance of germinating seeds. *Plant physiology*, 146(3), pp.1231–41.
- Syntichaki, P., Troulinaki, K. & Tavernarakis, N., 2007. eIF4E function in somatic cells modulates ageing in *Caenorhabditis elegans*. *Nature*, 445(7130), pp.922–926.
- Tadini, L. et al., 2016. GUN1 Controls Accumulation of the Plastid Ribosomal Protein S1 at the Protein Level and Interacts with Proteins Involved in Plastid Protein Homeostasis 1. *Plant Physiology*, 170(March), pp.1817–1830.
- Tanz, S.K. et al., 2012. The SCO2 protein disulphide isomerase is required for thylakoid biogenesis and interacts with LHCB1 chlorophyll a/b binding proteins which affects chlorophyll biosynthesis in Arabidopsis seedlings. *The Plant journal*, 69(5), pp.743–54.
- Tenson, T., Lovmar, M. & Ehrenberg, M., 2003. The mechanism of action of macrolides,

- lincosamides and streptogramin B reveals the nascent peptide exit path in the ribosome. *Journal of Molecular Biology*, 330(5), pp.1005–1014.
- Tiller, N. et al., 2012. The plastid-specific ribosomal proteins of *Arabidopsis thaliana* can be divided into non-essential proteins and genuine ribosomal proteins. *Plant Journal*, 69(2), pp.302–316.
- Tillich, M. et al., 2009. Chloroplast ribonucleoprotein CP31A is required for editing and stability of specific chloroplast mRNAs. *Proceedings of the National Academy of Sciences*, 106(14), pp.6002–6007.
- Torabi, S. et al., 2014. PsbN Is Required for Assembly of the Photosystem II Reaction Center in *Nicotiana tabacum*. *The Plant Cell*, 26(3), pp.1183–1199.
- Urbański, D.F. et al., 2012. Genome-wide LORE1 retrotransposon mutagenesis and high-throughput insertion detection in *Lotus japonicus*. *Plant Journal*, 69(4), pp.731–741.
- Wang, J. et al., 2016. Proteomic insight into the response of *Arabidopsis* chloroplasts to darkness. *PLoS ONE*, 11(5), pp.1–24.
- Wang, L. et al., 2010. The *Arabidopsis* chloroplast ribosome recycling factor is essential for embryogenesis and chloroplast biogenesis. *Plant Molecular Biology*, 74(1), pp.47–59.
- Wang, S. et al., 2016. Chloroplast RNA-Binding Protein RBD1 Promotes Chilling Tolerance through 23S rRNA Processing in *Arabidopsis*. *PLoS Genetics*, 12(5), pp.1–21.
- Weis, B.L. et al., 2014. The 60S associated ribosome biogenesis factor LSG1-2 is required for 40S maturation in *Arabidopsis thaliana*. *Plant Journal*, 80(6), pp.1043–1056.
- Woo, H.R. et al., 2002. Extended leaf longevity in the ore4-1 mutant of *Arabidopsis* with a reduced expression of a plastid ribosomal protein gene. *Plant Journal*, 31(3), pp.331–340.
- Yu, F. et al., 2008. Mutations in SUPPRESSOR OF VARIATION1, a Factor Required for Normal Chloroplast Translation, Suppress var2-Mediated Leaf Variegation in *Arabidopsis*. *the Plant Cell*, 20(7), pp.1786–1804.
- Yu, F., Park, S. & Rodermel, S.R., 2004. The *Arabidopsis* FtsH metalloprotease gene family: Interchangeability of subunits in chloroplast oligomeric complexes. *Plant Journal*, 37(6), pp.864–876.
- Yu, H. et al., 2012. Downregulation of Chloroplast RPS1 Negatively Modulates Nuclear Heat-Responsive Expression of HsfA2 and Its Target Genes in *Arabidopsis*. , 8(5).
- Zagari, N. et al., 2017. SNOWY COTYLEDON 2 Promotes Chloroplast Development and Has a Role in Leaf Variegation in Both *Lotus japonicus* and *Arabidopsis thaliana*. *Molecular Plant*, 10(5), pp.721–734.
- Zaltsman, A., Ori, N. & Adam, Z., 2005. Two types of FtsH protease subunits are required for chloroplast biogenesis and Photosystem II repair in *Arabidopsis*. *The Plant cell*, 17(October), pp.2782–2790.

- Zhang, J. et al., 2016. Plastid ribosomal protein S5 is involved in photosynthesis, plant development, and cold stress tolerance in Arabidopsis. *Journal of Experimental Botany*, 67(9), pp.2731–2744.
- Zhou, X. et al., 2015. Arabidopsis OR proteins are the major posttranscriptional regulators of phytoene synthase in controlling carotenoid biosynthesis. *Proceedings of the National Academy of Sciences*, 112(11), pp.3558–3563.
- Zybailov, B. et al., 2008. Sorting Signals, N-Terminal Modifications and Abundance of the Chloroplast Proteome K.-W. Koch, ed. *PLoS ONE*, 3(4), p.e1994.

## **8. Eidesstattliche Erklärung**

Ich versichere hiermit an Eides statt, dass die vorliegende Dissertation von mir selbständig und ohne unerlaubte Hilfe angefertigt ist.

München, 28-05-2019

Nicola Zagari

## **Erklärung über bisherige Promotionsversuche**

Diese Dissertation wurde keiner weiteren Prüfungskommission weder in Teilen noch als Ganzes vorgelegt. Ich habe nicht versucht, anderweitig eine Dissertation einzureichen oder mich einer Doktorprüfung zu unterziehen.

München, 28-05-2019

Nicola Zagari

## 9. Curriculum vitae

### Personal details:

Name: Nicola Zagari

Date of birth: 06-10-1987

Place of birth: Viterbo, Italy

Citizenship: Italian

Address: Zuiderkerksteeg 10a, 1601HJ Enkhuizen, The Netherlands

### Employment:

August 2018 - Currently

Junior researcher Cell Biology, Enza Zaden B.V. Enkhuizen, The Netherlands

May 2008 - Currently

Scientific explainer, ViterboScienza, Bologna Scienza in Piazza and other science festivals.

### Education:

May 2013 - Currently

PhD

Fondazione Edmund Mach, San Michele all'Adige, Italy (1.5 years)

Ludwig Maximilians Universitat, Munich, Germany (1.5 years)

Copenhagen Plant Science Center, Frederiksberg, Denmark (1.5 years)

Supervisor: Prof. Dr. Dario Leister (LMU)

February 2011 - March 2013

Master Degree Plant Biotechnology and Breeding, Wageningen University, The Netherlands

September 2006 - December 2010

Bachelor Degree, Agricultural Biotechnologies, University of Bologna, Italy

### Languages

Italian (native speaker), English (C2), French (C1), Spanish (B1), Dutch (A2)

### Publications

**Zagari N**, Sandoval-Ibañez O, Sandal N, Su J, Rodriguez-Concepcion M, Stougaard J, Pribil M, Leister D, Pulido P. 2017. SNOWY COTYLEDON 2 Promotes Chloroplast Development and Has a Role in Leaf Variegation in Both *Lotus japonicus* and *Arabidopsis thaliana*. *Molecular Plant*, 10(5), pp.721–734.

Pulido P\*, **Zagari N\***, Manavski N\*, Gawroński P, Matthes A, Scharff LB, Meurer J, Leister D. 2018. CHLOROPLAST RIBOSOME ASSOCIATED Supports Translation under Stress and Interacts with the Ribosomal 30S Subunit. *Plant Physiology*, 177(4), pp.1539–1554.

\*These authors contributed equally to this work.

## 10. Acknowledgements

I would like to express my deepest gratitude to several people that helped and supported me throughout my PhD.

At first to Prof. Dr. Dario Leister for giving me the opportunity to accomplish my PhD in his research group and to work in San Michele all'Adige, in Copenhagen and in Munich.

To FEM, CPSC and LMU for having financially supported my work.

To Dr. Pablo Pulido, for accepting to supervise me on different projects and to lead me through the publication jungle.

To Prof. Dr. Poul Erik Jensen and Prof. Dr. Paolo Pesaresi for having welcomed me in their groups and supported my research ideas.

To Dr. Lars Scharff, Dr. Mathias Pribil, Piotr, Omar and Kamil for having being great colleagues in Copenhagen and having helped me in the lab each time I was lost.

To the amazing colleagues at FEM in san Michele and to those in Munich that made my life nicer when my results were trying to make it terrible.

To Chiara, Cristina, Luise, Marcel, Bennet, for being great friends and smiling even when I was negative or unhappy and having me helped with all the bureaucracies of these years.

To Francesca, for having the patience to be at my side from the first day of my PhD, assisting my best and worst moments and being an amazing friend.

To my great friends in Bologna for being always positive and happy with me and to Giulia, Francesco and Marina, for being there in every moment of the last 20 years.

To Mum and Dad, who believed in me and always supported the choices I did and will do.